

MONITORING THE DEVELOPMENT OF PROPERTIES IN FRESH CEMENT  
PASTE AND MORTAR BY ULTRASONIC WAVES

A THESIS SUBMITTED TO  
THE GRADUATE SCHOOL OF NATURAL AND APPLIED SCIENCES  
OF  
MIDDLE EAST TECHNICAL UNIVERSITY

BY

ÖZLEM KASAP KESKİN

IN PARTIAL FULFILLMENT OF THE REQUIREMENTS  
FOR  
THE DEGREE OF DOCTOR OF PHILOSOPHY  
IN  
CIVIL ENGINEERING

JANUARY 2009

Approval of thesis:

**MONITORING THE DEVELOPMENT OF PROPERTIES IN FRESH  
CEMENT PASTE AND MORTAR BY ULTRASONIC WAVES**

submitted by **ÖZLEM KASAP KESKİN** in partial fulfillment of the requirements  
for the degree of **Doctor of Philosophy in Civil Engineering Department,**  
**Middle East Technical University** by,

Prof. Dr. Canan Özgen  
Dean, Graduate School of **Natural and Applied Sciences**

\_\_\_\_\_

Prof. Dr. Güney Özcebe  
Head of Department, **Civil Engineering**

\_\_\_\_\_

Prof. Dr. Mustafa Tokyay  
Supervisor, **Civil Engineering Dept., METU**

\_\_\_\_\_

Assoc. Prof. Dr. İsmail Özgür Yaman  
Co. Supervisor, **Civil Engineering Dept., METU**

\_\_\_\_\_

**Examining Committee Members:**

Prof. Dr. Turhan Y. Erdoğan  
Civil Engineering Dept., METU

\_\_\_\_\_

Prof. Dr. Mustafa Tokyay  
Civil Engineering Dept., METU

\_\_\_\_\_

Prof. Dr. Kambiz Ramyar  
Civil Engineering Dept., Ege University

\_\_\_\_\_

Assoc. Prof. Dr. Uğurhan Akyüz  
Civil Engineering Dept., METU

\_\_\_\_\_

Asst. Prof. Dr. Sinan T. Erdoğan  
Civil Engineering Dept., METU

\_\_\_\_\_

**Date:** January 27, 2009

**I hereby declare that all information in this document has been obtained and presented in accordance with academic rules and ethical conduct. I also declare that, as required by these rules and conduct, I have fully cited and referenced all material and results that are not original to this work.**

Name, Last Name : Özlem Kasap Keskin

Signature :

## **ABSTRACT**

### **MONITORING THE DEVELOPMENT OF PROPERTIES IN FRESH CEMENT PASTE AND MORTAR BY ULTRASONIC WAVES**

Kasap Keskin, Özlem

Ph.D., Department of Civil Engineering

Supervisor : Prof. Dr. Mustafa Tokyay

Co-supervisor: Assoc. Prof. Dr. İ. Özgür Yaman

January 2009, 170 pages

The determination and following up the development of properties during the fresh state and early ages of concrete are important in order to schedule the work and to obtain the desired properties in the hardened concrete. As the traditional methods such as Vicat and Penetrometer mostly depend on the experience of the operator and do not provide a continuous picture of the development of properties, reliable and objective non-destructive test methods are needed for the quality control of fresh concrete.

The purpose of this thesis is to observe the development of properties of fresh pastes and mortars continuously by longitudinal ultrasonic waves. For this purpose, cement pastes and mortars with three different w/c ratios were prepared with ordinary portland cement. The ultrasonic pulse velocities were determined

continuously during hydration. The setting times were also determined by standard test methods.

The flexural and compressive strength were determined at 1, 2, 3, 7 and 28 days by standard test method and the volume of permeable pores were also obtained at the same ages. Lastly, the heat of hydration of cement pastes of similar w/c ratios were determined by isothermal calorimetry.

UPV (Ultrasonic Pulse Velocity) development was compared with the results of standard tests applied on the samples. The results revealed that the UPV is a useful method in monitoring the hydration process of cementitious materials.

Keywords: Ultrasonic Wave Propagation, Fresh State Properties, Setting Time, Heat of Hydration

## ÖZ

### TAZE ÇİMENTO HAMURLARI VE HARÇLARINDA ÖZELLİK GELİŞİMİNİN ULTRASES DALGALARIYLA İZLENMESİ

Kasap Keskin, Özlem

Doktora, İnşaat Mühendisliği Bölümü

Tez Yöneticisi : Prof. Dr. Mustafa Tokyay

Ortak Tez Yöneticisi: Doç. Dr. İ. Özgür Yaman

Ocak 2009, 170 sayfa

Betonun taze haldeki ve erken yaşlardaki özelliklerinin belirlenmesi ve izlenmesi iş zamanlaması ve istenilen özelliklerde sertleşmiş beton elde etmek için önemlidir. Vicat ve penetrometre gibi standard deneyler, büyük ölçüde uygulayan kişinin tecrübesine dayandığı ve özelliklerin gelişimi ile ilgili olarak sürekli bir bilgi sağlayamadığı için, taze betonun kalite kontrolünde güvenilir ve objektif tahribatsız deney yöntemlerine ihtiyaç duyulmaktadır.

Bu tezin amacı, taze çimento hamuru ve harçlarında özelliklerin gelişimini basınç dalgalarının iletimi yoluyla sürekli olarak gözlemlemektir. Bu amaçla normal portland çimentosu kullanılarak üç farklı su/çimento oranında çimento hamurları ve harçları hazırlanmıştır. Hidratasyon sırasında ultrases dalgalarının hızları sürekli olarak belirlenmiştir. Priz süreleri de standard yöntemler kullanılarak belirlenmiştir.

Standard yöntemle 1, 2, 3, 7 ve 28 günlerde eğilme ve basınç dayanımları ve yine aynı günlerde geçirgen boşluk hacmi ölçülmüştür. Son olarak aynı su/çimento oranlarına sahip çimento hamurlarının hidrasyon ısıları izotermal kalorimetre yöntemi ile ölçülmüştür.

UPV (Ultras ses Hızı) gelişimi, numunelere uygulanan standard deneylerde elde edilen sonuçlar ile kıyaslanmıştır. Sonuçlar, UPV'nin çimento bazlı malzemelerin hidrasyonunun gözlemlenmesi için faydalı bir metod olduğunu göstermiştir.

Anahtar kelimeler: Ultrasonik Dalga İletimi, Taze Haldeki Özellikler, Priz Süresi, Hidrasyon Isısı

To My Parents,  
Tülay Kadriye and Hikmet Kasap

## ACKNOWLEDGEMENTS

I would like to express great appreciation to my supervisor Prof. Dr. Mustafa Tokyay and co-supervisor Assoc. Prof. Dr. İ. Özgür Yaman for their continuous suggestions, support and supervision throughout my PhD life.

I also would like to thank Prof. Dr. Turhan Y. Erdoğan and Prof. Dr. Kambiz Ramyar for their valuable suggestions and comments throughout this study.

I acknowledge the personnel of Materials of Construction Laboratory for their full support and contribution to the experiments.

I am also grateful to Dr. Oğuzhan Çopuroğlu, who conducted the ESEM analysis of the cement pastes at Delft University.

I am also thankful to Technical Research and Quality Control Department (TAKK) of State Water Works (DSİ) for conducting the isothermal calorimetric measurements of the cement pastes in their laboratories.

Lastly, I would like to express my sincere gratitude to my husband Mr. Süleyman Bahadır Keskin, my parents and my brother for their patience, understanding, encouragement, and full support not only during my PhD study but also throughout my life.

## TABLE OF CONTENTS

ABSTRACT .....	iv
ÖZ .....	vi
DEDICATION .....	viii
ACKNOWLEDGEMENTS .....	ix
TABLE OF CONTENTS .....	x
LIST OF TABLES .....	xiii
LIST OF FIGURES .....	xv

### CHAPTERS

1. INTRODUCTION .....	1
1.1 General .....	1
1.2 Objective and Scope .....	4
2. THEORETICAL CONSIDERATIONS .....	6
2.1 Hydration of Portland Cement .....	6
2.1.1 Reactions and Mechanism of Hydration .....	6
2.1.2 Setting .....	11
2.1.3 Heat of Hydration .....	13
2.2 Ultrasonic Testing Method .....	18
2.2.1 Basic Elements of Ultrasonic Waves .....	18
2.2.2 Wave Propagation Theory .....	20

2.2.3	Ultrasonic Testing of Hardened Concrete .....	26
2.2.4	Near-Field and Far-Field Concepts .....	32
3. LITERATURE SURVEY ON WAVE PROPAGATION		
	TECHNIQUES FOR FRESH CEMENTITIOUS MATERIALS.....	34
3.1	General .....	34
3.2	Impact-Echo Method .....	35
3.3	Vibroscope .....	37
3.4	Wave Reflection Method .....	41
3.5	Wave Transmission Method .....	47
3.6	Comparison of the Methods .....	58
3.7	Some Remarks on the Wave Transmission Method .....	60
4. EXPERIMENTAL STUDY .....		
4.1	Experimental Program .....	62
4.2	Materials .....	63
4.2.1	Cements .....	63
4.2.2	Aggregates .....	65
4.2.3	Water .....	66
4.3	Mortar Mixtures .....	66
4.4	Test Methods .....	67
4.4.1	Development of the mold .....	68
4.4.2	UPV determination .....	71
4.4.3	Setting time determination .....	75
4.4.4	Heat of hydration determination .....	77
4.4.5	ESEM analysis .....	78
4.4.6	Strength determination .....	78
4.4.7	Volume of permeable pores and absorption capacity determination .....	79

5. TEST RESULTS AND DISCUSSIONS .....	81
5.1 Progress of Hydration in Cements .....	81
5.2 Propagation of Ultrasonic Waves in Hydrating Cements .....	84
5.3 Development of Ultrasonic Pulse Velocity in Cement Pastes ....	91
5.4 Setting Time Test Results in Cement Pastes .....	96
5.4.1 Determination of initial setting time from UPV curves in cement pastes .....	97
5.4.2 Determination of final setting time from UPV curves in cement pastes .....	99
5.5 Heat of Hydration and Rate of Heat of Hydration Test Results ..	103
5.6 Development of Ultrasonic Pulse Velocity in Cement Mortars ..	109
5.7 Determination of Setting Time in Mortars .....	116
5.8 Alternative Approach for the Setting Time of Cement Mortars ..	118
5.9 Factors Affecting the Velocity Measurements on Fresh Mortars	123
5.9.1 Effect of path length .....	124
5.9.2 Effect of frequency range of transducers .....	130
5.10 Repeatability of the UPV Testing of Fresh Mortars .....	138
5.11 Properties of Hardened Mortars .....	139
5.11.1 Strength test results .....	140
5.11.2 Volume of permeable pore determination test results ...	147
6. CONCLUSIONS .....	154
7. RECOMMENDATIONS .....	161
REFERENCES .....	162
CURRICULUM VITAE .....	169

## LIST OF TABLES

### TABLES

Table 2.1.	Near-field zone for different velocity levels .....	33
Table 4.1.	Tests performed on cement .....	64
Table 4.2.	The chemical composition of CEM I 42.5 R cement .....	64
Table 4.3.	The physical and mechanical properties of CEM I 42.5 R cement .....	64
Table 4.4.	Tests performed on aggregates .....	65
Table 4.5.	Properties of aggregate .....	65
Table 4.6.	Gradation of the aggregate .....	65
Table 4.7.	Mixture proportions of mortar specimens .....	66
Table 4.8.	Zero reading correction for each frequency .....	74
Table 4.9.	UPV of plexiglass sheet for each frequency .....	75
Table 5.1.	Setting time test results and corresponding UPVs .....	97
Table 5.2.	The intersection points of linear portions and corresponding UPVs .....	98
Table 5.3.	Comparison of Vicat and UPV for initial setting time determination .....	99
Table 5.4.	The characteristic points of RUPV curves and the corresponding UPVs .....	101
Table 5.5.	Comparison of Vicat and UPV Methods for final setting time determination .....	102
Table 5.6.	Slopes of linear portions in UPV development curves .....	113

Table 5.7.	The intersection points of linear portions and corresponding UPVs .....	114
Table 5.8.	The characteristic points of RUPV development curves and the corresponding UPVs .....	116
Table 5.9.	Initial and final setting times of mortars and corresponding UPVs .....	117
Table 5.10.	Initial setting time as determined by standard method and UPV method .....	118
Table 5.11.	Initial and final setting times of mortars according to new approach .....	123
Table 5.12.	Comparison of intersection points of linear portions in UPV curves .....	129
Table 5.13.	Comparison of characteristic points of linear portions in RUPV curves .....	129
Table 5.14.	The wavelength for different velocity and frequency .....	131
Table 5.15.	Comparison of determined setting times with different frequencies .....	137
Table 5.16.	Comparison of determined setting times at different times ...	138
Table 5.17.	Flexural and compressive strength test results of mortar specimens .....	141
Table 5.18.	Volume of permeable pores, absorption, apparent and bulk density .....	148

## LIST OF FIGURES

### FIGURES

Figure 2.1.	Schematic representation of rate of heat of hydration of portland cement paste obtained by isothermal conduction calorimetry .....	16
Figure 2.2.	Schematic representation of heat of hydration of portland cement paste obtained by isothermal conduction calorimetry	17
Figure 2.3.	Basic elements of a wave .....	19
Figure 2.4.	Particle motion for different wave types .....	21
Figure 2.5.	The reflection and refraction of a P-wave with mode conversion .....	23
Figure 2.6.	Attenuation of a wave while propagating in a medium .....	25
Figure 2.7.	Schematic representation of ultrasonic apparatus .....	28
Figure 2.8.	Arrangements in placing transducers .....	28
Figure 2.9.	Near-field/Far-field concept .....	32
Figure 3.1.	Experimental set-up for impact-echo developed for testing fresh concrete .....	37
Figure 3.2.	A schematic representation of Vibroscope .....	39
Figure 3.3.	Apparatus for wave reflection of shear waves .....	43
Figure 3.4.	Apparatus for reflection factor determination of longitudinal waves .....	47
Figure 3.5.	The mold developed at Stuttgart University .....	53

Figure 4.1.	The wooden molds used in the experiments and attachment of transducers .....	70
Figure 4.2.	The schematic representation of data acquisition system ...	71
Figure 4.3.	The raw and processed waveforms of ultrasonic pulses .....	73
Figure 5.1.	Schematic representation of setting and hardening process ..	82
Figure 5.2.	Cement paste structure (a) before setting, (b) at initial setting, (c) at final setting .....	83
Figure 5.3.	The change in waveforms during hydration for mortar specimen .....	86
Figure 5.4.	Development of UPV in cement pastes for different w/c ratios .....	91
Figure 5.5.	The stages of UPV development in cement pastes with different w/c ratios .....	93
Figure 5.6.	Rate of UPV change with time in cement pastes for different w/c ratios .....	95
Figure 5.7.	Setting time values for each w/c ratio .....	96
Figure 5.8.	The stages of RUPV development curves of cement pastes with different w/c ratios .....	100
Figure 5.9.	Rate of heat of hydration of cement for different w/c ratios ..	103
Figure 5.10.	Comparison of UPV and RHH development in cement pastes .....	105
Figure 5.11.	Comparison of RUPV and RHH development in cement pastes .....	107
Figure 5.12.	Heat of hydration of cement pastes for different w/c ratios ...	108
Figure 5.13.	Development of UPV in cement mortars for different w/c ratios .....	109
Figure 5.14.	Development of UPV in cement mortars for the first 24 hours .....	111
Figure 5.15.	The stages of UPV development in mortars for each w/c ratio .....	112

Figure 5.16.	Rate of UPV change with time in mortars for different w/c ratios .....	115
Figure 5.17.	Comparison of UPV development in pastes and mortars for different w/c ratios .....	120
Figure 5.18.	Comparison of RUPV development in pastes and mortars for different w/c ratios .....	121
Figure 5.19.	Effect of path distance on UPV and RUPV of mortars with 0.5 w/c ratio .....	125
Figure 5.20.	Effect of path distance on UPV and RUPV of mortars with 0.6 w/c ratio .....	127
Figure 5.21.	Effect of path distance on UPV and RUPV of mortars with 0.8 w/c ratio .....	128
Figure 5.22.	Effect of frequency on UPV development for each travel path .....	133
Figure 5.23.	Effect of frequency on RUPV development for each travel path .....	135
Figure 5.24.	Development of compressive strength in mortar specimens ..	141
Figure 5.25.	Development of flexural strength in mortar specimens .....	142
Figure 5.26.	Relation between flexural and compressive strength in mortar specimens .....	143
Figure 5.27.	Development of UPV in hardened cement mortars .....	144
Figure 5.28.	Relation between UPV and compressive strength for different travel path lengths .....	145
Figure 5.29.	Relationships between UPV and compressive strength .....	146
Figure 5.30.	Absorption of mortar specimens .....	149
Figure 5.31.	Volume of permeable pore space of mortar specimens .....	150
Figure 5.32.	Relation between volume of permeable pores and w/c ratio	151
Figure 5.33.	Relation between UPV and permeable pore volume in mortars .....	152

# **CHAPTER 1**

## **INTRODUCTION**

### **1.1 General**

Cement-based materials are generally the most widely-used construction materials throughout the world. When the cementitious material is mixed with water, at the beginning it is in a plastic and shapeable state. This plastic state is defined as the fresh state. After the medium loses its plasticity, it starts to gain strength and rigidity, and this state is defined as the hardened state.

The properties of fresh concrete is one of the most important topics in concrete technology as the properties of hardened concrete are in close relation to those of fresh state and the curing conditions. It is obvious that in order to obtain the desired properties in the hardened concrete, it should have proper properties in the fresh state and the necessary operations such as mixing, placing, compacting, finishing and curing should be done appropriately. Control of the early age properties of cement based materials will lead to a better quality in the later stages.

Additionally, the determination of the properties of fresh concrete is also important for scheduling the work in construction sites and precast plants. As the concrete is workable only for a limited period of time, timing for mixing, placing, compacting

and finishing should be arranged properly. Form removal time should also be scheduled properly so that the structure can carry the construction loads safely. Therefore, it is indisputable that the determination and following up the development of properties during fresh state and early ages of concrete is a crucial issue from both technical and economical points of view.

The most commonly used test methods for determining the properties of fresh cement paste, mortar and concrete are setting time determination by Vicat apparatus or Penetrometer; consistency determination by flow or slump tests. Although these tests are cheap and easy to apply, they mostly depend on the experience of the operator, they only determine a single property and most importantly they do not provide a continuous picture of the development of properties. Therefore, reliable and objective test methods which provide continuous information about the condition of the medium are needed for fresh concrete.

Non-destructive test methods can be more appropriate for continuous observation as the specimen is not damaged and they allow testing the same specimen many times.

Another advantage of non-destructive testing is the possibility of in-situ application. If the appropriate experimental set-up can be designed, then it may be possible to apply the test not only in the laboratory but also at the site. As the environmental conditions and the specimen geometry can be different in laboratory and on site, in-situ testing is more reliable in determining the properties. It is known that the rate of cement hydration is affected by the ambient temperature. Sometimes the specimen geometry may also be important in testing procedure. Therefore, new and reliable methods for testing the fresh properties of cement mortar and concrete non-destructively should be developed and standardized.

The investigations for new methods on fresh concrete properties have increased over the last decade. These new methods may be listed as nuclear magnetic

resonance, electrical methods, impact-echo, acoustic emission, maturity method, radon exhalation method and methods based on ultrasonic wave propagation (Grosse et. al, 2005).

Ultrasonic testing method is one of the most widely used non-destructive testing methods in hardened concrete. The main idea is to send ultrasonic waves from one point of the material and receive them at another point. The travel time between these points is measured. Knowing the distance between the measurement points, the velocity of the ultrasonic waves throughout the medium can be calculated easily. According to ASTM C 597, ultrasonic pulse velocity method can be used to control the uniformity and relative quality of concrete, to determine the presence of cracks and voids and to estimate the crack depth.

Ultrasonic waves have a frequency range higher than 20 kHz, which is beyond the limits of the human ear. The wave propagates through the medium by small vibration of particles. Although, it does not give exact information about the strength of concrete, it is a useful technique for uniformity and quality inspection of hardened concrete. The ultrasonic waves travelling through a medium give information about the elastic properties of the medium as the velocity of waves is directly related to the elastic properties (Krautkrämer, 1983). Ultrasonic pulse velocity is also related to the density of the medium (Neville, 2003). In a material with high density, ultrasonic pulse wave can propagate faster, which means the velocity will be higher.

As mentioned before, just after the cement and water is mixed, initially the medium is in a state like liquid which contains voids. As time passes, the hydration reactions proceed leading to the gaining of rigidity and strength. The hydration products fill the pores within the medium. Ultrasonic pulse waves cannot propagate through the voids. When the wave comes across a void, it cannot pass across the void, but it passes around it. As a result of increase in hydration products, the amount of pores decreases within the body. Therefore, as time passes, the total path

that the ultrasonic pulse wave travels decreases leading to an increase in velocity. Moreover, as the material stiffens, the elastic properties develop in the fresh cementitious material. As the ultrasonic pulse velocity is related to the elastic properties and the density of the material, the increase in density and elastic properties by time will lead to an increase in ultrasonic pulse velocity (UPV). Therefore, the stages of the hydration process of cementitious materials can be monitored by following the changes in ultrasonic pulse velocity in time starting just after the mixing and placing operations.

## **1.2 Objective and Scope**

The purpose of this dissertation is to monitor the properties of fresh cementitious materials continuously by longitudinal ultrasonic waves in through transmission. For this purpose, the properties determined by standard test methods were compared with the development of ultrasonic pulse wave velocity, and the relation between the results of standard test methods and UPV development was investigated.

One of the most challenging parts of monitoring fresh cementitious material properties by ultrasonic test method is the design of a suitable experimental set-up. The importance of the mold in testing the fresh material by ultrasonic wave propagation arises due to the necessity of testing the specimen which is still inside the mold. Firstly, an experimental set-up for UPV measurements was designed.

After the experimental set-up was prepared, cement pastes and mortars with different water/cement (w/c) ratios were prepared by using CEM I 42.5 R cement. Three different w/c ratios (0.5, 0.6, 0.8) were tested.

In cement paste specimens, UPV measurements were taken for 24 hours continuously right after the paste is placed in the molds. Besides the UPV measurements, setting time of cement pastes prepared with different w/c ratios

were determined by Vicat needle according to ASTM C 191. In order to observe hydration process, rate of heat of hydration of cement pastes were also determined by isothermal calorimetry. Lastly, the ESEM images of pastes with 0.5 w/c ratio was taken during setting.

In mortar specimens, UPV measurements were taken continuously with a time interval of 15 minutes for the first 72 hours. Additional UPV measurements were taken at 7 and 28 days. The setting time of mortar specimens were determined according to ASTM C 403 by the penetration resistance method. The flexural and compressive strength of 4\*4\*16 cm mortar specimens were determined at 1, 2, 3, 7 and 28 days. Lastly, the volume of permeable pores of specimens having dimensions similar to strength determination test specimens were obtained according to ASTM C 642 for the 1, 2, 3, 7 and 28 day-old mortar specimens.

As there is no standard for observation of hydration of cement by ultrasonic wave propagation method, each researcher used his/her own mold dimensions and frequency ranges; detailed information about which will be given in Chapter 3. In order to see the effect of dimension of specimen and the frequency used in testing, different travel path distances and different narrow-band transducers were used for mortar mixtures. Travel path lengths of 15, 10, and 5 cm were used for determining the effect of mold dimension for each w/c ratio. Three different frequencies of 54, 82, and 150 kHz were applied separately to each travel path length for mortars having w/c ratio of 0.5.

Thus, the early age hydration process of cement was monitored continuously by ultrasonic wave propagation method in conjunction with various standard methods.

## **CHAPTER 2**

### **THEORETICAL CONSIDERATIONS**

#### **2.1 Hydration of Portland Cement**

##### **2.1.1 Reactions and Mechanism of Hydration**

Cement gains binding property only when mixed with water. The strength and rigidity gaining of cement are the results of chemical reactions between cement particles and water, which is known as hydration (Mehta and Monteiro, 2006).

Two mechanisms have been proposed for hydration of portland cement; through-solution hydration and solid-state hydration. In through-solution hydration, first the anhydrous compounds of the cement dissolves into their ionic constituents, then the hydrates are formed in the solution, and lastly the hydrates are precipitated. In solid-state or topochemical hydration, the reactions occur directly at the surface of the anhydrous cement compounds. It is proposed that while at the early stages of hydration the through-solution mechanism is dominant, at later stages solid-state mechanism may be effective in the hydration of residual cement particles (Mehta and Monteiro, 2006).

As portland cement consists of several compounds, its hydration process is rather complex. The hydration process consists of a series of reactions proceeding

simultaneously and successively with different rates, the participants of which are alite (impure tricalcium silicate), belite (impure dicalcium silicate), tricalcium aluminate, calcium alumino ferrite, free calcium oxide, alkali sulfates, calcium sulfate, and mixing water (Odler, 2005). Among these, tricalcium silicate ( $C_3S$ ), dicalciumsilicate ( $C_2S$ ), tricalcium aluminate ( $C_3A$ ), and tetracalcium alumino ferrite ( $C_4AF$ ) are the major compounds of the portland cement. Although it is not completely correct, in most cases, from a practical point of view, it is reasonable to assume that the hydration of each cement component occurs independently (Mindess and Young, 1981).

The stiffening and setting characteristics of cements are mostly controlled by the hydration of the aluminates whereas the strength development of cement is largely dependent on the hydration of silicates (Mehta and Monteiro, 2006). Additionally, the rate of hydration of aluminates is faster than the rate of hydration of silicates.

The total amount of tricalcium silicate ( $C_3S$ ) and dicalciumsilicate ( $C_2S$ ) makes up approximately 75% of ordinary portland cement. The completed hydration reactions of silicates are very similar in nature:



The chemical formula  $C_3S_2H_3$  is not accurate, as the hydrate is variable over quite a wide range (Mindess and Young, 1981). The major output of these reactions is, in a more general sense, calcium-silicate-hydrate gel (C-S-H). C-S-H is the major constituent of hardened cementitious systems and it is responsible for strength development as well as many other important properties. If 100 parts by mass are assumed to react according to both reactions separately, approximately similar amounts of water will be consumed by both silicates, however, amount of CH produced will be twice and the amount of C-S-H gel will be less in the case of  $C_3S$

hydration compared to C<sub>2</sub>S hydration (Neville, 2003). As the increase in the CH amount reduces the resistance of cements against acidic and sulphate solutions, high-C<sub>2</sub>S cement will have a higher durability compared to high-C<sub>3</sub>S cement. Additionally, high-C<sub>2</sub>S mixtures will also have a higher ultimate strength due to the higher amount of C-S-H gel produced (Mehta and Monteiro, 2006).

Although the total amount of aluminates in cement is significantly less than the total amount of silicates, their behaviour in cementitious systems and effect on concrete properties, especially from durability point of view, is important. The hydration reaction of C<sub>3</sub>A with water progresses very rapidly with evolution of a high amount of heat (Mehta and Monteiro, 2006). Therefore, to slow down the reaction and to prevent the “flash set” which is the immediate stiffening of the fresh concrete, a small amount of gypsum is added into the cement composition during the production (Neville, 2003). When C<sub>3</sub>A reacts with gypsum and water, one or both of the following reactions occur:



The mineral group containing three molecules of sulphate as the ettringite produced in reaction 2.3 is labelled as Aft. Additionally, the mineral group containing one molecule of sulphate as the product of reaction 2.4 is named as Afm. During hydration of cements, the Aft phase transforms into Afm phase when the gypsum is completely consumed due to the reduction of sulphate ions in the medium (Mindess and Young, 1981).

Lastly, the hydration of C<sub>4</sub>AF with the presence of gypsum is analogous to that of C<sub>3</sub>A. In the hydration product, the iron oxide and alumina occur interchangeably in

the compound. The products of this reaction may be written as  $C_4(A, F)\bar{S}H_{12}$  and  $(C_6(A, F)\bar{S}_3H_{32})$  (Mindess and Young, 1981).

The hydration process of portland cement can be divided into several stages such as pre-induction period, induction period, acceleration period and post-acceleration period. These stages of cement hydration are described below (Odler, 2005; Mindess and Young, 1981):

Pre-induction period:

This is the stage of dissolution of ionic species into the liquid phase which starts immediately after cement particles and water come into contact and lasts for only a few minutes. Alkali sulfates of cement dissolve completely giving  $K^+$ ,  $Na^+$ , and  $SO_4^{2-}$  ions and calcium sulfate dissolves until saturation giving  $Ca^{2+}$  and  $SO_4^{2-}$  ions into the liquid phase. A very small portion of  $C_3S$  hydrates in this stage forming C-S-H gels, which precipitates on the surface of cement grains, and thus  $Ca^{2+}$  and  $OH^-$  concentration increases and silicate ions are produced.  $C_3A$  in the cement dissolves and produces AFt by reacting with  $Ca^{2+}$  and  $SO_4^{2-}$  ions. This also precipitates at the surface of the cement grains.  $C_4AF$  reacts similarly to  $C_3A$  producing AFt phase. Only a minor portion of  $C_2S$  hydrates during this stage producing C-S-H and  $Ca^{2+}$  and  $OH^-$  ions. This fast hydration phase is stopped due to the deposition of hydration products at the surface of cement particles so that a barrier is formed between non-hydrated cement grains and the solution.

Induction (dormant) period:

After the fast hydration stage, a period of relative inactivity which lasts for a few hours is seen. In this stage, the rate of hydration reactions slows down significantly. In the dormant period, the concentration of  $SO_4^{2-}$  ions remains constant, because the dissolution of additional calcium sulfate compensates for the consumption of  $SO_4^{2-}$  ions as the result of AFt phase formation. The end of the induction period

and the start of the main reactions is said to be due to the nucleation of the second-stage C-S-H from the bulk liquid.

Acceleration period:

In this stage, the hydration reactions which are controlled by the nucleation and growth of the hydration products accelerate again. This period lasts about 3-12 hours depending on the cement composition and curing temperature. The rate of hydration of  $C_3S$  accelerates, the hydration of  $C_2S$  also progresses, and the second-stage C-S-H phase starts to be produced. The concentration of  $Ca^{2+}$  ions declines gradually as the result of precipitation of crystalline calcium hydroxide. The concentration of  $SO_4^{2-}$  ions also declines due to the formation of AFt phase and adsorption of the ions on the surface of formed C-S-H phase.

Post-acceleration period:

Due to the fact that the amount of non-reacted cement decreases and the rate of hydration starts to be controlled by diffusion, the rate of hydration slows down. As the result of on-going hydration of  $C_3S$  and  $C_2S$ , C-S-H phase continues to increase. The concentration of  $SO_4^{2-}$  ions decreases after the calcium sulfate is exhausted. As a result, the AFt phase starts to react with additional  $C_3A$  and  $C_2(A,F)$  by through-solution mechanism producing monosulfate. If there is sufficient water in the medium, the hydration reactions continue until there are no unhydrated cement particles. However, this is not the general case in real applications. After the hydration process has been stopped, an aging of the hydration products may take place.

Later on, the material has reached its long-term structure, strength and properties. The stage after the completion of hydration reactions is classified as a fifth period of hydration process, namely “steady-stage” by some researchers (Schindler et al., 2002).

### 2.1.2 Setting

Setting is a term used to describe the stiffening of the fresh cement paste (Neville, 2003). Stiffening is described as the loss of consistency of the plastic cement paste (Mehta and Monteiro, 2006). By setting process, the fresh cementitious material is converted from a liquid state into a solid state. The solidification of the fresh cement paste does not occur suddenly; instead it requires some time to become totally rigid. The beginning of the solidification is called initial set, and it describes the time when the cement paste is not workable anymore. The end of the solidification is called final set, and it describes the time for full solidification (Mehta and Monteiro, 2006).

Sometimes abnormal setting of cement may take place in the form of “flash set” or “false set”. As mentioned in the previous section, flash set is the result of hydration of  $C_3A$  in the absence of gypsum. If the amount of gypsum is not sufficient, flash set occurs with a high amount of heat liberation. This situation is irreversible and the paste does not gain much strength (Erdoğan, 2002). On the other hand, false set is different from flash set, because no heat liberation occurs and by remixing without addition of any water, the paste restores its plasticity again. Then the material sets and gains strength in a normal manner (Neville, 2003). Possible causes of false set can be dehydration of gypsum when interground with too hot clinker and carbonation of alkalis of cement during storage (Erdoğan, 2002, and Neville, 2003).

Setting and strength gain are different phenomena. Hydration of cement particles continues after setting as long as there exist unhydrated cement particles and water within the medium. As the hydration reactions proceeds, the voids are filled with hydration products leading to a decrease in porosity and permeability and increase in strength (Mehta and Monteiro, 2006). Strength gain of a set cement paste is called hardening (Neville, 2003).

As the material is only workable up to setting which means mixing, transporting, placing, compacting and surface finishing processes should be finished before setting occurs, time required for setting is important. Too short a setting time will lead to problems in treatment of fresh concrete while too long a setting will lead to delays in construction. Therefore, knowledge of setting time is required in order to schedule and apply the processes for fresh concrete properly. Setting time of cement paste is determined by Vicat apparatus according to ASTM C 191 and the setting time of concrete is determined by penetrometer according to ASTM C 403. Actually, in both of the standards, the initial and final setting time values are described as arbitrarily chosen stages of the setting, by declaring the amount of penetration values for initial and final setting times, separately.

In the Vicat test, the depth of penetration of the needle under the own weight of the apparatus into the cement paste is measured. The initial set is said to be occurred when a penetration depth of 25 mm from the top of the paste is obtained. Final set is said to occur when the needle of the apparatus no longer penetrates into the paste.

Setting time test cannot be applied directly to concrete sample, due to the fact that the presence of coarse aggregate particles may violate the penetration resistance readings. Therefore, the test is applied on the mortar part of the concrete sample which is obtained by sieving through a No 4 sieve to separate the coarse aggregates. After the mortar is separated from the concrete mix, the material is placed in a mold for following the increase in the penetration resistance value. Penetration resistance is determined by measuring the force required to penetrate the 25 mm-long needle with known cross sectional area into the medium. Penetration resistance is calculated by dividing the obtained force by the cross sectional area. According to ASTM C 403, initial setting is reached when a penetration resistance strength of 3.5 MPa is obtained. For final setting time, the designated value of penetration resistance strength is 27.6 MPa.

If the procedures for determination of setting time for cement paste and mortar according to the relevant standards are examined, it becomes doubtful whether these methods determine the beginning and the end of setting as described by their physical meanings, since they only determine two arbitrary points during the setting stage as initial and final setting time values.

### **2.1.3 Heat of Hydration**

The hydration of cement is an exothermic reaction; i.e. heat is evolved during the reaction. Cement is produced by burning raw materials at very high temperatures of about 1450 °C in a rotary kiln. As the compounds of cement are non-equilibrium products of high-temperature reactions, they are in a high-energy state. When cement is mixed with water, the cement particles react with water in order to reach a more stable state, hence lowering their energy levels. Hence hydration reactions lead to heat liberation (Mindess and Young, 1981; Mehta and Monteiro, 2006).

The total amount of heat released during the hydration reaction is called “heat of hydration”. It is expressed in terms of calories/gram (cal/g) or joules/gram (j/g). As cement is composed of different compounds which have different hydration rates and hydration heats, cement composition is one of the most important factors that affect the heat of hydration of cement (Neville, 2003). At the early stages of hydration, the surface area of the cement is effective in the rate of heat evolution. However, as the hydration proceeds, the total heat of hydration is not affected by the fineness of cement (Neville, 2003). The temperature during the hydration also affects the rate of heat evolution (Neville, 2003). In summary, it can be stated that cement composition, cement fineness and the temperature are the three main factors that influence the heat of hydration and rate of heat of hydration evolution.

The heat released during the hydration reactions of cement may be beneficial for some cases whereas it may be destructive for concrete in other cases. For example, during cold weather, high heat of hydration is needed in order to compensate to

some degree the adverse effects of low ambient temperature, such as freezing of water in capillary pores, on the setting and hardening properties of concrete. However, in a massive structure, high heat of hydration may lead to cracks in the concrete body. As the structure starts to cool from the outer surface, the inner parts will cool more slowly. Due to this temperature difference between inner and outer parts of the concrete mass, thermal stresses occur in the structure. Especially at early ages, while the tensile strength of concrete is very low, these thermal stresses cause cracks and strength loss in the structure. Therefore, having the knowledge of the heat of hydration of cements may provide considerable benefits during the construction process.

There are three main methods for determining the amount of heat released as the result of the hydration reactions of cement. These methods can be explained briefly as follows:

#### Heat of Solution Method:

Determination of heat of hydration by heat of solution method is described in ASTM C 186. According to this method, the heats of solution of unhydrated and hydrated cements are measured by dissolving them in a mixture of nitric acid and hydrofluoric acid. The heat of hydration is calculated by subtracting the heats of solution of hydrated and unhydrated cement.

This method suggests testing the heat of hydration of cement pastes at 7 and 28 days. Before dissolving in the acidic solution, the pastes should be ground so that it passes through No. 200 sieve. This implies that the cement paste should gain enough rigidity to be ground, which means the method can only be applied on hardened cement pastes. Although the heat of solution method is a reliable method for hardened cement paste as long as carbonation and loss of moisture is prevented during the grinding process, it is not possible to observe the heat of hydration of cement at early ages, i.e. the method is not appropriate for monitoring the hydration process.

### Adiabatic or Semi-Adiabatic Calorimetry:

In the adiabatic method, the temperature rise in the specimen during the hydration process is measured. In order to measure the temperature rise in the specimen due to the heat of hydration, the specimen should be well insulated so that no heat can flow from the system. As the sample cannot exchange heat with the surrounding, the heat of hydration will be completely transformed into the temperature rise of the specimen. However, in order to convert the temperature rise to the heat of hydration of the cement, the specific heat of the sample should be known. The heat capacities of the specimen and the system components must be determined separately (RILEM TC119-TCE1, 1997).

This method can be applied not only to the cement paste but also to the concrete specimens. Additionally, using the adiabatic method, the heat of hydration measurements can start just after mixing and placing, there is no need to wait until the material hardens as in the case of heat of solution method. However, still the need of knowledge about the specific heat of the material is a disadvantage.

The semi-adiabatic method is also known as the Langavant Calorimetry. In semi-adiabatic method, the heat generated during the hydration process of cement is measured by using a thermally isolated bottle. This method is mentioned in Spanish and French standards (Sanchez et al., 1993).

### Isothermal Conduction Calorimetry:

The isothermal conduction calorimeter method is described in NT Build505. In this method, the specimen and the environment are kept at an isothermal temperature of 20°C and the heat of hydration of cement is measured directly by monitoring the heat flow from the specimen by comparing it with the heat flow from the reference material. In the calorimeter, the heat produced in the sample is measured as it conducts away from the sample. Therefore, the test should be done at constant

temperature and during the test the temperature increase in the sample should be a negligible amount.

A small amount of cement is mixed with water and placed in the calorimeter as soon as possible. Then the thermal power from the sample is measured, the data is acquired at sufficiently short time intervals continuously for 3 to 7 days. However, the method is reported to be not suitable for measurements beyond 7 days. The heat of hydration is calculated by taking the integral of measured heat flow which is the rate of heat of hydration with respect to time.

A schematic representation of rate of heat of hydration of cement paste obtained by isothermal conduction calorimetry is given in Figure 2.1.

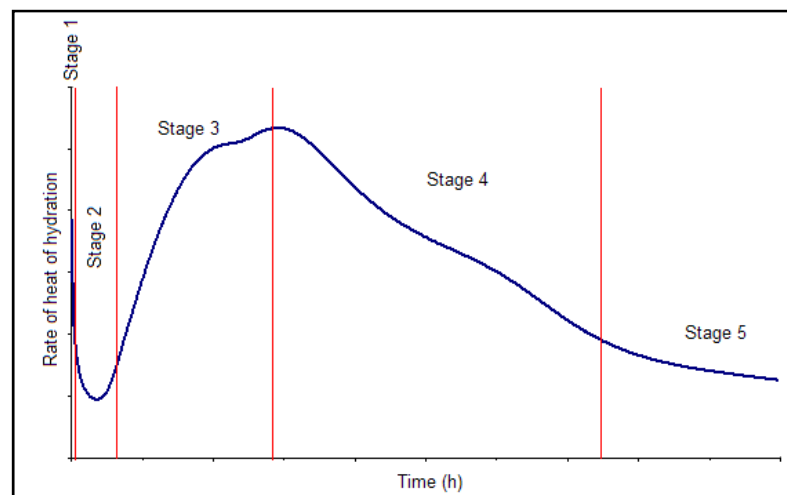


Figure 2.1. Schematic representation of rate of heat of hydration of portland cement paste obtained by isothermal conduction calorimetry (Mindess and Young, 1981)

In the rate of heat of hydration curve, the five stages of hydration described above are shown. Several peaks are seen in rate of hydration curves. The first initial peak observed within minutes just after mixing with water indicates the rapid hydration of  $C_3S$  and  $C_3A$  in the pre-induction period. The minimum point occurs in the

dormant period, in which the hydration is slowed down. Thereafter, a main peak is observed which is probably due to the hydration of  $C_3S$  and the formation of C-S-H phase. This main peak occurs in the acceleration stage of hydration. In most cements, a second peak is observed. Renewed Aft is probably the reason of this second peak. A third peak may also be formed as the result of Aft-AFm conservation during the cement hydration. As time proceeds the rate of hydration heat slows down and reaches very small values which is described as the post-acceleration stage of hydration (Odler, 2005; Young et al., 1998).

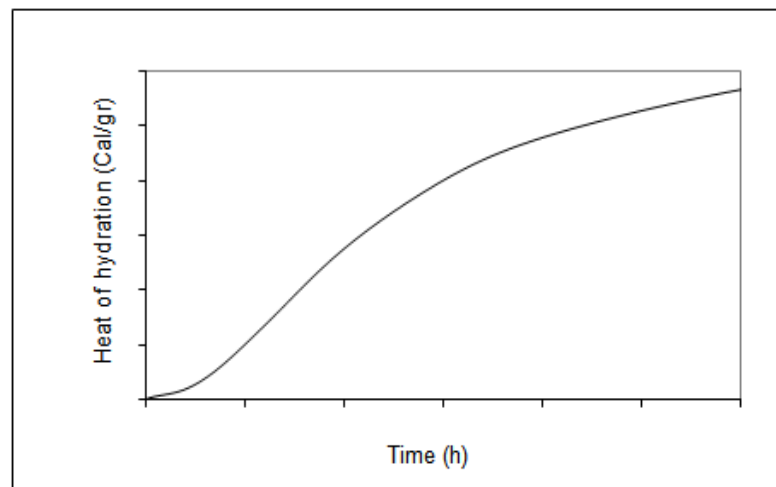


Figure 2.2. Schematic representation of heat of hydration of portland cement paste obtained by isothermal conduction calorimetry

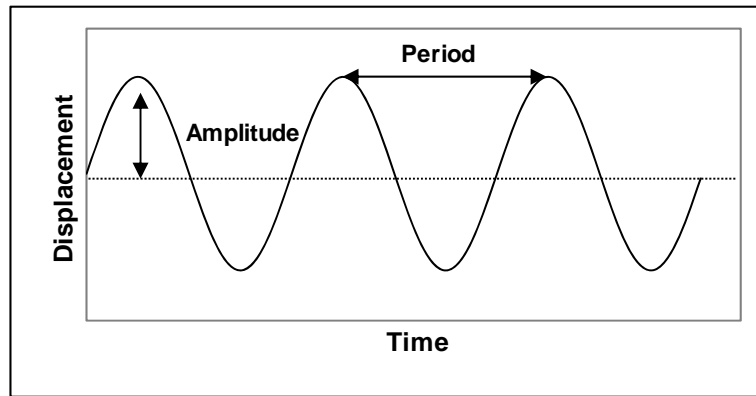
The heat of hydration of cement is calculated by integrating the area under the rate of hydration curve. A typical heat of hydration curve for portland cement paste is given in Figure 2.2. As seen from Figure 2.2, heat of hydration of cement paste increases with time and approaches an asymptotic value at later ages.

## 2.2 Ultrasonic Testing Method

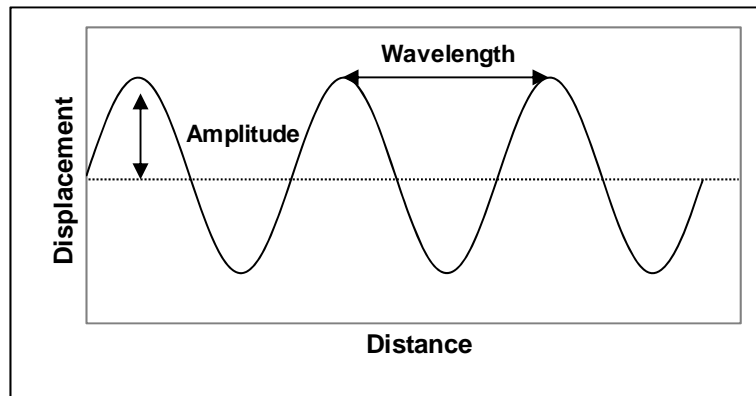
### 2.2.1 Basic Elements of Ultrasonic Waves

A wave is defined as “a periodic disturbance or variation of a physical quantity, e.g. electric or magnetic intensity or air pressure, by which energy is transferred progressively from one point to another either through space or through a physical medium, e.g. water or air, by transient local displacement of the particles of the medium but without its permanent movement” (Penguin English Dictionary). Simply, a wave is the oscillation of discrete particles in a material through which it is propagating like the movements created in still water when a piece of stone is dropped. As also seen in the definition, in a wave, the propagating part is not the particles, but the energy.

The waves are represented by some parameters; amplitude, wavelength, and frequency. In order to describe the mentioned parameters, consider a periodical sinusoidal waveform as shown in Figure 2.3. The amplitude,  $A$ , is the maximum displacement of the particles. As seen in Figure 2.3-a, the distance between the two crests of the wave is the period,  $T$ , which means that it is the time for a complete cycle. Number of cycles in one second is the frequency,  $f$ , which is the reciprocal of  $T$ . When the wave is considered in space domain as in Figure 2.3-b, the distance between two crests of the wave gives the wavelength,  $\lambda$ . (Malhotra and Carino, 2004; Mehta and Monteiro, 2006):



(a) Time domain



(b) Space domain

Figure 2.3. Basic elements of a wave

For a given homogeneous medium, the velocity of sound or ultrasound is typical for that medium. The frequency ( $f$ ) and wavelength ( $\lambda$ ) are related with velocity ( $V$ ) as given in Equation (2.5):

$$V = \lambda * f \quad (2.5)$$

As seen in Equation (2.5), higher frequencies will result in shorter wavelengths. This fact permits to arrange the wavelength by changing the frequency so that the medium can behave as a homogeneous material.

### 2.2.2 Wave Propagation Theory

When the surface of a large solid elastic body is influenced by a dynamic load, three types of stress waves (or mechanical waves) are created; longitudinal waves (compressional or primary waves), transverse waves (shear or secondary waves) and Rayleigh waves (surface waves). These waves propagate through the solid medium as the sound waves do in air (Malhotra and Carino, 2004). The only difference between a sound wave and an ultrasound wave is the frequency range. The ultrasonic waves have higher frequency which is above the limits of the human ear, i.e. above 20 kHz.

These three types of waves differ in the direction of motion and the velocity of the wave. In longitudinal waves, the particles move in a direction parallel to the wave propagation, while in transverse waves, the particles move perpendicular to the direction of wave propagation. On the other hand, in Rayleigh waves the particles on the surface move in a counter clockwise direction on an elliptical path. The particle motion for the different wave types are shown in Figure 2.4.

Transverse waves cannot propagate through liquids, because the shear stresses cannot be formed in fluids. On the other hand, longitudinal waves can propagate both in solids and liquids (Krautkrämer, 1983).

Among these three types of waves, longitudinal waves are the fastest. This is the reason why they are called the primary waves, because, they are the first type of waves that arrive at a point within the medium. Transverse waves arrive secondly, hence called secondary waves. Surface waves are the slowest. As an example, in a good quality concrete, the longitudinal wave velocity is about 4500 m/s, the transverse wave velocity is 2700 m/s (about 60% of primary wave velocity) and the Rayleigh wave velocity is 2500 m/s (about 55% of primary wave velocity) (Malhotra and Carino, 2004).

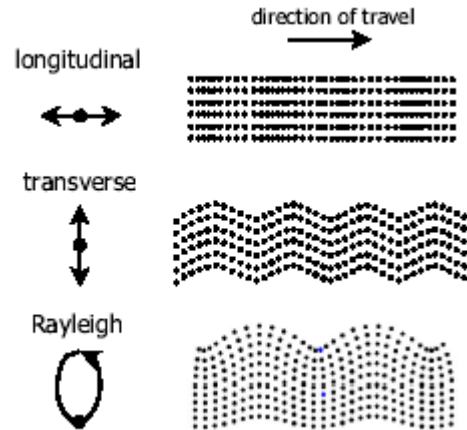


Figure 2.4. Particle motion for different wave types (Voigt et al., 2001)

The velocity of a wave through a medium depends on the elastic properties and density of the material through which it propagates. The mathematical expressions for wave velocity according to the wave type are given below in terms of the material properties for an infinite, elastic, homogeneous and isotropic material (Malhotra and Carino, 2004, Mehta and Monteiro, 2006):

$$V_L = \sqrt{\frac{E}{\rho} \frac{(1-\mu)}{(1+\nu)(1-2\nu)}} \quad (2.6)$$

$$V_T = \sqrt{\frac{E}{\rho} \frac{1}{2(1+\nu)}} = \sqrt{\frac{G}{\rho}} \quad (2.7)$$

where;

$V_L$ : longitudinal wave velocity (m/s)

$V_T$ : transverse wave velocity (m/s)

$\rho$ : density ( $\text{kg/m}^3$ )

$E$ : Modulus of Elasticity ( $\text{N/m}^2$ )

$G$ : Modulus of Shear ( $\text{N/m}^2$ )

$\nu$ : Poisson's ratio

When a wave comes to a boundary which can be an inhomogeneity within the medium or an interface between two different materials, it partially passes to the other part and partially reflects back. While passing through the boundary, it changes its direction depending on the acoustic properties of the materials. The part of the wave that penetrates to the other side with a different angle is termed the refracted wave. In the reflection and refraction phenomena, the reflection angle is same as the incident angle as in the reflection of light rays. The refraction angle depends on the incident angle and the velocity ratios of the two materials (Malhotra and Carino, 2004).

Although the geometry of reflection of stress waves is analogous to the geometry of light rays, it differs from that of light rays in the manner that the waves can change mode during reflection. The mode conversion can also occur during refraction.

The reflection and refraction of a P-wave at an oblique plane is shown in Figure 2.5. The incident P-wave strikes the interface with an incident angle of  $\theta$ , which is the angle between the longitudinal beam and the normal of the surface. Part of the incident wave can reflect back as P-wave with the same angle of  $\theta$ , and can partially reflect back as S-wave with an angle of  $\theta_s$ , which is smaller than  $\theta$  as the speed of S-wave is always less than the speed of P-wave. The incident wave can also refract as P-wave with an angle of  $\beta_p$  and as S-wave with an angle of  $\beta_s$ . In refraction again the  $\beta_p$  will always be greater than  $\beta_s$  due to the same reason (Malhotra and Carino, 2004).

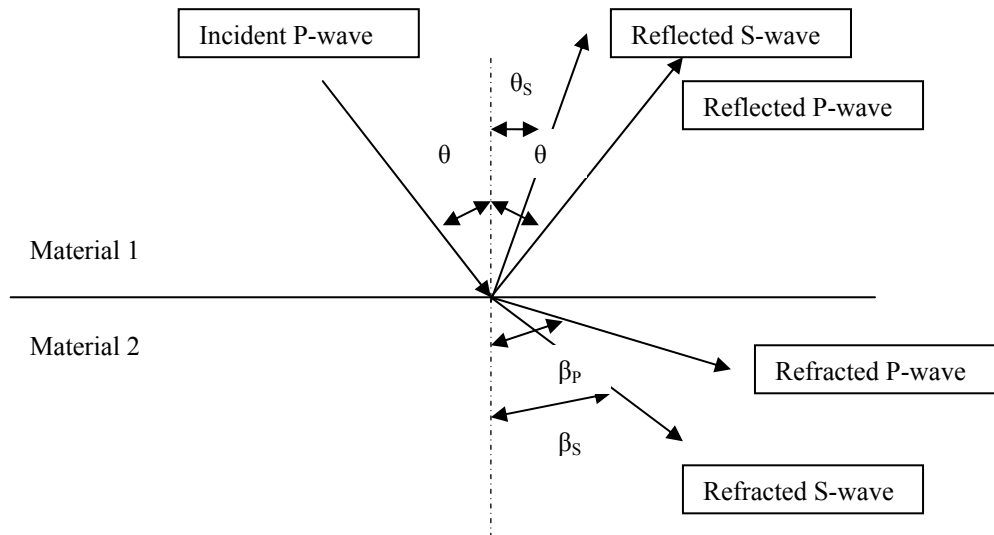


Figure 2.5. The reflection and refraction of a P-wave with mode conversion (adopted from Malhotra and Carino, 2004)

The relation between the wave speed in the materials and the angles obey Snell's law which is defined below in Equation (2.8):

$$\frac{\sin \theta}{V_{P1}} = \frac{\sin \theta_s}{V_{S1}} = \frac{\sin \beta_p}{V_{P2}} = \frac{\sin \beta_s}{V_{S2}} \quad (2.8)$$

where;

$\theta$ : incident angle

$V_{P1}$ : longitudinal velocity of Material 1

$\theta_s$ : reflection angle in S-wave mode

$V_{S1}$ : shear velocity of Material 1

$\beta_p$ : refraction angle in P-wave mode

$V_{P2}$ : longitudinal velocity of Material 2

$\beta_s$ : refraction angle in S-wave mode

$V_{S2}$ : shear velocity of Material 2

The portion of the wave which will reflect at the boundary depends on the specific acoustic impedances of the two materials. When the incident angle equals to zero, i.e. the wave beam is normal to the boundary, the amplitude of the reflected angle will be the maximum (Malhotra and Carino, 2004). The ratio of the amplitude of the reflected wave to the amplitude of the incident wave is known as the wave reflection factor (WRF). As the acoustic impedance equals to the density times velocity of the ultrasonic wave through the medium, the WRF is calculated according to the following equation:

$$WRF = \frac{Z_2 - Z_1}{Z_2 + Z_1} = \frac{V_2\rho_2 - V_1\rho_1}{V_2\rho_2 + V_1\rho_1} \quad (2.9)$$

where:

WRF: wave reflection factor

$Z_1$ : acoustic impedance of Material 1

$Z_2$ : acoustic impedance of Material 2

$V_1$ : velocity in Material 1

$V_2$ : velocity in Material 2

$\rho_1$ : density of Material 1

$\rho_2$ : density of Material 2

As seen in equation (2.9), if the acoustic impedance of Material 1 is greater than the acoustic impedance of Material 2, the wave reflection factor will be negative. This negative sign implies a change in the mode of the wave, which means a longitudinal wave reflects as a transversal wave or vice versa. If the acoustic impedance of Material 2 is greater than that of Material 1, no change in mode occurs (Malhotra and Carino, 2004).

During the propagation of the wave through the medium, its energy decreases. This loss of the energy is known as attenuation. The loss of energy shows itself as a decrease in the amplitude as shown in Figure 2.6.

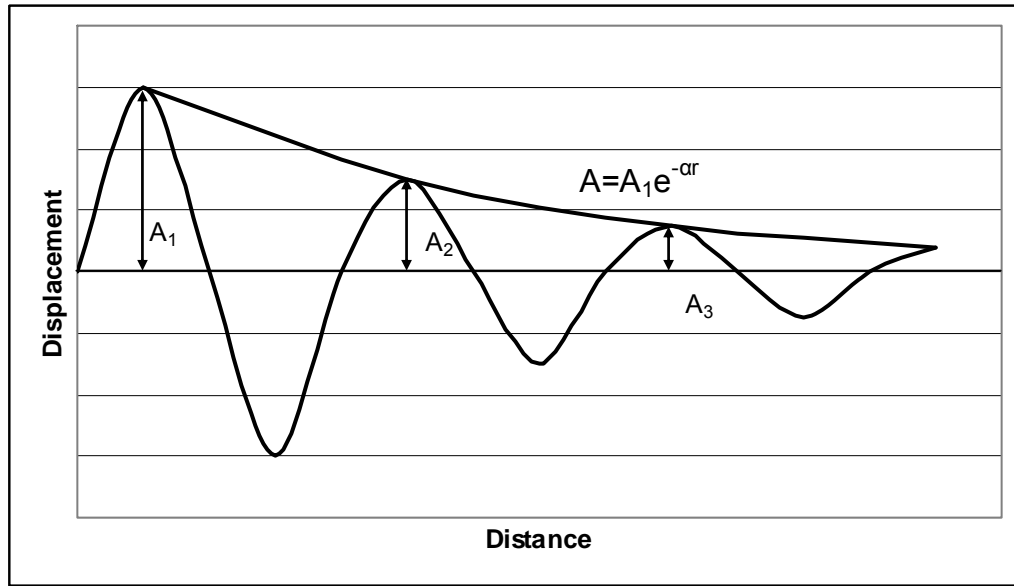


Figure 2.6. Attenuation of a wave while propagating in a medium

The attenuation of the sound pressure consists of two components as geometric divergence and energy dissipation (Krautkrämer, 1983). Travelling away from the source results the divergence of the sound beam. Energy dissipation may be due to the scattering which is mainly caused by non-homogeneity of the material and absorption which is mainly caused by the internal friction and is a loss of energy as heat (Tharmaratnam and Tan, 1990).

The attenuation can be calculated from the decrease of the amplitude by the ratio of the amplitude or by fitting a logarithmic curve to the peak points as seen in the Figure 2.6. For the determination of attenuation, the following equation is used:

$$A = -20 * \log \frac{A_2}{A_1} \quad (\text{dB}) \quad (2.10)$$

In Equation (2.10),  $A_2$  is the first pulse amplitude of the medium and  $A_1$  is the initial amplitude (Tharmaratnam and Tan, 1990).

Attenuation can also be determined as following:

$$A = \frac{1}{L} * \ln \frac{A_m}{A_r} \quad (2.11)$$

In Equation (2.11), L is the length of the material,  $A_m$  is the amplitude of the measured signal and  $A_r$  is the amplitude of the reference signal. For the determination of reference signal, a shorter sample of the same material or a low-attenuating material can be used as a reference material. When a shorter sample of the same material is used, the length difference between the original sample and the shorter sample should be taken as L in the equation (Kaczmarek, 2001).

### **2.2.3 Ultrasonic Testing of Hardened Concrete**

Ultrasonic pulse velocity test method was started to be developed for testing concrete at about the same time in England and Canada and the method has been applied on hardened concrete at construction sites since 1960s (Malhotra and Carino, 2004). There are several applications (Malhotra and Carino, 2004) of the method in concrete technology such as uniformity and quality control, flaw and crack detection, deterioration estimation. Although there is no physical relation between strength and ultrasonic pulse velocity, the method can be used to estimate the strength of concrete from previously establishing graphical correlations for the specified concrete. The method is suitable for the homogeneity and quality control of a structure. Measuring the ultrasonic pulse velocity with time, the effect of environmental factors such as freeze-thaw, sulphate attack, etc. can be established. The method can also be used to detect the cracks within the structure and the depth of cracks. As the ultrasonic pulse velocity test is related to the elastic properties, the dynamic modulus of the material can be estimated from pulse velocity measurement if the density and Poisson's ratio are known. One of the recent

studies about the ultrasonic pulse velocity is to study the hydration of cement which will be discussed in detail in the next chapter.

The test method is described in ASTM C 597, “Standard Test Method for Pulse Velocity Through Concrete”. The principle in ultrasonic testing is to generate stress wave pulses and measure the travel time of the stress wave through the medium. The ultrasonic pulse velocity (UPV) is calculated by dividing the travel distance to the travel time:

$$V = \frac{L}{t} \quad (2.12)$$

where;

V: ultrasonic pulse velocity (m/s)

L: travel distance (distance between the receiver and the transmitter) (m)

t: time for travel of the ultrasonic pulse (s)

A schematic representation of test equipment is shown in Figure 2.7. As also seen from the figure, the test apparatus consists of several units such as a pulse generator, a receiver, a transmitting transducer, a receiving transducer, a time measuring circuit, a time display unit and connecting cables. The transmitting transducer sends the pulse wave and the receiving transducer receives the pulse wave, the time between transmitting and receiving is measured and displayed in the display unit. The accuracy of the method depends on the accuracy of measuring the travel path and travel time. For measuring the travel time accurately, a full contact should be supplied between the transducers and the specimen. Otherwise, the air pockets between the transducers and the specimen may lead to error in travel time reading. In order to have a full contact, a coupling agent such as oil, petroleum jelly or grease is applied between the transducers and the surfaces of the specimen.

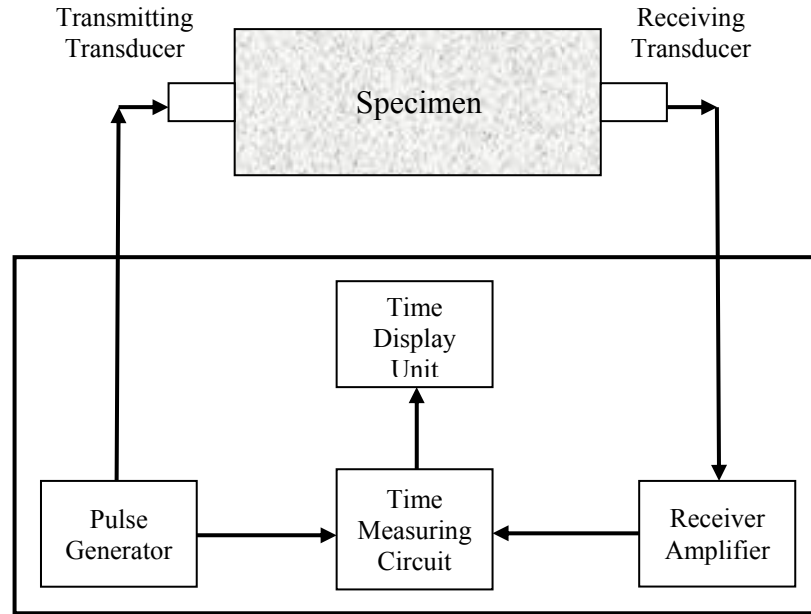


Figure 2.7. Schematic representation of ultrasonic apparatus (ASTM C 597)

While measuring the UPV of a test specimen, the transducers can be placed in three different arrangements as shown in Figure 2.8.

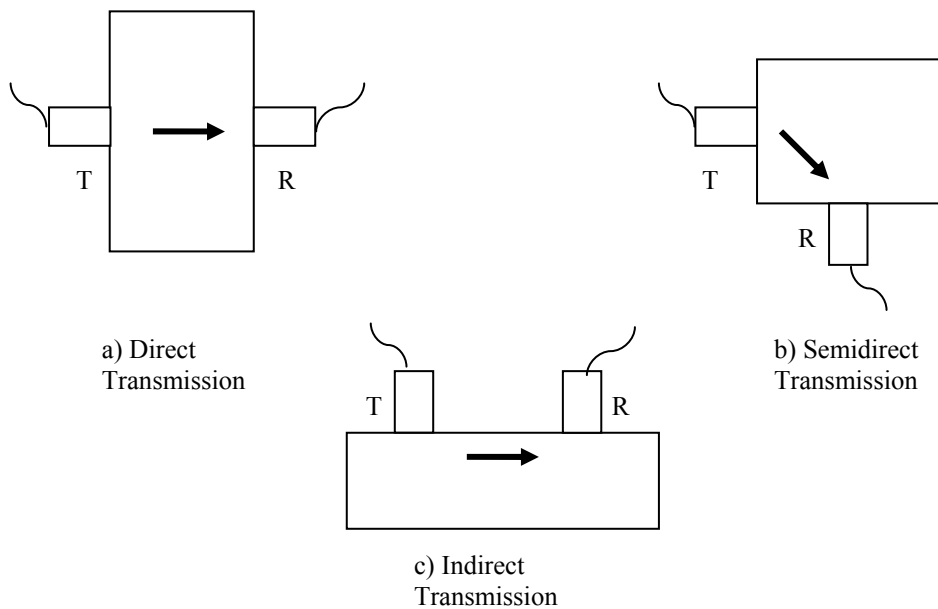


Figure 2.8. Arrangements in placing transducers

When the transducers are placed directly opposite to each other on opposite surfaces of the specimen, the energy of the pulse transmitted between transmitter and the receiver is the maximum. Therefore, direct transmission which is shown in Figure 2.8-a is the most preferred arrangement (Malhotra and Carino, 2004). However, when the distance between the transducers is too far, due to the attenuation, the signal may be weakened and might not be detected by the receiver. The semi-direct transmission is less sensitive and accurate compared to direct transmission. On the other hand, indirect transmission shall not be used unless only one face of the structure is available as this type of arrangement is the least sensitive and accurate and additionally, this method may give information about only the surface layer (ASTM C 597). When indirect transmission has to be applied, the transmitter is fixed at a point and the receiver is placed at different distances. After several measurements are taken, the reciprocal of the slope of the transit time versus travel path graph gives the velocity. If there is a layer of different characteristics, it can be detected from the change of slope, because, when the stress wave passes also through the second layer, then the travel time will be affected both by the velocity of first and second layers.

There are several factors that affect the ultrasonic pulse velocity measurements in a concrete specimen. Some of them are related directly to the concrete properties and the others are test conditions. These factors are listed and discussed briefly below (ASTM C 597; Neville, 2003; Malhotra and Carino, 2004; and Mehta and Monteiro, 2006):

Amount and type of aggregate:

Aggregates make up approximately 75 % of the concrete volume. The ultrasonic pulse velocity of aggregates is generally higher than that of cement paste. As a result, the amount and type of aggregate in concrete obviously affects the UPV value of concrete significantly.

#### Cement Type:

Actually, cement type does not directly influence the UPV of concrete, but the rate of hydration, which is affected by cement type, is related to the pulse velocity. As the degree of hydration increases, the elastic modulus increases which means the UPV increases.

#### Water/Cement (w/c) Ratio:

Water/cement ratio affects the modulus of elasticity. It is also related to the porosity of the concrete specimen. As the w/c ratio increases, the compressive strength and the ultrasonic pulse velocity of the concrete decreases.

#### Age of Concrete:

As the hydration of cement proceeds with time, the porosity of the concrete decreases and the ultrasonic pulse wave propagates faster through the concrete body. The behaviour of pulse velocity with age is similar to behaviour of strength with age. It increases rapidly at the beginning but later reaches an asymptotic value. However, UPV reaches its asymptotic value much earlier than the strength.

#### Moisture Condition:

When the concrete is saturated, the ultrasonic pulse velocity will be higher. If the pores in the concrete specimen are dry, then the wave cannot propagate and have to travel around the pores which results in increase in path length and the velocity seems to decrease. However, if the pores are filled with water, the stress wave will propagate through the water and the velocity will not decrease as in the dry case.

#### Temperature of Concrete:

The ultrasonic pulse velocity is reported not to be affected from a change in temperature as long as the temperature stays in the range of 5 and 30 °C.

### Transducer Contact:

The contact between the transducer and the specimen is important in measuring the pulse velocity correctly. If there exist air pockets between the contact surfaces, the total wave energy cannot be transmitted and the measurements can be erroneous. In order to improve the contact, coupling agents are used.

### Path Length:

Theoretically, the path length does not affect the pulse velocity. However, in practice, due to the near-field effect, which will be discussed in the next section, shorter path lengths give more variable thus less accurate results. Additionally, due to the attenuation, very long path lengths will also cause inaccuracy as most of the energy is lost during the propagation.

### Size and Shape of the Specimen:

The ultrasonic pulse velocity is known to be independent from the shape and the size of the specimen. However, Equations (2.6) and (2.7) are only valid for infinite, homogeneous and elastic materials. The vibrations of the particles caused by wave propagation are so small that the concrete is in the elastic range. The homogeneity of the specimen can be achieved by using the proper frequency range. If the wavelength is larger than the maximum particle dimension, then the material is accepted as a homogeneous material. For having an infinite specimen, the minimum lateral dimension of the test specimen should again be greater than the wavelength of the stress wave.

### Micro-cracking:

Microcracks develop in the concrete due to the environmental conditions or the stress level above the 50% of the ultimate strength. The presence of microcracks reduces the modulus of elasticity and as a result, reduces the wave velocity of the concrete.

### Presence of Reinforcing Steel Bars:

The ultrasonic pulse wave velocity is higher in steel than in concrete. Therefore, the presence of steel bars in the vicinity of the measurement point will lead higher velocity readings.

### **2.2.4 Near-Field and Far-Field Concepts**

One of the important points about the path length is a phenomenon called near-field/far-field effect. In the transducer, the pulse is generated at multiple points on the crystal. As the wave from each piece of crystal travels through the medium, they eventually merge to form one wave. The region after this unification is called far-field. However, within the region in front of the far-field, the waves may interfere with each other at some points. This region is known as near-field, and the inspection in the near-field cannot be trusted and should be avoided (Houf, 2003). The near-field/far-field concept is shown schematically in Figure 2.9.

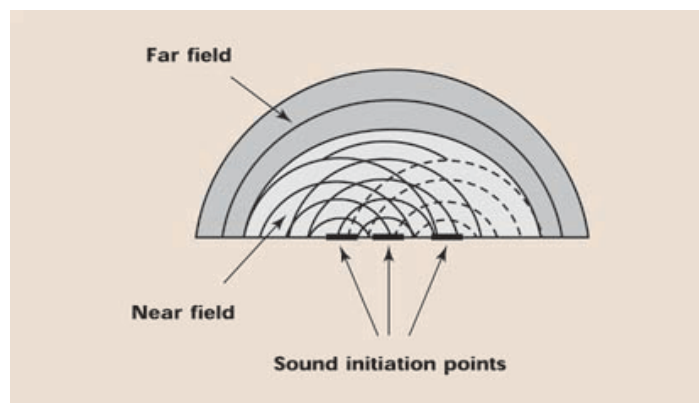


Figure 2.9. Near-field/Far-field concept (Houf, 2003)

The length of near-field region depends on frequency and the diameter of the transducer:

$$N = \frac{(D^2 - \lambda^2)}{4\lambda} \quad (2.13)$$

where;

- N: near-field length (m)
- D: diameter of the transducer (m)
- $\lambda$ : wavelength of the stress wave (m)

Therefore, as the velocity changes, length for near-field also changes. The calculated values of near-field zone for two different frequency transducers of 54 and 150 kHz at different velocity levels are given in Table 2.1.

Table 2.1. Near-field zone for different velocity levels

Frequency: 54 kHz (D=50mm)			Frequency: 150 kHz (D=25mm)		
Velocity (m/s)	Wavelength (m)	Near-field (mm)	Velocity (m/s)	Wavelength (m)	Near-field (mm)
4000	0.074	-10.0	4000	0.027	-0.9
2000	0.037	7.6	2000	0.013	8.8
1000	0.018	30.2	1000	$6.667 \cdot 10^{-3}$	21.8
500	$9.259 \cdot 10^{-3}$	65.2	500	$3.333 \cdot 10^{-3}$	46.0
200	$3.704 \cdot 10^{-3}$	167.8	200	$1.333 \cdot 10^{-3}$	116.9
100	$1.852 \cdot 10^{-3}$	337.0	100	$0.667 \cdot 10^{-3}$	234.1

As seen from Table 2.1, near-field can be very large when the pulse velocity is small and the diameter of the transducer is large which means the frequency is small. However, for high velocity values, the near-field/far-field concept does not seem to cause a problem. As the path length is a part of this concept, the effect of path length may be an important research topic in ultrasonics.

## **CHAPTER 3**

### **LITERATURE SURVEY ON WAVE PROPAGATION TECHNIQUES FOR FRESH CEMENTITIOUS MATERIALS**

#### **3.1 General**

The phase change of cement paste from fresh state to hardened state is a continuous process. The hydration reactions start just after the cement and water come into contact. The amount of hydration products increases with time and the medium transforms from a liquid suspension to a porous solid after setting and hardening processes.

Traditional test methods for fresh cementitious materials like Vicat and Penetrometer tests, do not take the continuous character of setting and hardening into consideration, but only a short time period of hydration process can be controlled by these tests. For the continuous monitoring of the hydration process at early ages, various non-destructive test methods may be utilized.

The continuous monitoring and quality control of fresh concrete is important during construction for determining the construction speed, and obtaining the desired properties in the hardened state. Therefore, the investigations for new and non-destructive test methods on fresh concrete have increased over the last decade. RILEM established a Technical Committee on “Advanced testing of cement based

materials during setting and hardening” (TC 185 ATC) in 1999. This committee published a report about several techniques to monitor the setting and hardening processes of fresh cementitious materials (RILEM Report 31). These methods can be listed as nuclear magnetic resonance, electrical methods, acoustic emission method, maturity method, radon exhalation method and methods based on wave propagation. The methods which are based on wave propagation are impact-echo, vibroscope, wave reflection and through transmission methods. In impact-echo method, longitudinal waves are observed, in vibroscope, shear and longitudinal waves are measured simultaneously, in wave reflection method mostly shear waves are used and in through-transmission method both the longitudinal and shear waves can be applied separately. More detailed information about the methods based on wave propagation will be given in the following sections.

### **3.2 Impact-Echo Method**

Impact-echo method is a non-destructive test method which uses transient stress waves to detect the internal flaws in concrete or the thickness of the concrete element. The method is also used to measure the P-wave velocity if the dimensions of the concrete element are known. On the surface of the concrete specimen, a stress wave with low-frequency is generated by an impact of a steel ball, and at a point adjacent to the impact point, the surface displacements are obtained by a transducer. The stress waves are reflected when they touch a boundary. From the multiple reflections between the flaw or external surfaces and the surface of impact, information about the flaws inside the concrete or the dimensions of the structure is detected from the amplitude-frequency curves (Sansalone, 1997).

Pessiki and Carino (1988) evaluate the applicability of the impact-echo technique to fresh concrete to determine the setting time and to monitor the strength development. As it was not possible to apply impact directly on the fresh concrete, thick plastic plates were placed on the surface for applying impact with sphere balls

and placing the transducer. By knowing the thickness of the specimen, the velocity of the stress wave is calculated as follows:

$$C_p = 2 * f_p * T \quad (3.1)$$

where;

$C_p$  : P-wave velocity

$f_p$  : the peak frequency

T : thickness of the specimen

They applied the tests directly on the concrete and on mortar sieved from the concrete. The setting time was also determined according to ASTM C 403 from the mortar sieved from the concrete. Concrete samples of two different w/c ratios were tested. As the result of the investigation, the initial setting time was defined as the point where the P-wave velocity begins to increase or where a specified P-wave velocity is reached. Additionally, a relation between early strength and P-wave velocity was also reported.

The method was applied to concrete to investigate the early-age strength in several researches. Pessiki and Johnson (1996) estimated the early-age strength in plate elements using impact-echo test method applied directly on the slab and on the core elements taken from the slab. It was concluded that the method could be applied successfully at very early ages. Pessiki and Rowe (1997) investigated the effect of reinforcing bars on the velocity of longitudinal waves at early-ages. According to this study, the presence of reinforcing steel bars only increases the measured velocity by about 100 m/s which do not hinder the successfulness of the method. Irwin and Pessiki (2004) applied the impact-echo method to measure the early-age mechanical properties of precast concrete elements. From the obtained strength-age curves and strength-velocity curves, it is concluded that the P-wave velocity is more sensitive to concrete strength at early ages compared to later ages.

Impact-Echo testing method is also one of the topics in RILEM Report 31. An experimental set-up was developed for testing fresh cementitious materials. The set-up is shown in Figure 3.1. Specimens of different thicknesses were tested at 10-minute time intervals. The results showed that as time passes and the hydration progresses, the frequency increases. As a conclusion, it is said that the impact-echo technique can be used to improve the existing techniques of through transmission or reflection. The advantage of the method is that access to only one side of the specimen is sufficient. However, the method needs more reliable impact generation.

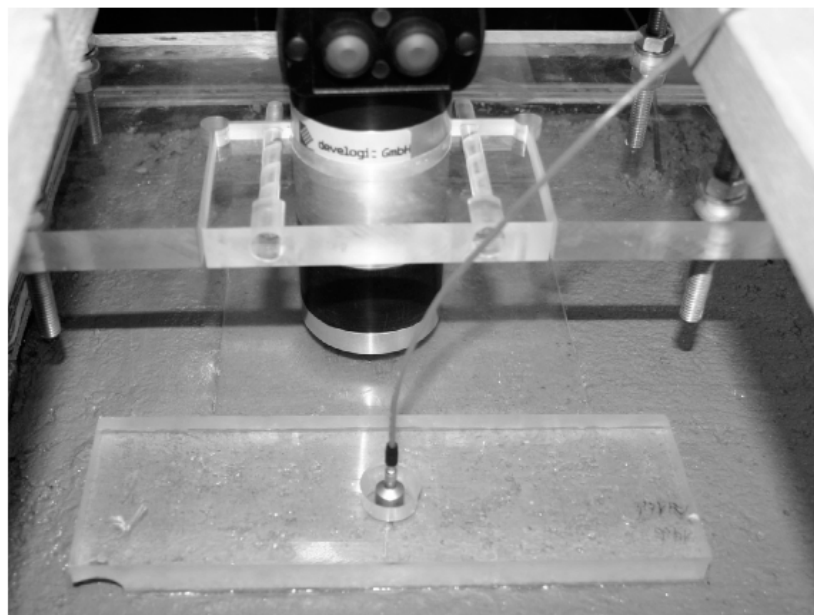


Figure 3.1. Experimental set-up for impact-echo developed for testing fresh concrete (RILEM Report 31)

### 3.3 Vibroscope

A vibroscope is an apparatus which allows studying the longitudinal and transversal waves at the same time in the same specimen. By a vibroscope, wave velocity in transmission is determined. The difference of vibroscope from ultrasonic measurement is the range of frequency used. A vibroscope is a vibratory

test which uses low frequencies of order 20 Hz - 1 kHz (RILEM Report 31). The reason for low frequency is the heterogeneity of the material. Fresh cementitious materials are very attenuative due to the presence of air bubbles. If the wavelength is smaller than the diameter of the bubbles, the wave scatters at the heterogeneities. Therefore, low frequencies are preferred to obtain high wavelengths.

The compressional waves show the macroscopic variations in the compressibility during the phase change from liquid to solid. On the other hand, transversal waves directly show the shear properties of the material (RILEM Report 31).

In the vibroscope device three dynamic pressure transducers are used so that the tridimensional behaviour of the material can be investigated (Boutin and Arnaud, 1995). These transducers are embedded in the material. Two transducers are placed in the direction of wave propagation and the third transducer is placed in the direction perpendicular to the wave propagation for compressional waves (Boutin and Arnaud, 1995). Same type of transducers are placed in the material along the main stress directions, i.e. with an inclination of  $\pm\pi/4$  with respect to the direction of the wave propagation, for shear waves. The material is tested in an adiabatic environment not to disturb the kinetics of the hydration reactions (RILEM Report 31). A schematic representation of a vibroscope device is shown in Figure 3.2.

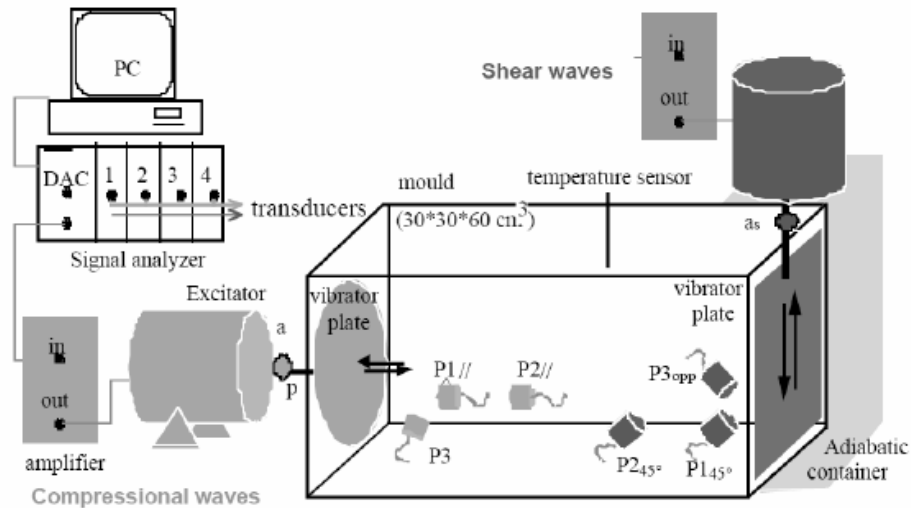


Figure 3.2. A schematic representation of Vibroscope (RILEM Report 31)

Boutin and Arnaud (1995) used a vibroscope to study the mechanical characterization of crude cellular concrete during setting. The characteristic of cellular concrete is the high heterogeneity level due to the air bubbles. The manufacturing procedure of cellular concrete is composed of three steps. In the first step, sand mud, cement, quick lime and aluminum powder are mixed and poured in the container. In the second stage, hydrogen is released, the diameter of air bubbles increases up to 1 mm and the temperature increases as the result of the crystallization of quick lime, and at the end of this step the paste transforms from liquid to solid. As the last stage, the material is placed in an autoclave to obtain the final product. By vibroscope the velocity, damping coefficient and the ratio of normal stresses in two orthogonal directions were determined in the research. The damping coefficients were determined from the pressure levels on the transducers. In the first stage very low values for velocity were obtained, while in the second stage velocity increased rapidly. The transition between these two steps which was considered as the setting could be obtained accurately by this method. Additionally, it was found out that in the first stage the damping ratios decreased and in the second stage, they increased. After obtaining good results in cellular concrete, the theory was applied to mortar and concrete, and it was concluded that the method is

appropriate in order to monitor the rheological properties of heterogeneous materials such as concrete.

Arnaud and Thinet (2000) used a vibroscope to test hydraulic concrete during setting. They prepared concrete mixtures at two different w/c ratios of 0.4 and 0.6 and cured specimens at three different temperatures of 10, 20 and 30 °C. The velocity and the damping coefficients were determined both for longitudinal and transversal waves. The change of these parameters was all consistent. From the velocity and damping ratio change with time, two phases were realized, the transition thought to be related to the threshold percolation. It was concluded that with this device it was possible to follow the mechanical evolution of the concrete qualitatively and to calculate the rheological parameters.

Arnaud (2004) tested cellular concrete, mortar, hydraulic concrete and cold bituminous mixes with a vibroscope to monitor the rheological properties during setting and hardening. Although they have very different characteristics, all of these civil engineering materials are common in their heterogeneity due to being composed of solid particles, binder, fluids and air bubbles. The wavelengths were chosen large as compared to the size of heterogeneity for all material, for example in mortar and concrete, the frequency for P-wave is 800 Hz and for S-wave is 100 Hz. Two different phases were observed from velocity-time curves. In the first phase the mechanical evolution was slow, whereas in the second velocity increased strongly. The transition between these phases was linked to the percolation threshold. Additionally, a characteristic time which describes the start of mechanical evolution by fitting an exponential function to the velocity-time curve was determined. When the exponential function was normalized with the initial velocity, similar curves were obtained for all mortar and concrete types tested.

The disadvantage of the method is the necessity of embedding the transducers in the material. This means the test should be stopped before the material hardens completely in order to remove the transducers. This time approximately

corresponds to a longitudinal velocity of 2000 m/s. However, at that moment the mechanical setting is not finished (RILEM Report 31). Therefore, after removing the transducers the test should be continued by another means of testing method such as ultrasonic wave propagation so that a complete picture of setting and hardening process can be obtained.

### **3.4 Wave Reflection Method**

The wave reflection method depends on the rule that an ultrasonic wave is partially reflected back and partially transmitted to the adjacent material when it meets a boundary while travelling through a material. In order to test fresh cement-based materials during setting, a buffer material is placed in the fresh concrete, and the reflection at the interface between the buffer material and the fresh concrete is observed. The wave reflection factor (WRF) which describes the amount of wave energy reflected at the boundary is calculated according to Equation (2.9).

The method is applicable to both shear and longitudinal waves. In the case of shear waves, all the wave energy is reflected back as the shear waves cannot propagate through liquid. Therefore, the WRF is unity just after the cement-based material is mixed with water. When the material changes into solid structure as the result of hydration, the WRF starts to decrease as the transversal wave starts to propagate through the medium. Later on, the WRF approaches an asymptotic value. On the other hand, in the case of longitudinal waves, the initial value of WRF is below the unity as the compressional waves can propagate through liquids as well as through solids. The WRF will remain constant initially, and then start to decrease until an asymptotic value as in the case of shear waves. However, it is reported for the wave reflection method that the shear wave reflection coefficient is more sensitive than that of longitudinal waves for testing the hydration of cement (RILEM Report 31).

The first application of this method to cementitious materials was in 1981 (Stepisnik et al. 1981). Quartz bar was used as the buffer material. It was reported that the method was sensitive to hydration process of cement paste at early ages.

Öztürk and collaborators (1999) used the method both for longitudinal and shear waves for observing the setting and hardening characteristics of plain concrete, and concretes containing admixtures of accelerator, retarder, superplasticizer and silica fume. They correlated the results with the heat of hydration and the times of initial and final setting. The bottom of the steel mold was used as the buffer material and a frequency range of 2-5 MHz were applied. It was concluded that the wave reflection factor was a good indicator for hydration behaviour of concrete mixtures containing different admixtures. The end of the induction period which was determined from temperature measurements was correlated to the time when the wave reflection coefficient started to decrease.

Using the wave reflection method, Rapoport and his friends (2000) investigated the wave reflection factor of shear waves for concretes containing admixtures such as accelerator, retarder, superplasticizer and silica fume. The temperature change in the concrete specimens, the initial and final setting times and the dynamic modulus were also determined. Three different parts were observed for each type of concrete from the WRF-time curves. Initially, the curve was constant at approximately unity. In the second stage, the WRF started to decrease. Finally, it reached an asymptotic value. The point where WRF started to decrease and the point where WRF started to approach the limiting value were determined and correlated with the critical points of hydration process. In order to determine the critical points of WRF curve, first derivative was used. However, differentiating at every point resulted in too much noise so that those points could not be determined accurately. As a new method, in the investigation, the derivative was taken for each sixth point. This means, the derivative of seventh point was determined by subtracting the first point from the thirteenth point. As the result of this study, it was concluded that WRF was sensitive to hydration and presence of admixtures. The point where

WRF started to decrease corresponded to the end of dormant period. At early age, WRF was dominated by setting action while at later ages, it was dominated by modulus development.

A nondestructive test method for investigating the setting and the hardening process of cementitious materials was developed at Northwestern University (Voigt et al. 2001). Steel was used as a buffer material. The steel plate was placed on the surface of the fresh concrete and the measurements were performed on the surface of the specimen. A broadband frequency range with a centre frequency of 2.25 MHz was used. The apparatus developed is shown in Figure 3.3.

The method was used not only to monitor the hydration process but also to estimate the compressive strength. A linear relationship was observed between the attenuation and early-age strength of concrete.

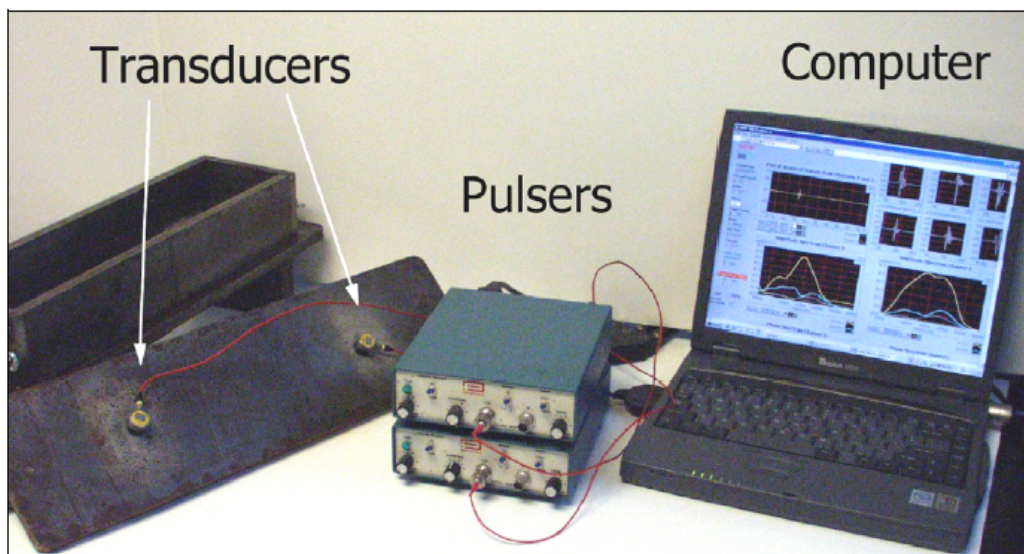


Figure 3.3. Apparatus for wave reflection of shear waves (Voigt et al. 2001)

Using the same apparatus, mortar and concrete specimens cured under different conditions were tested (Voigt et al. 2002). Constant curing conditions of 4, 22 and 30 °C and variable curing conditions were applied on the specimens. The

compressive strength values were determined from 12 hours to 3 days after mixing. The temperature development was also observed by embedding thermocouples in the specimens. It was concluded that the reflection between steel and hydrating mortar and concrete was sensitive to the hydration kinetics. The compressive strength development at early ages was linearly correlated with the attenuation for all curing conditions. It was also possible to predict the compressive strength for 3 days if a strength-attenuation relation could be established for the first hours. The repeatability of the method was also checked and a good repeatability in mortars was observed, however, in the case of concrete samples the repeatability was not good. This was explained as the result of non-homogeneity of concrete compared to mortar. In non-homogeneous materials the attenuation is not consistent due to local differences in w/c ratio, cement and paste content, and aggregate dispersion.

In another study, the relationship between the WRF and dynamic elastic modulus, compressive strength and the degree of hydration was investigated (Voigt, et al. 2003a). The dynamic elastic modulus was determined from the fundamental resonant frequency method and the ultrasonic pulse velocity, separately. Thermogravimetric analysis which determines the amount of non-evaporable water in the cement paste was used to obtain the degree of hydration. Mortar specimens of different w/c ratios were tested. The results revealed that all three parameters were linearly related to the WRF at early ages. The relation between compressive strength and reflection loss up to 4 days was composed of two lines, the transition point being dependent on the w/c ratio. The linear relationship with the degree of hydration showed that the reflection factor was highly sensitive to the microstructural changes of cement-based materials due to hydration process.

Voigt et al. (2003b) compared the wave reflection method for the application on cement mortar and concrete. The linear relationship between the reflection loss and early compressive strength was also obtained as the result of experiments applied. It was concluded that tests on mortar specimens were repeatable, almost unique relationship was obtained for the same mix. However, in the case of concrete

specimens, different relations were obtained for the same mix. Although the repeatability tests on concrete gave different final results for the wave reflection loss curves, the distinct points in the graphs occurred at the same points of time.

The effects of different curing conditions and mixture proportions were also explored to see the sensitivity of the wave reflection factor to the development of hydration process (Akkaya et al., 2003). Results similar to those of previous studies were obtained. Based on the slope of strength-reflection loss curve, a method for strength prediction was proposed. However, it was concluded that in order to estimate strength accurately, a calibration should be applied to strength-reflection loss relationship. Additionally, the inflection point of reflection loss curve which is the point with maximum slope was found out to be related with the initiation of compressive strength development.

Voigt and Shah (2004) studied the wave reflection on steel-mortar interface for mortars with different w/c ratios. Besides the WRF setting time, heat of hydration, compressive strength, dynamic shear modulus and degree of hydration were also determined for characterization of the hydration behaviour of the samples. Compressive strength tests were applied on 5 cm cube specimens. The setting time was determined according to ASTM C403. The temperature rise in the mortar specimens were obtained by semi-adiabatic calorimeter. The dynamic shear modulus was obtained by resonant frequency test, shear wave velocity and wave reflection methods, separately. Thermogravimetry was used for degree of hydration. According to the results obtained, it was seen that the adiabatic heat release and reflection loss were related as both parameters started to increase at the same time and followed similar trends. The bilinear behaviour of compressive strength and reflection loss relation was also observed. The transition time corresponded to the time when the character of compressive strength alters from power equation to hyperbolic equation. The dynamic shear values calculated by three different methods exhibited similar behaviour. The slope of degree of hydration-reflection loss curve was reported to be dependent on w/c ratio. Lastly, it

was concluded that the gel-space ratio and reflection loss had a unique relation for all mortars tested which means WRF is related to most of the fundamental physicochemical parameters of the cement-based materials.

Öztürk and colleagues (2006) used longitudinal wave reflection factor for monitoring the setting behaviour of cement pastes. Longitudinal wave reflection between cement paste and an acrylic glass plate was determined for the first 12 hours after mixing for different cement types. The obtained WRF values were normalized with the WRF between the acrylic glass and air in order to eliminate the influence of coupling condition of the transducer. The setting time of cement pastes were determined by Vicat needle. The heat evolution was also measured continuously with thermocouples. The effect of frequency range was also tested. For this purpose, center frequency of 200 kHz, 500 kHz and 1 MHz were applied for longitudinal wave reflection determination. It was concluded that the initial and final setting time could be detected accurately for all frequency ranges tested. By this method, the initial and final setting time of cement paste were reported to be obtained accurately. The initial setting time corresponded to the minimum of first numeric derivative of WRF, while the final setting time corresponded to the point where the first numeric derivative crosses the zero.

Labouret and friends (1998) used a different buffer material with longitudinal waves for determination of wave reflection coefficient. A right angled plexiglass prism as seen in Figure 3.4 was used as the buffer material. The reflection occurred twice within this reference material; therefore, the loss was related to the square of the reflection coefficient. The method was developed for the industrial processes. It was concluded that the method allowed following the setting characteristics of the medium. Although it was tested for cement and concrete, it was reported that the method can be used for other materials mechanical properties of which changed with time.

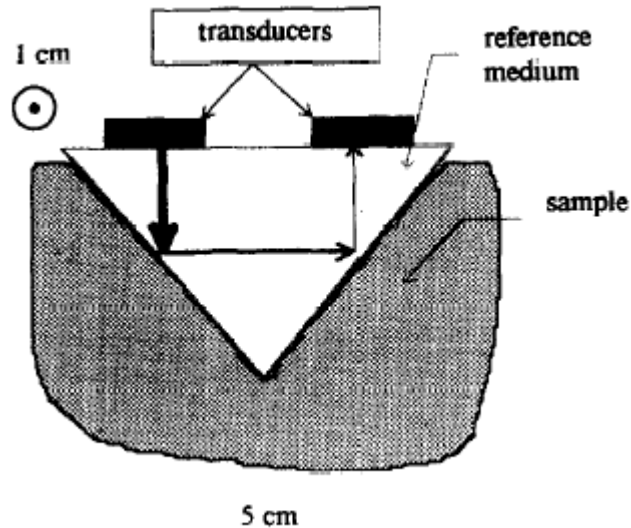


Figure 3.4. Apparatus for reflection factor determination of longitudinal waves (Labouret et al. 1998)

### 3.5 Wave Transmission Method

The basic principle of the wave transmission method is to measure the velocity of the stress wave travelling from one side of the specimen to the other side. Actually, the pulse is generated on one side of the specimen and the travel time of the pulse to the other side is measured. The ultrasonic pulse wave velocity is calculated by dividing the travel length to the travel distance. In a hydrating cement-based medium, initially the velocity is very low and the attenuation is very high due to the air bubbles. However, as the material starts to stiffen due to the hydration products, the wave velocity increases rapidly first and slowly later, approaching an asymptotic value. Typically S-curves are obtained in a hydrating cementitious material as velocity-time diagrams (RILEM Report 31).

The main difference between the vibroscope and ultrasound is the frequency range used. In the ultrasonic method, higher frequencies are preferred. As the frequency increases, the wavelength decreases. Larger wavelengths are required for the

heterogeneous materials; because unless the wavelength is greater than the level of heterogeneity, the wave scatters at the heterogeneities. However, the dimension of heterogeneity is not the only limitation in stress wave testing of materials. In order to obtain an infinite medium and to get rid of the effects of reflections at the sides, the wavelength should be smaller than the least lateral dimension. According to ASTM C 597, the least dimension must be greater than one wavelength. In the test method ASTM D 2845 which is about the ultrasonic testing of rocks, it is recommended to have the minimum lateral dimension at least 5 times the wavelength of the compressional wave.

The method is valid for both P- and S- waves. Although the early studies of through transmission technique for cementitious materials in fresh state seem to prefer the shear waves, the recent studies mainly focus on the use of longitudinal waves.

Keating and collaborators (1989a) studied the properties of fresh cement pastes used in oil well cementing. The cement slurries are used to fill the gap between the casing and rock to support the casing. Cement slurries of four different mixture compositions were tested in this research. The frequency of longitudinal waves was 200 kHz. Besides the ultrasonic pulse velocity, the shear moduli of cement pastes were also determined. It was shown that after the initial setting, the pulse velocity method was an effective method for differentiating the differences in rate of structural development of different slurries, however, before the initial setting shear modulus was more sensitive.

In the same year, the same authors compared the ultrasonic pulse velocity, compressive strength and volume change of the same type of oil cement slurries for the first 24 hours (Keating et al. 1989b). The pulse velocity increased with the highest rate between the 4<sup>th</sup> and 7<sup>th</sup> hours after mixing. While no correlation between volume change and cube strength could be established, the ultrasonic pulse velocity and strength was reported to be correlated for the first 24 hours. The

compressive strength was estimated by ultrasonic pulse velocity measurements in oil well cements with an error of  $\pm 25\%$ .

Sayers and Grenfell (1993) studied both the velocity of shear and longitudinal waves and the temperature change in the oil field drilling cement slurries with various additives. Broadband transducers with a nominal center frequency of 0.5 MHz were used for stress waves. A PMMA mold with the dimensions of 14\*12\*1.208 cm was used in the measurements. Fast longitudinal waves were observed at early times and shear waves at later times. The bulk modulus of cement slurry was found out to be linearly related to the effective shear modulus after the slurry became interconnected. At that time the Poisson's ratio was observed to decrease from 0.5 to values characteristic of porous solids.

Sayers and Dahlin (1993) performed a study on cement paste of American Petroleum Institute class G cement. It was concluded that the ultrasonic waves were sensitive to the point at which the solid phase became interconnected as the result of the hydration process. Initially, the propagating waves had the characteristics of motion in fluids, while at later ages the characteristics of motion in solids were observed. They reported that the longitudinal velocity decreased slightly due to the increased tortuosity of the pore space during the first few hours and then started to increase steeply.

D'Angelo et al. (1995) compared the shear and longitudinal waves in oil field cement slurries after de-aerating together with the temperature which was used as an indicator of the chemical activity. Three different types of oil field cements were tested for the first 24 hours after mixing. The inner dimensions of the PMMA mold were 15.24\*12.70\*1.27 cm. The wall thickness of the mold was 2.54 cm to buffer the reflections. The transducers were broadband type with a center frequency of 1 MHz. The setting point of cement was defined as the time that the slurry reached the percolation threshold. It was concluded that the shear waves were more sensitive to the connectivity of the cement matrix.

Boumiz and colleagues (1996) studied the development of mechanical properties in relation with the hydration reaction in cement pastes and mortars. For this purpose, they applied ultrasonic, calorimetric and conductimetric methods on cement-based materials. The ultrasonic technique was applied to determine the velocity, frequency and attenuation of longitudinal and shear waves. Additionally, the Young's and shear modulus and the Poisson's ratio were calculated from the velocity measurements. A perspex mold with a wall thickness of 3 cm was used. The transducers with center frequency of 0.5 MHz were attached on the walls of the mold for longitudinal and shear waves. For cement pastes the travel distance of the waves was 1 cm, while it was 4 cm in cement mortars. The setting time by Vicat apparatus and compressive strength of mortars were also determined. It was said that the velocity of ultrasonic waves increased rapidly during setting and hardening. The Young's and shear moduli increased rapidly at early ages, and slowed down as the hydration slowed. The Poisson's ratio decreased from 0.5 which is a typical value of fluids to 0.2 which is a typical value of a cementitious material. For the development of mechanical properties, two mechanisms had been proposed; the first one was the connection of cement particles and the second one was the filling of capillary pores.

As a part of the round robin test carried out by RILEM, a device for velocity, frequency spectrum and energy measurement by transmission of longitudinal waves was developed at Stuttgart University (RILEM Report 31). The studies about this device were started earlier in 1991 (Grosse et al. 1999). The historical information about the development of the experimental set-up is explained in detail by Grosse (2002). The summary of this set of studies is explained in the following paragraphs:

Reinhardt and Grosse (1996) investigated the effects of w/c ratio, retarder and cement type by ultrasonic wave propagation. Velocity, transmitted energy and frequency spectrum of the longitudinal waves were the parameters determined. The container used for measurements were made up of styrofoam with two aluminum

plates at the top and bottom. The transducers were in contact with the aluminum plates. For the frequency analysis the wave was generated by a steel ball, while for the other tests it was generated by transducers. The wave velocity, energy and frequency spectra reported to be sensitive to the age and the composition of the concrete. All the parameters were reported to increase with time. The difference in w/c ratio was detected from the measured values; however, the effect of blast furnace slag could not be detected.

In 1996, Reinhardt and his collaborates (1996) studied the influence of w/c ratio, paste volume, effect of aggregate size and superplasticizer by longitudinal wave propagation. The stress wave was generated by an impact of a steel ball and the frequency range of the impact was up to 100 kHz in the early stages of the development of the experimental set-up. The container was made up of PMMA and a rubber was placed between the PMMA walls. The distance between the walls that is the path length of the waves was 70 cm. The initial velocity within the fresh concrete was about 500 m/s which was below the velocity in water. This initial velocity remained approximately same for the first 2 hours, and then increased steeply approaching an asymptotic value. The velocity development with time was divided into stages by the authors. In the first stage the velocity was low and it was dependent on the paste volume and w/c ratio. In the second stage the velocity increased steeply and it was concluded that the w/c ratio was ineffective on the wave velocity. It was also reported that the retarding effect of superplasticizer on hydration was clearly seen.

The application of the method on mortars is explained by Grosse et al. (1999). The same PMMA mold was used for testing the mortars. The frequency range of 20-300 kHz was generated by transducers. The waveforms of longitudinal waves propagating through the fresh mortars were taken in 10 minute time intervals by a data acquisition system and processed automatically for determination of velocity, energy and frequency spectra. The applicability of the method on mortars was proved by testing the reproducibility of the data curves. It was reported that the

method gave a comprehensive picture of the stiffening process and special mixtures and new admixtures were able to be characterized in a new and promising way.

The apparatus mentioned above was developed as a result of several investigations at Stuttgart University. The development history was given in Grosse, 2002. A semi adiabatic temperature measurement system was also added to the experimental set-up. A computer program was developed which continuously recorded the waveform, temperature in the specimen, temperature in the calorimetric device and the air temperature, and which calculated the velocity, energy and frequency spectrum from the waveforms of the ultrasonic waves. A wavelet transformation was tried to be applied on the signals. It was concluded that typical S-shaped curves were obtained for compressional wave development for cement-based materials. In the beginning the velocity values were small and increased slowly, later on, the velocity in the cementitious medium increased steeply. Curve smoothening was applied on the data in order to deal with some erroneous data points. It was seen that the velocity in concrete specimens was higher compared to that of mortar specimens.

The container developed for mortars as the result of several studies had only a volume of 45 cm<sup>3</sup>. The distance between the transducers was 22 cm. The mold consisted of two long PMMA walls and a U-shaped rubber foam which was placed in between. This mold was used for the following researches at Stuttgart University (Grosse and Reinhardt, 2001; Grosse et al. 2001; Reinhardt et al. 2004; Belie et al. 2005; Voigt et al. 2005). The shape of the mold is shown in Figure 3.5. For testing concrete similar mold with greater dimensions were used.

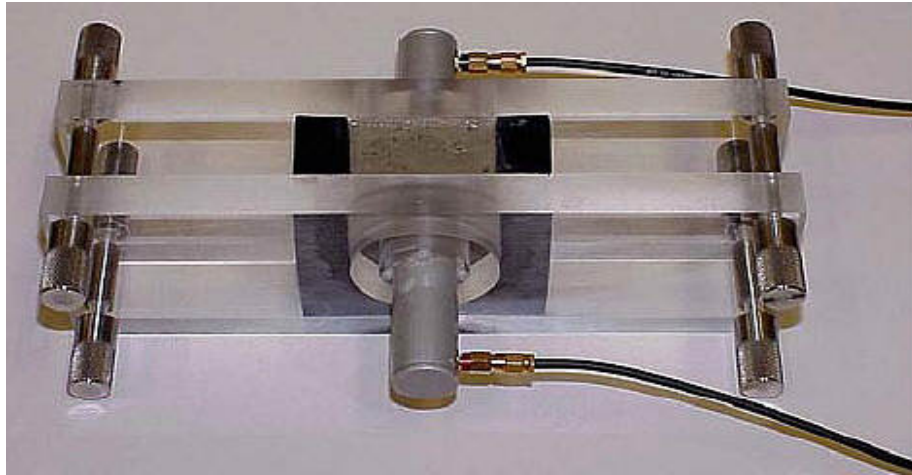


Figure 3.5. The mold developed at Stuttgart University (Grosse, 2002)

The applicability of the ultrasound method for quality control of cement-based materials was explained by Grosse and Reinhardt (2000). Velocity, energy and frequency content of the waves were claimed to be related to the hydration of the mortar as those parameters described the behaviour of the material. The velocity was calculated from the onset times of the ultrasonic waves as the travel distance was already known. The energy was the cumulative sum of the wave amplitudes. The frequency was obtained from the signal data by Fast Fourier Transform (FFT). The parameters were extracted automatically from the waveform data by an algorithm developed at Stuttgart University.

Grosse and Reinhardt (2001) explained how the software for analysis was operating by giving some examples of applications in another paper. The software analysed the wave signals during the experiment. The software showed on the screen the ultrasound signal in time and frequency domain, the change in velocity and energy during time and the wavelet transform of the signal. The wavelet transformation made it possible to correlate the certain regions in the ultrasonic signal and the different frequencies of the wave. In the early stages, mainly signals with low frequency were observed, while in the later stages higher frequencies were observed.

Newly developed methods for monitoring fresh state of cement-based materials were compared (Grosse et al. 2001). The methods compared were ultrasound in through transmission, calorimetry, Scanning Electron Microscopy (SEM) and Nuclear Magnetic Resonance (NMR). In ultrasonic testing, mortar specimens with different w/c ratios and with different types of cements were observed during the first 24 hours after mixing. From the UPV curves it was seen that for lower w/c ratio the hydration occurred faster. The effect of cement type was also detected by ultrasonic measurements and the mortars with CEM I 52.5 had higher velocity compared to CEM I 42.5 and CEM III. Temperature change of the similar mortars was measured by Langavant calorimetry. The results of temperature test showed similar results with the velocity measurements. In order to take the SEM micrographs of the cement pastes, the specimens were immersed in the alcohol which absorbed water of the specimen and then dried in the oven. The SEM micrographs were taken at 2, 5 and 24 hours after mixing. The SEM results proved the densification of the structure of the fresh cement paste with time. While in the 2 hour observation the cement particles were separated, in the 8 hour observation the particles were interconnected and at 24 hour observation the cement particles were nearly changed into gel form. However, it was reported that comparing ultrasonic measurements with SEM was not suitable as the drying process of specimens for SEM application might affect the hydration process in the cementitious material. NMR method applied on the cement pastes with different w/c ratios showed a close correlation with ultrasonic measurement technique.

Reinhardt and Grosse (2004) determined the initial and final setting time values from the ultrasonic pulse velocity curves. They tested mortar specimens with different cement type and different w/c ratio. The effect of admixtures was also tested. A method for determination of onset times and for denoising of ultrasonic signals based on Hinkley criterion and wavelet transformation was explained. According to Hinkley criterion, if the difference between the energy value and a predetermined value was greater than a certain value, then it was assumed that the increase was due to the real signal other than the noise. Wavelet transformation

allowed observing the frequency and the time domain together, so it was possible to distinguish the time each frequency was dominant. The test was applied to three mortars with same composition in order to check the reproducibility, and it was concluded that the method is reproducible with only a variation of 1% in velocity measurements. Lastly, the initial setting time was reported as the first maximum in curvature of the velocity-age curve which could be determined mathematically; however, the final setting time was determined empirically as the time that the longitudinal velocity corresponded to 1500 m/s.

This method was applied to shotcrete (Belie et al. 2005). Before applying the procedure a calibration is applied to the mold by taking ultrasonic measurements of empty mold and a reference material with known properties. Mortars were prepared from two types of cements (CEM I 42.5 R and CEM II/A-LL 42.5 R) with two types of admixtures of alkaline aluminate based solution and alkali-free solution based on aluminium sulphate at different dosages. The effect of those admixtures on the compressive strength, tensile strength and density of the specimens were also tested. When the ultrasonic velocity development of the mortars was investigated, it was seen that the velocity values started at 100-700 m/s and increased up to 4000 m/s. The ultrasonic measurements were said to be sensitive to the cement type, accelerator type and dosage. For non-accelerated mortars a dormant period of 30 minutes was detected while for the accelerated mortar no dormant period was observed. Depending on the energy data of the ultrasonic waves, it was concluded that the rate of energy was dependent on the type and dosage of admixtures. The first maximum point of energy curve was found to occur 20 minutes after the velocity reached a value of 1500 m/s, which was reported to be the final setting of concrete in the literature. Therefore, the maximum of energy curve was related to the end of workability. For the frequency content, it was observed that the peak frequency changes from 20 kHz to 50 kHz as the age of the specimen increased. This shifting point was reported to correspond to the point where the increase in velocity started to decrease. This point was correlated to the point where the hydration products of cement formed a totally connected solid

frame. After this point it was suggested that the ultrasonic pulse velocity measurements followed the evolution of the total solid volume fraction.

The same mold was used for the investigation of high performance concrete in Korea (Lee et al. 2004). The travel distance for P-wave in concrete was 145 mm and a broadband transducer with a center frequency of 54 kHz was used. Mortar and concrete specimens having different w/c ratios made from ordinary portland cement with and without low-calcium fly ash. Water/cementitious material ratio changes in the range of 0.27 to 0.50. The initial and final setting times of the specimens were determined according to ASTM C 403. However, the difficulty of sieving mortar from the concrete for low w/c ratios was mentioned. Mortar specimens were prepared separately with the same w/c ratio and fly ash content. Three steps in hydration process were distinguished in the velocity curves. In step 1, hydrates were reported to begin to form after a dormant period in which the material could be characterized as a water-like viscous suspension. During this step velocity decreases slightly due to the tortuosity. In step 2, ultrasonic wave velocity increased steeply. In this step percolation occurred and the material changed into a water-saturated porous solid structure as the medium became more connected due to the increased amount of hydration products. In the last step, the increase in velocity decreased by approaching an asymptotic value in the solid structure as the volume of pores decreased due the products of hydration reactions. When the ultrasonic pulse values of mortar and concrete specimens were compared, it was seen that at the beginning mortar and concrete specimens having same water/cementitious material ratio had similar velocity, however, at later ages the concrete specimens had higher velocities than mortar specimens. This was explained as in the early ages, the ultrasonic waves propagated through the water-like viscous phase so that the presence of coarse aggregates was ineffective; however, in later ages, the waves propagated through solid structure so the aggregate could affect the pulse velocity. In this research, the initial setting of mortars made from ordinary Portland cement was reached in a velocity range of 800-980 m/s and for mortars blended with fly ash, it was in between 920-1070 m/s.

From velocity curves 2 critical points were determined and compared with the initial and final setting times. The first point was the transition point between steps 1 and 2, and the second point was the point where the increasing rate of velocity was the maximum which occurred in step 2. It was concluded that these points reflected the microstructural changes better than the points determined by penetration resistance method. Lastly, the slope of step 1 observed to increase when the water/cementitious material ratio decreased. The change in the frequency content of specimens with time was also investigated. The dominant frequency content of 5 kHz was measured 10 hours after mixing. At 2 hours, the frequency was determined as 55 kHz and at 21 hours it was determined as 53 kHz which were very close to the center frequency of the transducer. This event was explained as the result of the microstructural changes occurring within the concrete during the setting and hardening.

Ye and his colleagues used a more practical mold in their research (Ye et al. 2004). Two holes were opened on opposite walls of a steel mold and covered with plastic membrane. The holes were a little bit larger than the diameter of the transducers and the transducers were fixed by PVC rings. The dimensions of the steel mold were 150\*150\*200 mm, and the frequency used in the test was 54 kHz. Effect of different w/c ratios and curing conditions were investigated in order to develop a three-dimensional model for the hydration of cement. During the first 5 hours, the ultrasonic velocity values were very slow for all concrete types. The point where pulse velocity started to increase was reported to depend on the w/c ratio and curing temperature. After this point the velocity increased steeply for approximately 40 hours. Lastly, the velocity reached a plateau after 60 hours. For higher curing temperatures, this plateau was reached earlier and the ultrasonic pulse velocity increased faster for the first 24 hours. As the w/c ratio increased, the ultrasonic pulse velocity decreased due to the higher porosity. A model for microstructural development of cement hydration based on the three stages of the ultrasonic measurements was developed.

Kamada and collaborators (2005) investigated the hydration of cement paste through ultrasonic measurements. They used a steel mold with holes on the sides in which brass plates placed for the attachment of the transducers. The distance of the travel path of ultrasonic waves was chosen as 35 mm so it was greater than the wavelength. The resonant frequency of the transducers was 140 kHz. Wave velocity, maximum amplitude and frequency content were determined through the ultrasonic measurements. The viscosity of the specimen was also determined. The initial and final setting times were measured according to the penetration test. In order to observe the chemical properties of the cement pastes, SEM and X-Ray diffraction analysis were applied after the hydration was stopped by replacing the water with acetone. According to the ultrasonic pulse velocity curves, the hydration of cement was also divided into three stages in this research. The frequency content of the waves was reported to be around resonant frequency of the transducers in stage 1, around 29 kHz in stage 2 and around 35 kHz in stage 3. The maximum amplitude ratio which was determined as the ratio of wave amplitude to the maximum amplitude during the measurement was reported to reflect the changes in shear stress resistance. From the SEM measurements it was concluded that the ettringite crystals formed in the stage where the ultrasonic velocity increased suddenly. This was explained as the result of densification of the cement paste due to the formation of acicular ettringite crystals.

Lastly, in RILEM Report 31, the initial setting time was reported as the inflection point of velocity-time curve and the final setting time was reported to correspond to time when ultrasonic pulse velocity reached to a value of 1500 m/s as defined by Reinhardt and Grosse (2004).

### **3.6 Comparison of the Methods**

The methods for testing the fresh cementitious materials mainly depend on two principles: wave reflection and wave refraction. Wave reflection and impact-echo methods depend on the principle that a wave reflects back when touches a

boundary. These methods have the advantage of one sided-contact. However, this one sided measurements give information about only the vicinity of the point of impact and the surface of the application. Vibroscope and wave transmission methods observe the propagation of waves generated at one point through another point so that the measurements are related to the whole path travelled by the stress wave. The impact-echo and vibroscope methods work in relatively low frequency and hence high wavelength, on the other hand wave reflection and wave transmission methods work in higher frequency ranges. Low frequencies result in less attenuation; however, in standards it is mentioned that the wavelength should be greater than the least dimension of the test specimen. In the vibroscope method the test should be stopped before the material completely hardens for removing the transducers from the specimen. The other three methods can be applied as long as the material reaches the desired age.

Wave reflection, wave transmission and impact-echo techniques for early age properties of cement mortar and concrete were compared by Beutel and collaborators (2005). Temperature rise of the specimens was determined using embedded thermocouples as an indicator for the hydration process. When the change in temperature with time was compared with the development of longitudinal wave velocity, it was seen that the temperature started to increase when the longitudinal wave velocity reached the maximum rate. Additionally, when the temperature reached its maximum, the longitudinal wave velocity gained approximately 90% of its final value. In the case of transversal wave velocity, it started to increase later compared to longitudinal wave velocity as the transversal waves could only propagate in the existence of shear strength. The temperature and the shear wave velocity started to increase at the same time which meant both parameters were governed by the same mechanism. The wave reflection factor initially decreased until the acoustic properties were equal to the material of the mold (acrylic glass), after reaching a minimum point it started to increase again. The minimum point of the curve corresponded to the point of increase in temperature curve. The resonant frequency data obtained from impact-echo test

started to increase just after the mixing and then reached a plateau. As the result of the study, it was concluded that those three methods were sensitive to the setting and hardening processes of the cement hydration.

In a more comprehensive study, the wave reflection method and wave transmission method were compared under the additional information about the penetration resistance, in-situ temperature rise, adiabatic heat release and chemical shrinkage for the two concrete and six mortar specimens having different compositions (Voigt et al. 2005). When the change in penetration resistance with time was investigated, it was seen that wave reflection factor and penetration resistance started to increase at the same time which meant that both parameters were governed by the development of the rigid bonds. On the other hand, longitudinal wave velocity started to increase earlier which explained as the fact that the velocity was affected by the formation of ettringite which had no affect on the penetration resistance. It was observed that the wave reflection factor had a linear relationship with chemical shrinkage and adiabatic heat release while longitudinal wave velocity had an exponential relation with those parameters. As a result it was concluded that although the reflection loss measured with transverse waves is related to the dynamic shear modulus and the velocity measured with longitudinal waves is related to the dynamic Young's modulus, both methods have direct relationship to the cement hydration.

### **3.7 Some Remarks on the Wave Transmission Method**

When the studies in the literature about testing cement-based materials in fresh state by through transmission of ultrasonic waves were investigated, it was seen that there is no standard test method for the application and the procedure is still under development.

First of all, in each study, the researchers used their own experimental set-up for testing the specimen. As during the testing period the material should be in the mold, the shape, size and the material of the mold may become important. Although the travel path of the ultrasonic wave was reported as ineffective in the velocity, fresh mortar and concrete are highly attenuative materials, which means the energy of the pulse will decrease while travelling within the medium. In this case, the travel length is important especially at the beginning of the hydration while the velocities are rather small. Another restrictive point in the travel path is the near-field/far-field concept which was explained in part 2.2.4. As mentioned, in order to have reliable data, the travel distance of the pulses should be greater than the near-field zone.

Secondly, for through-transmission of longitudinal ultrasonic waves, usually broadband frequency transducers are employed in the literature in order to observe the frequency spectrum during setting and hardening. However, the case of narrow-band transducers have not been studied much. The effect of different frequencies has not been investigated yet. Although theoretically the frequency should not affect the velocity, it affects the wavelength and hence the attenuation in the nonhomogeneous materials.

As the method seems appropriate for quality control of cement-based materials in the fresh state, a standard test method is needed to be developed. Therefore, the behaviour of the velocity curves for different travel path lengths of the pulses should also be investigated under different frequency ranges.

## **CHAPTER 4**

### **EXPERIMENTAL STUDY**

#### **4.1 Experimental Program**

The aim of this research is to correlate the ultrasonic pulse velocity (UPV) development of hydrating cement-based materials with the hydration process. For monitoring cement hydration non-destructively by ultrasonic pulse velocity technique the hydration of the cement was investigated in two phases; cement paste and mortar. Besides the UPV measurements, related standard test methods were also applied to the paste and mortar specimens in the fresh state. Some later-age properties of the specimens were also determined in order to check the correlation between the properties of fresh state and hardened state.

In order to measure the UPV of the fresh material, first of all, a test set-up was developed, the details of which will be explained in the following sections.

For cement paste specimens, besides the ultrasonic pulse velocity determinations, the setting time measurements and the rate of heat of hydration measurements were applied for three different water/cement (w/c) ratios. The ESEM images at different stages of hydration were obtained for paste with 0.5 w/c ratio. For UPV tests in cement pastes, the development of UPV during hydration with the single variable of w/c ratio was observed.

For cement mortar specimens, ultrasonic pulse velocity and setting time determinations were done in the fresh state for the w/c ratio similar to that of paste specimens. For the hardened state of the same mixes, compressive strength and volume of permeable pores were determined. The UPV measurements were also taken for the hardened mortars. While testing the applicability of the UPV test on hydrating cement-based materials, the variables in UPV test method such as path length and frequency range were also tested for a selected w/c ratio.

The curing conditions for all specimens were similar during the experimental program. They were stored in a room with a relative moisture of 60 % and a temperature of  $27\pm 1$  °C during the fresh state tests and until the test age for the hardened state tests. After the specimens on which compressive strength and volume of permeable pores would be determined were demolded, they were placed in water in the same room until the time of test.

The waveforms obtained by ultrasonic tests were analysed by Matlab. In the analysis part of the research, the results obtained from UPV were compared with the results obtained from the standard test methods in order to monitor and to follow the hydration process of the cement.

## **4.2 Materials**

### **4.2.1 Cements**

Ordinary Portland cement of CEM I 42.5 R type which was obtained from the same source was used in all experiments. The chemical and physical properties of the cement were obtained before preparing the test pastes and mortars according to relevant ASTM standards. The types of tests applied on the cements in order to determine their physical and chemical properties are listed in Table 4.1. The results of tests conducted to determine the chemical and physical properties of the cement are given in Table 4.2 and Table 4.3, respectively.

Table 4.1. Tests performed on cement

<b>Tests</b>	<b>Related Standards</b>
Chemical Analysis	ASTM C 114
Density	ASTM C 188
Fineness	ASTM C 204
Normal Consistency	ASTM C 187
Setting Time	ASTM C 191
Compressive Strength	ASTM C 109

Table 4.2. The chemical composition of CEM I 42.5 R cement

<b>Component</b>	<b>(%)</b>
SiO <sub>2</sub>	18.90
Al <sub>2</sub> O <sub>3</sub>	4.74
Fe <sub>2</sub> O <sub>3</sub>	3.03
CaO	67.01
MgO	1.76
SO <sub>3</sub>	2.88

Table 4.3. The physical and mechanical properties of CEM I 42.5 R cement

<b>Property</b>	<b>Value</b>
Density (g/cm <sup>3</sup> )	3.03
Blaine Fineness (cm <sup>2</sup> /g)	3045
Normal Consistency (%)	28
Setting Time (min)	
Initial Set	185
Final Set	240
Compressive Strength (MPa)	
3 days	31.50
7 days	36.15
28 days	41.22

#### 4.2.2 Aggregates

Crushed sand was used as the fine aggregate in preparing the mortar mixtures. The specific gravity and absorption capacity of sand were determined before designing the mixture proportions of the mortars. The particle size distribution of the aggregate sample was also determined by sieve analysis. The tests applied on the aggregate are listed in Table 4.4. The results of specific gravity and absorption tests are shown in Table 4.5, and the gradation of the sand is given in Table 4.6.

Table 4.4. Tests performed on aggregate

<b>Tests</b>	<b>Related Standards</b>
Specific Gravity and Absorption	ASTM C 128
Sieve Analysis	ASTM C 136

Table 4.5. Properties of aggregate

<b>Property</b>	<b>Value</b>
Apparent Specific Gravity	2.72
SSD Specific Gravity	2.64
Dry Specific Gravity	2.59
Absorption (%)	1.81

Table 4.6. Gradation of the aggregate

<b>Sieve size</b>	<b>Passed through (%)</b>
3/8"	100
No 4	99.31
No 8	68.28
No 16	44.24
No 30	30.39
No 50	21.68
No 100	16.39

### 4.2.3 Water

Municipal tap water was used for the preparation of paste and mortar mixtures. The water used was assumed to be free from oil, organic materials and alkalis.

### 4.3 Mortar Mixtures

In order to have mortar mixtures with different hydration characteristics, mortars having three different water/cement ratios of 0.5, 0.6 and 0.8 were prepared. While mixture proportions were calculated cement content was chosen as  $500 \text{ kg/m}^3$  in all mixtures. However, the assumed air content for mixture proportions and the measured air content during tests were not the same. So after the exact air content was determined by pressure method, the total volume was recalculated and the mixture proportions were corrected. The corrected amounts of contents of mortar mixtures are given in Table 4.7. The air content measured according to ASTM C 138 and unit weight determined according to ASTM C 231 are also shown in the same table.

Table 4.7. Mixture proportions of mortar specimens

	w/c ratio		
	0.5	0.6	0.8
Cement ( $\text{kg/m}^3$ )	494	514	513
Water ( $\text{kg/m}^3$ )	247	308	411
Sand ( $\text{kg/m}^3$ )	1487	1370	1138
Total ( $\text{kg/m}^3$ )	2228	2192	2062
Unit Weight ( $\text{kg/m}^3$ )	2230	2200	2070
Air content (%)	2.9	1.3	0.8

The mortar mixtures were compacted with a rod when placing in the molds. For the mortars with high w/c ratio, compaction was much more easier. The smaller air

content results for higher w/c ratio are probably due to the ease of compaction. As the same procedure was applied for each mixture, the degree of compaction became higher as the w/c ratio increased.

In the initial stage of the experimental program, it was decided to test mortar mixtures with a w/c ratio of 0.4. However, when the mixture was prepared, it was observed that the mixing, placing and compacting processes were very difficult. Although compaction process was applied carefully, when the specimens were demolded, it was realized that the mixture was not placed well. The results of this mixture would probably mislead the analysis part; therefore, this group of experiments was cancelled.

Additionally, beyond the ease of compaction, the increased w/c ratio leads to an increase in the possibility of segregation and bleeding. For the test mixture with w/c ratio of 0.8 some bleeding was observed.

#### **4.4 Test Methods**

In this investigation, tests were applied on cement paste and mortar specimens. The main aim of the study was to monitor the hydration process by ultrasonic pulse velocity measurements non-destructively; therefore, the UPV test was applied to both pastes and mortars. The setting time was also determined in both specimen groups. The heat of hydration was determined only on paste specimens whereas the strength and volume of permeable pores were only determined on mortar specimens. However, before beginning the experimental program the first step was to develop the experimental set-up for UPV determination. After the experimental set-up for ultrasonic test of fresh cementitious materials was established, the experimental part of the investigation was started. In the following sections, the details of the aforementioned tests are given:

#### 4.4.1 Development of the mold

The most challenging part in testing fresh cementitious materials by ultrasonic waves non-destructively was the design of the experimental set-up as during the testing procedure the material must stay inside the mold. Only one face of the specimen is available for testing. However, if the transducers of the UPV apparatus were placed on the top surface, they would sink into the specimen as the medium was not rigid enough to carry their weight yet. Additionally, in UPV testing direct measurement is more reliable than indirect measurement as explained in Chapter 2. In order to have direct measurement, the sending and receiving transducers should be placed on the two opposite faces of the specimen. However, the waves would prefer the path that they could travel in the shortest duration. Therefore, if the transducers were attached on the sides of the mold, the ultrasonic longitudinal waves could travel through the sides of the mold instead of the medium itself.

In order to choose the material and the shape of the mold, some preliminary experiments were done. First of all, when a steel mold was used, it was not possible to observe the hydration process, because throughout the whole test, the ultrasonic waves travelled through the sides as it took the shortest time period due to the high velocity in steel which was about 5900 m/s. The mold needed to be produced from such a material that the velocity through it should be slower than the mortar. Therefore, a material of low density should be used for placing the fresh cementitious material. As a second trial, a plastic mold having the dimensions of 15\*15\*15 cm<sup>3</sup> was used. Before placing the mortar mixture in the container, the UPV of the empty mold was measured. In the empty mold, the waves would prefer to travel through the walls of the mold. After the material was placed in the mold, the UPV measurements started. At the beginning, same value as the empty mold was taken for a while, because as the velocity of ultrasonic pulse in fresh cement mortar was very low, the waves preferred to pass through the mold walls. However, as time passed, the travel time between the transmitting and the receiving transducers started to decrease compared to the initial value, which meant that the

mortar started to gain rigidity and the velocity of the mortar began to be higher than the velocity of the mold material. This preliminary experiment was applied for two different w/c ratios in order to check whether the difference in the UPV development for different hydrating properties could be detected with the proposed method. The results were encouraging for monitoring the progress of hydration in cement by UPV test if an appropriate set-up could be performed.

Although it seemed possible to observe hydration of cement mortar with this system, the initial stages of hydration could not be captured using this set-up. A mold with less density needed to be used or the contact between the sides of the mold and the transducers of the ultrasonic apparatus needed to be prevented. Unfortunately, it was not possible to give shape to the plastic conventional standard mold. Therefore, it was decided to produce molds using wooden pieces with desired shape and dimensions. For this purpose the mold used by Ye et al. (2004) was adopted. Circular holes with dimensions a little larger than the transducers were cut on opposite sides. These holes needed to be somewhat covered in order to prevent the viscous material from flowing outside. However, using plastic sheets for the holes as done by Ye et al. (2004) was not appropriate as due to the pressure applied on the transducers, the material deformed. In order to prevent direct touch, plexiglass sheets were employed inside the mold on the sides with the holes. With the use of plexiglass sheets not only direct contact was prevented but also the risk of transmission of the ultrasonic waves through the sides of the mold was decreased as the result of attenuation between wooden sides and the plexiglass sheets. Another advantage of this system was the possibility to obtain a mold in the desired shape and dimension in an economical way. The disadvantage of the wood was the possible capacity of the material to absorb water which could alter the water content in the mortar mixture. However, this problem was solved by covering the inside of the mold with a plastic sheet.

After the mold material and shape was decided, the second problem was the attachment of the transducers to the mold. As the aim was to take measurements

continuously for at least 24 hours, the transducers needed to be attached to the mold so that similar pressure could be applied during the test. The contact and the pressure level between the transducers and the specimen affect the wave amplitude measurement. If the contact was good, the wave could be detected precisely, however, in the case of poor contact, the wave could not be captured precisely and the wave parameters might not be measured correctly. The contact between the transducer and plexiglass sheet was achieved by applying vaseline on the surfaces. In order to hold the transducers attached on the container continuously, the transducers were tied by rubber bands. The shape of the empty molds of different dimensions and the attachment of the transducers are shown in Figure 4.1.



Figure 4.1. The wooden molds used in the experiments and attachment of transducers

Using an appropriate mold is one of the most important parts of this experimental procedure due to previously mentioned reasons. After the mold for the testing system was designed, the data acquisition system and UPV measurement of the experimental set-up needed to be designed in order to visualize the longitudinal waves travelling through the medium and to calculate the UPV of the specimens.

#### 4.4.2 UPV determination

The velocity of ultrasonic pulses travelling through the cement pastes and mortars were determined by using an ultrasonic apparatus together with a data acquisition system which was attached to a computer. The schematic representation of experimental system is shown in Figure 4.2.

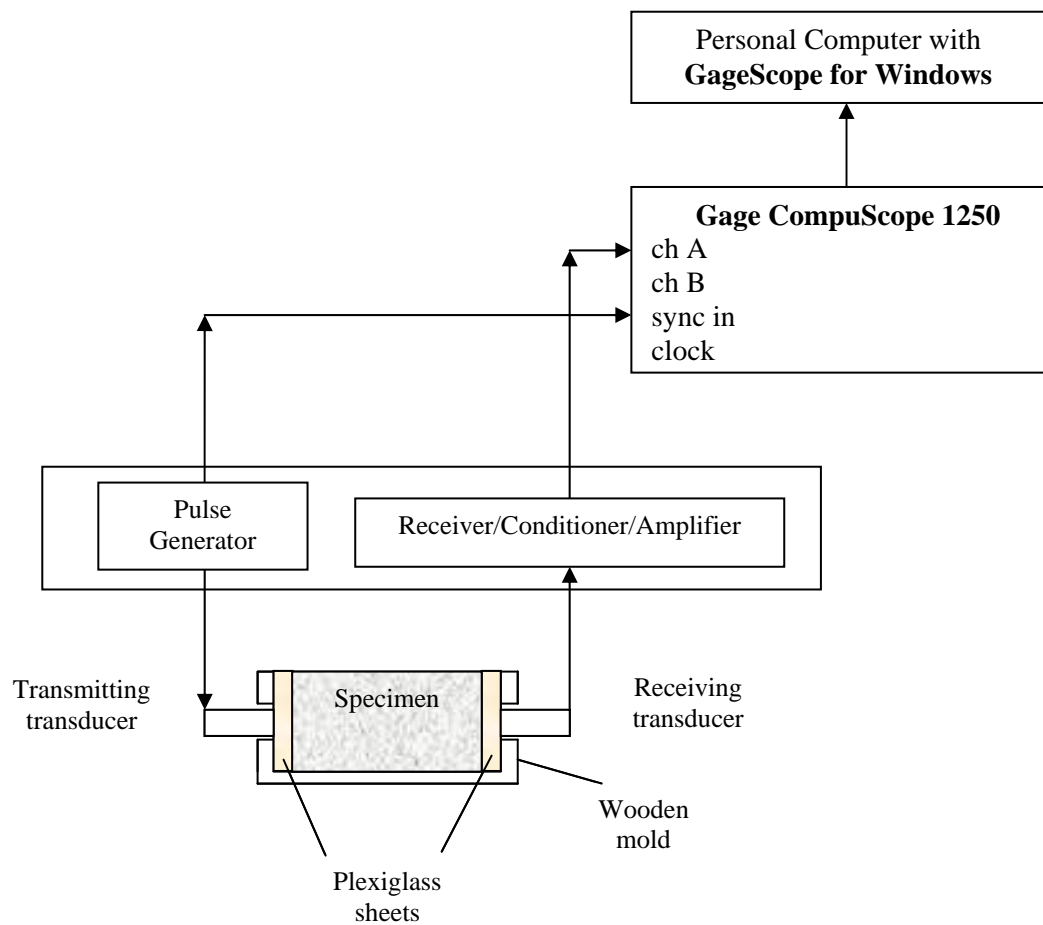


Figure 4.2. The schematic representation of data acquisition system

In the experimental set-up the ultrasonic pulses were generated by an ultrasonic apparatus. A data acquisition card was inserted in the computer and the oscilloscope software was installed so that the features of the data acquisition card

could be used. The ultrasonic apparatus was connected to the data acquisition card with coaxial cables. The signals sent and received by ultrasonic apparatus were transferred simultaneously to the hardware so the ultrasonic waves could be observed directly on the computer display as shown in Figure 4.2. The oscilloscope software had the capability to save the data at desired time intervals. The data saved by the system was then processed and analysed using Matlab.

Taking multiple records was possible with the set-up. The saved waves were the average of the 16 readings which was automatically calculated by the oscilloscope software. Although the system could record data from 2 channels, only one channel was used as the ultrasonic apparatus was single. When one channel option was used, the sampling rate could be as high as 50 MS/s. Additionally, the number of data points could be selected. In order to monitor the total wave and to observe the attenuation more than 120000 points were chosen for each wave. As in one second 50000000 samples could be collected, 120000 points corresponded to a time period of 2400 microseconds, which was a very long duration when ultrasonic testing of concrete was considered. The first arrival time of the ultrasonic wave, the waveform and the decrease in the amplitude with time until zero amplitude could be observed with these parameters.

As some vibrations from the environment could also be captured by the system, the noise needed to be eliminated by smoothening methods. For this purpose, while the data was being analysed by Matlab, the moving average method of 10 points was applied. The average of first 10 points was taken and recorded as the first point, then the points from 2 to 11 were averaged and recorded as second point, then the points from 3 to 12 were averaged and recorded as the third point, and this process continued until the end of the data points. After the signals were smoothened with this method, the first arrival time of the ultrasonic wave was determined. For this purpose, the first peak of the wave signal was determined by the analysis program and the whole wave was amplified so that the first peak corresponds to 2 Volts. Later on, the arrival time was selected as the point where the signal corresponded

to a threshold of 0.06 V which was 3% of first peak. The onset times of the waves were calculated in this manner.

Filtering the data clears the electrical noise while amplifying simplifies the determination of first arrival time of the pulse wave. As an example, the raw and processed waveforms are shown in Figure 4.3. The example belongs to the mortar specimens of 0.5 w/c ratio at an age of 4 hours.

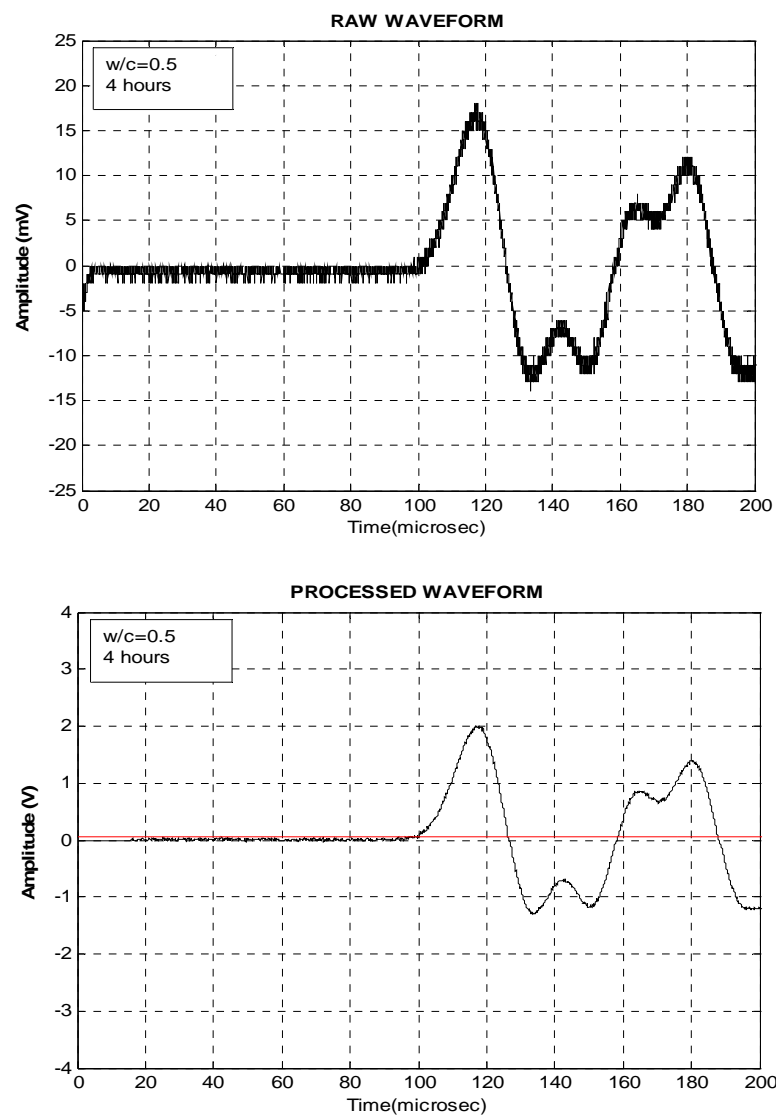


Figure 4.3. The raw and processed waveforms of ultrasonic pulses

In Figure 4.3, the units in the y-axes are different; in the raw data the axis is given in millivolts, while in the processed data it is given in volts. In the processed form, the wave is filtered, amplified and the baseline corrected. The threshold for the arrival time determination is also given on the processed waveform.

After the onset times were obtained from the processed waveforms, the velocity could be calculated as the travel path length was known. However, some corrections needed to be applied before calculating the velocity.

The first correction was for the zero reading of the transducers. When the sending and receiving transducers were in touch, the time for arrival of the wave should be zero as the wave did not travel through any medium. However, due to signals travelled through long cables, and conversions of the signals between different phases, some time passed so, the system could not read zero for that case. First of all, the constant time value for each frequency was determined for zero reading by taking the average of at least 20 readings obtained at different times for the direct touch of the transducers. This value was subtracted from the determined time values before calculating the velocity. The values for zero correction for each frequency transducers are given in Table 4.8.

Table 4.8. Zero reading correction for each frequency

Frequency (kHz)	Correction time ( $\mu$ s)
54	2.27
82	1.77
150	2.17

The second correction was applied for the plexiglass sheets. As the wave travels through plexiglass sheets for a while, the time spent through those sheets should also be considered. For this purpose with the same set-up 3 different sheets were tested 10 times and the travel times for each frequency were calculated by Matlab. By dividing the thickness of each sheet by the travel time calculated after applying

zero time correction; the ultrasonic pulse velocity was determined by taking the average of all readings for each frequency range. The UPV of plexiglass sheets are given in Table 4.9.

Table 4.9. UPV of plexiglass sheet for each frequency

Frequency (kHz)	UPV (m/s)
54	2407
82	2452
150	2535

Thus, the data collected by experimental set-up was processed by Matlab and the travel time through the mold which contained the test specimen was determined. Later on, the zero time correction and the time spent through plexiglass sheets were subtracted. The final velocity was determined by dividing the length of the test specimen to the corrected time. The UPV values were obtained with 15-minute time intervals for each test specimen. For the first group of experiments, which is composed of mortars with different w/c ratios, different travel path lengths were tested for the first 72 hours. Additionally, at 7 and 28 days, the UPV values were also determined on the specimens which were kept in the same mold until the test age. However, it was observed that the UPV did not change significantly after 24 hours. Therefore, the remaining experiments which were for the paste specimens and for the frequency effect were tested only during the first 24 hours. After the UPV values were determined at the desired time interval and duration, the change of UPV with time was monitored.

#### 4.4.3 Setting time determination

In order to correlate the values with the UPV development of the medium the initial and final setting times of the cementitious materials were determined in two phases; cement paste and mortar. Setting time determination of cement paste and

cement mortar are explained in different ASTM standards. In each test, the related standard was used.

In cement pastes, the initial and final setting times were determined according to ASTM C 191 by Vicat apparatus. Although in the standard the test method was said to be applied on pastes at normal consistency, in order to correlate the setting characteristics of pastes with different w/c ratios to the UPV development of the same pastes, the test was applied on the cement paste specimens having different w/c ratios. Cement pastes with w/c ratios of 0.5, 0.6, and 0.8 were prepared and placed in the container of the apparatus. The depth of penetration of Vicat needle into the specimen which were kept in the same conditions with the UPV test specimens was measured at 15 minutes time intervals until the needle could no longer sink into the specimen so that the change in the penetration depth with time could be obtained. According to ASTM C 191, the initial setting time corresponds to a penetration depth of 25 mm from the top surface of the paste and the final setting time corresponds to a penetration less than 1 mm. The initial setting time values were determined from the penetration depth-time curves and the final setting times were determined during the test as the point when penetration is no longer observed which corresponded to the end of the test. While obtaining the penetration depth-time curves for each w/c ratio, the test was applied on two different specimens and the average was taken at each time interval before constructing the curves representing change of penetration depth with time.

In cement mortar, the initial and final setting times were determined according to ASTM C 403 by penetrometer. In order to determine the initial and final setting times of the mortar specimens, the mortar specimens were placed in 15\*15\*15cm cube molds in two layers by compacting each layer 25 times with the steel rod. The molds were kept under the same conditions with the specimens of UPV determination test. The penetration resistance was measured at 15-minute time intervals and the development of penetration resistance with time was obtained. From the penetration resistance-time curves the initial and final setting times of

mortar specimens for each w/c ratio were determined. According to ASTM C 403, initial setting time is reached when a penetration resistance strength of 3.5 MPa is obtained and final setting time is reached when a penetration resistance strength of 27.6 MPa is reached. The measurements were continued until no reading with the apparatus could be taken due to high amount of force was needed to penetrate into the specimen. While determining the penetration resistance-time curves, the average of the results obtained from two different specimens were used. Additionally, as the mortar specimens had to be tested at different times for each travel path length, the penetration test was applied at each time to the specimens stored together with the UPV test specimen. By this way, it was also checked whether similar properties were obtained at the mortar batches mixed at different days. The curves obtained were similar, so the average of the all tests was taken to draw the penetration resistance-time curves.

By the Vicat and penetration resistance tests the setting characteristics of the cement pastes and mortars were obtained. These properties were used to correlate the hydration of cementitious material with the UPV development.

#### **4.4.4 Heat of hydration determination**

As the hydration of cement is a chemical reaction, the heat of hydration and rate of heat of hydration give information about how much the reaction has progressed at any time. The rate of heat of hydration and the heat of hydration of cement pastes in this study were monitored in order to observe the hydration process chemically.

The heat of hydration of cement pastes with different w/c ratios were determined by isothermal conduction calorimetry for the first 72 hours at every minute. The pastes having w/c ratios of 0.5, 0.6, and 0.8 were prepared by mixing cement and water so that the total weight of the paste would be 7.5 grams. Immediately after the paste was mixed it was placed in the special mold of the apparatus and put in the calorimetry. The temperature of the apparatus and the environment was set

constant at 20 °C. The heat flow from the medium was measured automatically and by comparing with a reference material the rate of heat of hydration of the cement paste was determined. The heat of hydration was calculated by integrating the rate of heat of hydration curve with respect to time.

By isothermal conduction calorimetry method the rate of heat of hydration and heat of hydration of cement pastes were determined during the first 72 hours, the peaks and the stages of the hydration of the cement pastes were observed. The information obtained from the hydration of cement pastes could be useful while interpreting the UPV development of cement pastes and cement mortars.

#### **4.4.5 ESEM analysis**

In order to observe the microstructural changes due to hydration in cement pastes, the ESEM (Environmental Scanning Electron Microscopy) analyses were applied on the paste specimens having 0.5 w/c ratio at different stages of hydration. The hydration process was stopped by immersion in liquid nitrogen. After the hydration was stopped, the ESEM micrographs were obtained in BSE (Back-Scattered Electron) mode on the polished surfaces of the specimens. This analysis was applied at different stages of very early hydration so that the structural changes during setting could be observed. As the initial and final setting times were known due to the standard test method, the corresponding ESEM images were taken. From these images, the dormant period, initial and final setting stages could clearly be observed. The results are given in Chapter 5 in detail.

#### **4.4.6 Strength determination**

In order to determine the flexural and compressive strength of mortar mixtures 4\*4\*16 cm<sup>3</sup> prismatic specimens were used. The prisms were tested for flexural strength by mid-point loading as described in ASTM C 348. After the prisms were

divided into two pieces, the compressive strength was determined from those two pieces having  $4*4\text{ cm}^2$  cross-sectional area according to ASTM C 349.

The mortar prisms were mixed at three different w/c ratios of 0.5, 0.6, and 0.8. The prisms were kept in the same temperature as the ultrasonic test specimens. The prisms were kept in the molds for 24 hours. After 24 hours, the specimens were cured in lime-saturated water until the test age. The flexural and compressive strength values were determined at 1,2, 3, 7 and 28 days. At each time, 3 prisms were used to measure the flexural strength and 6 pieces obtained from the prisms tested by flexural load were used to measure the compressive strength.

While determining the UPV development in mortar specimens having different w/c ratios, the batches were prepared and tested at different days for each travel path length. The prisms for strength determination were also prepared and tested for each batch in order to observe whether similar properties were obtained at each three batch for UPV test of one mixture. It was seen that the results are approximately same for each batch of same type of mortar mixture. Therefore, the average of flexural and compressive strength values of mortar mixtures of similar properties prepared at different days was taken at each test age. Although 3 results existed at each test age due to the different batches, the results were decreased to one for each test age and each w/c ratio by averaging.

#### **4.4.7 Volume of permeable pores and absorption capacity determination**

The volume of permeable pores and the water absorption of the mortar specimens were determined according to ASTM C 642. For measuring the volume of permeable pores,  $4*4*16\text{ cm}^3$  prismatic specimens were used as in the case of the strength determination test. The prisms were prepared at the same time with the specimens for strength test, UPV test and penetration resistance for setting time test. They were cured same as the strength test prisms; after 24 hours the specimens

were demolded and kept in lime-saturated water until the test age together with the strength test specimens at the same temperature with the UPV test set-up.

At each test age, 3 specimens were tested. At the test age, firstly the specimens were placed in the oven to obtain the oven-dry mass. After the oven dry mass was obtained, the specimens were placed in the water for 48 hours, the saturated mass after immersion was measured by drying the surface with a towel. Later on, the specimens were boiled for 5 hours, the weight after boiling was determined after the specimens were cooled to room temperature and surface moisture was removed by a towel. Lastly, the specimen was weighed in water by placing in a wire basket. The absorption, bulk density and volume of permeable voids were calculated according to ASTM C 642.

As in the case of compressive strength determination, the average of three results obtained from different batches at the same mixture were taken for each test age.

## **CHAPTER 5**

### **TEST RESULTS AND DISCUSSIONS**

#### **5.1 Progress of Hydration in Cements**

This research was aimed to monitor the hydration process of cement-based materials by the propagation of longitudinal ultrasonic waves. By observing the development of ultrasonic pulse velocity (UPV) within the body during the hydration process, the setting behavior in different cementitious materials were planned to be determined. For this purpose, different stages of hydration process of cements obtained by standard test methods such as conduction calorimetry and Vicat needle are compared with UPV development through the material with time.

In order to relate the test results obtained in this research with the development of hydration, the schematic representation of the hydration process is given in Figure 5.1.

According to the schematic model given in Figure 5.1, right after mixing, the medium behaves as a suspension which is composed of individual cement particles suspended in water. However, with time hydration process proceeds and the solidification occurs. As the hydration products increase, the medium gains strength and rigidity becoming a solid material.

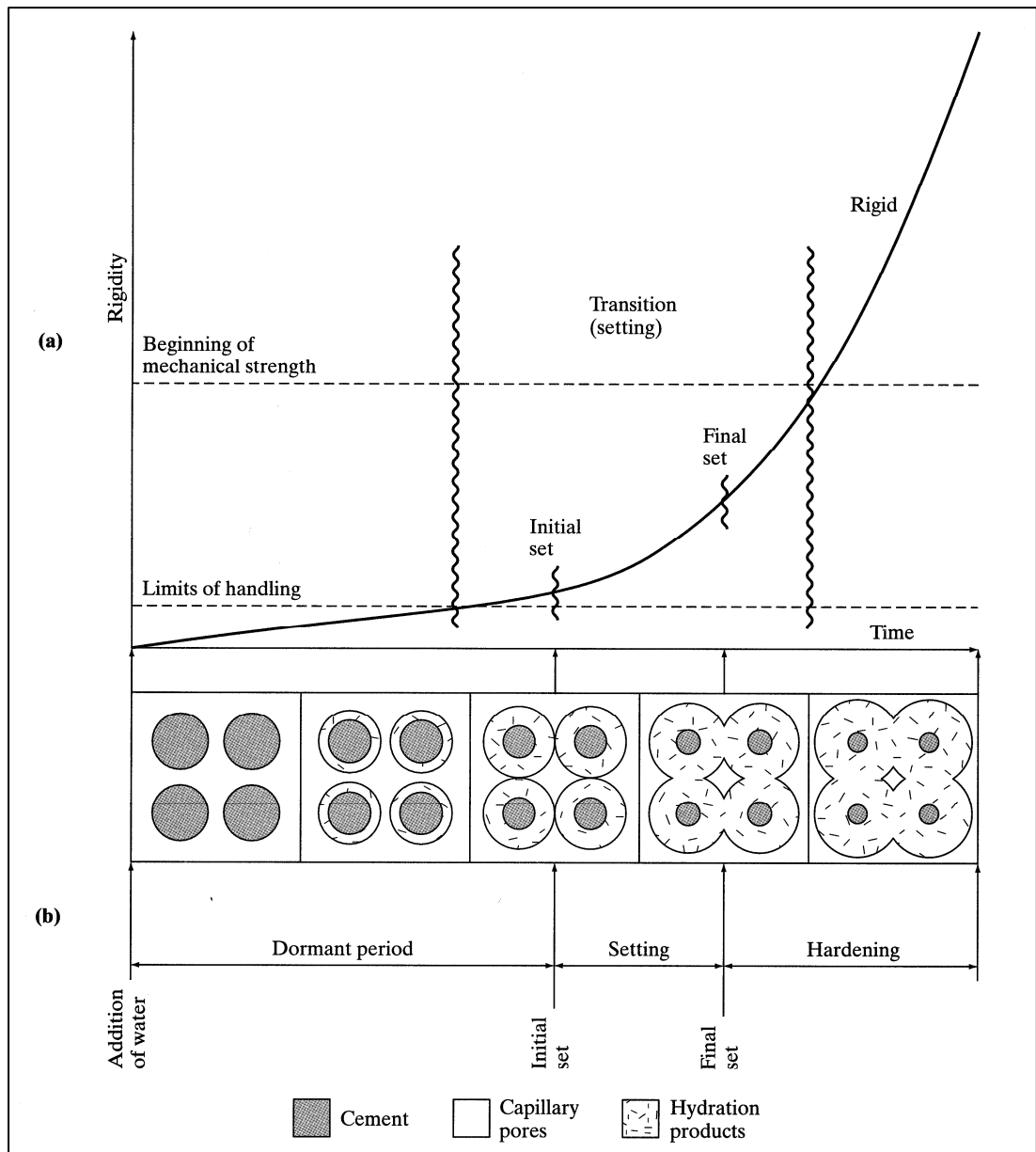


Figure 5.1. Schematic representation of setting and hardening process (Young et al. 1998)

The ESEM micrographs of cement paste having 0.5 w/c ratio were also obtained at different ages during the early hydration. The images were obtained after stopping hydration by liquid nitrogen. The micrographs are shown in Figure 5.2 for three different ages so that each represents different stages of the hydration process.

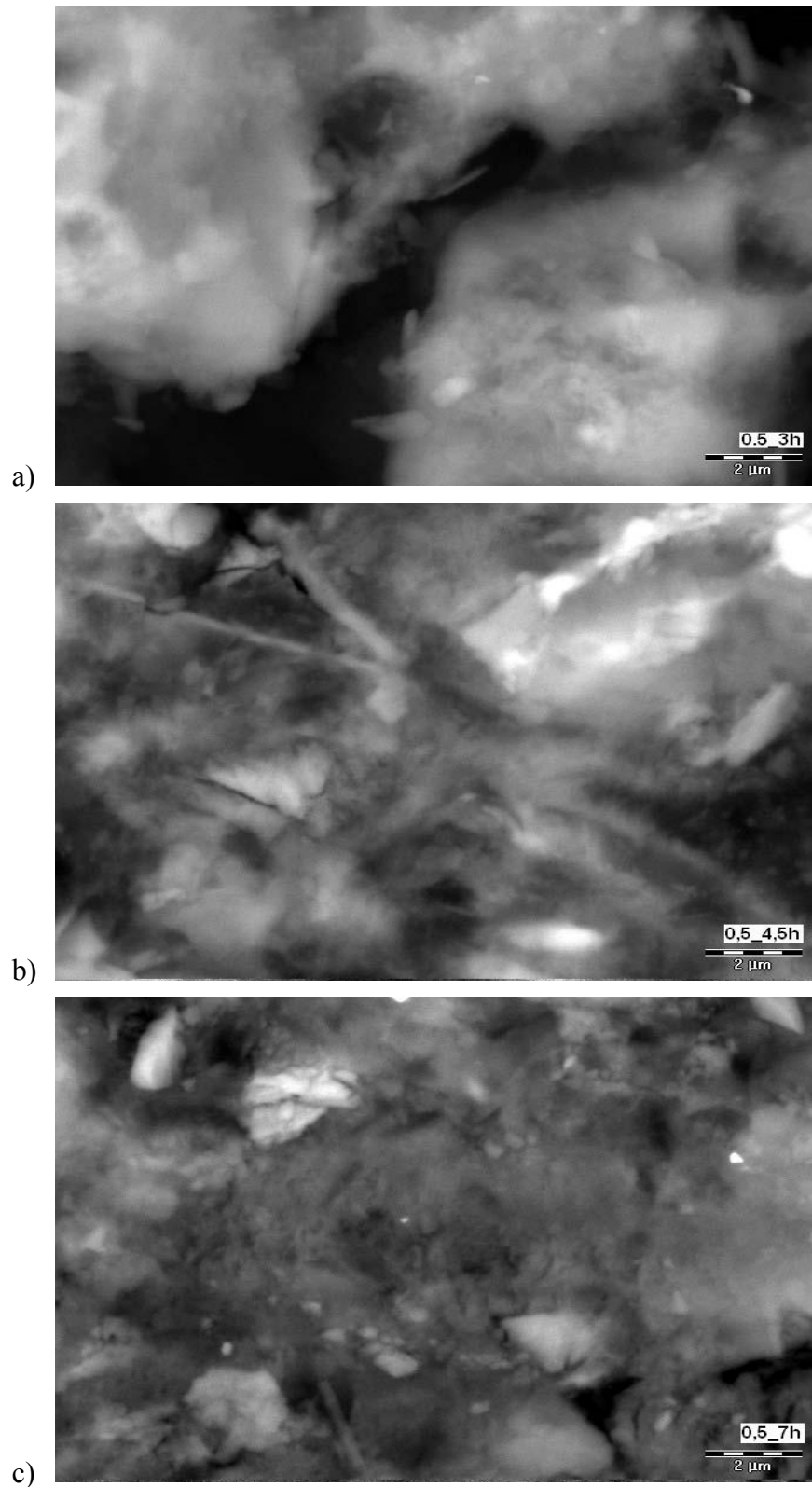


Figure 5.2. Cement paste structure (a) before setting, (b) at initial setting, (c) at final setting

In the cement paste shown in Figure 5.2, it is known that initial setting time occurs at about 4.5 hours and final setting time occurs at about 7 hours after mixing. Therefore, the different ages of cement paste in Figure 5.2 correspond to dormant period, initial setting and final setting. As seen in the figure, during the dormant period, the cement particles are not connected. However, as the hydration progresses the hydration products occur on the cement particles by reducing the distances between the individual particles. At the initial setting the hydration products obtained on adjacent cement particles seem to touch each other. After final setting the amount of hydration products increases by filling the voids between the particles. The stages of hydration process which are shown schematically in Figure 5.1 are obtained from the ESEM images of the cement paste during setting.

## **5.2 Propagation of Ultrasonic Waves in Hydrating Cements**

In order to obtain the development of UPV in hydrating cements, an experimental set-up was established so that the waveforms could be monitored continuously during the hydration process of cementitious medium. The arrival time of the ultrasonic longitudinal wave was determined from the waveforms of the longitudinal waves travelling through the body. Afterwards the ultrasonic pulse velocity (UPV) was calculated by dividing the travel length by the arrival time.

As soon as the material was placed in the mold, compacted and covered with plastic sheets in order to prevent moisture loss from the surface, the ultrasonic apparatus was attached and the set-up was started for acquiring the waveforms. The measurements were started within 30 minutes after the mixing operation.

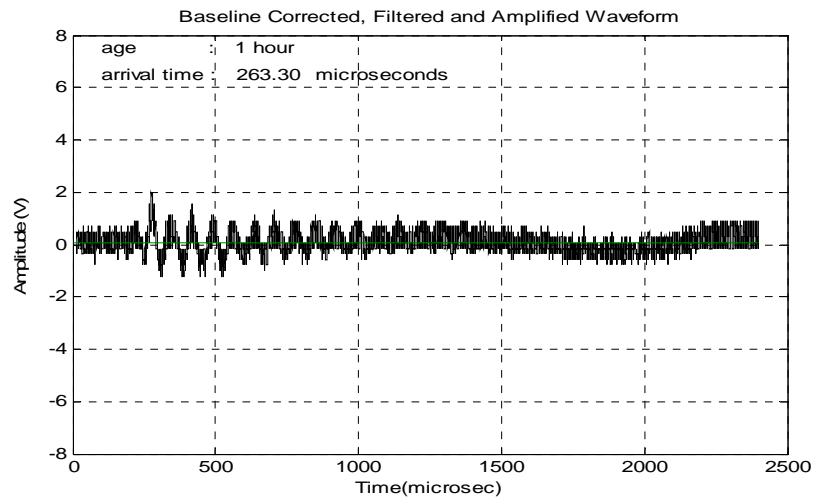
Just after the mixing process the medium is like a solid suspension containing many voids through which the waves cannot propagate fast. However, as time passes, the material becomes like a solid due to gaining of rigidity and the waves can propagate faster. In the early hours, the attenuation in the medium is very high.

Due to the weakness of the waves reaching the receiving transducer, the effect of noise is also high. As a result, at the beginning of the hydration process, the waves are not clearly observed. The change of waveforms with time is given for the mortar specimen having a w/c ratio of 0.5 tested with a frequency of 54 kHz for a travel path distance of 15 cm in Figure 5.3. The waveforms shown in the figure are the filtered and the amplified waves. The waves were processed and analyzed by Matlab and the arrival times were determined for each waveform by considering a threshold value of 0.06 V. The determined arrival times together with the threshold line are shown on each graph.

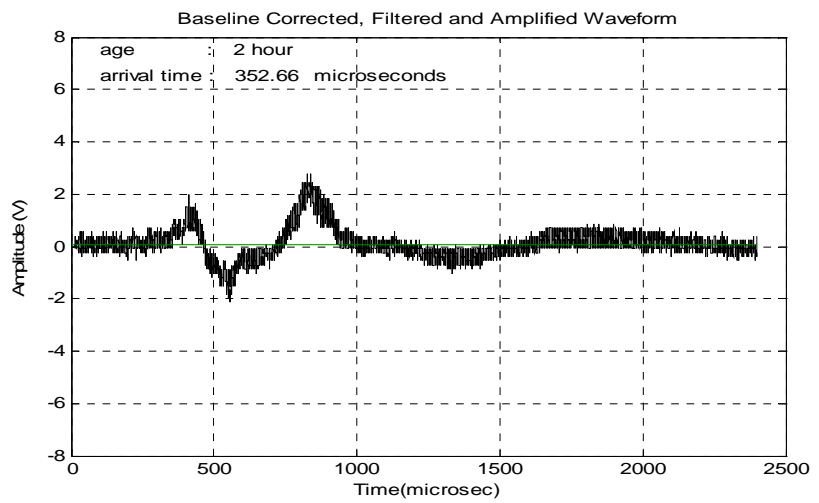
As seen in Figure 5.3, the waveforms change with time. The arrival time for the ultrasonic waves also changes such that as the hydration progresses the arrival times decrease. While during the early hours the change in arrival time is more significant, at later ages it is rather slow.

From the curves of Figure 5.3, it is seen that at very early ages the waveforms are not very clear. The electrical noise and the attenuation of the waves deteriorate the waveforms, and the arrival times cannot be accurately calculated. As seen in the figure, the arrival time for 1 hour-old mortar is 263.30  $\mu\text{s}$  while for 2 hour-old specimen it is 352.66  $\mu\text{s}$ . When the waveforms are examined, the high amount of electrical noise for the 1<sup>st</sup> and 2<sup>nd</sup> hours can be realized. The waves travelled through the medium and captured by the receiving transducer are very weak during the early ages due to the attenuation. However, at about beginning of setting as seen in the 3 hour-old mortar specimen, waveforms start to become clearer. After the initial set, in the cementitious medium an interconnected system starts to be formed. As the hydration proceeds, the medium becomes more solid and the UPV increases. Until final setting time, the maximum amplitude seems to increase. After the medium sets completely, the change in the waveform becomes less significant.

1 hour



2 hours



3 hours

(initial set:  
3.06 hours)

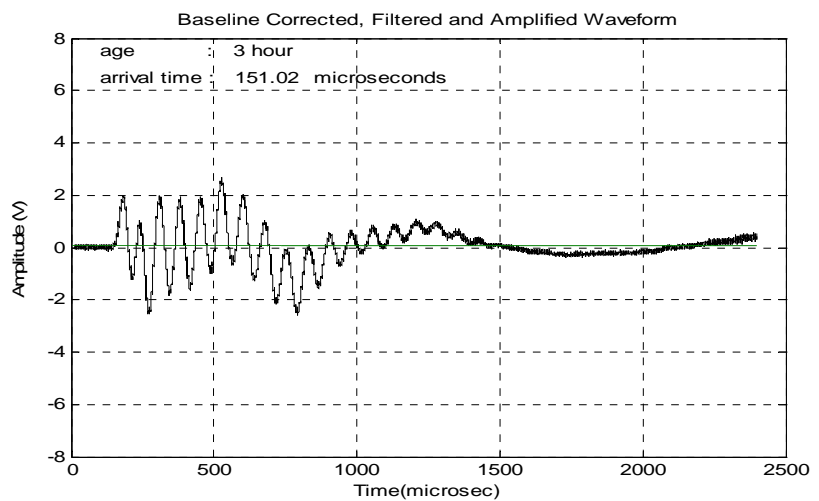
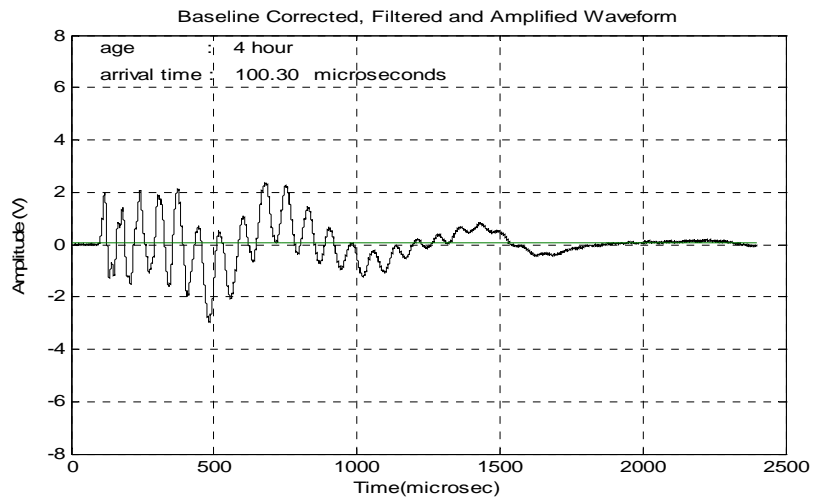


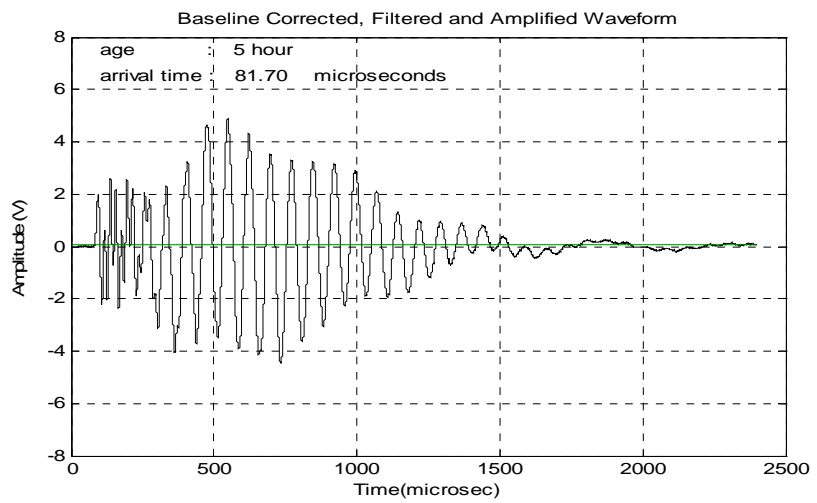
Figure 5.3. The change in waveforms during hydration for mortar specimen

4 hours



5 hours

(final set:  
5.49 hours)



6 hours

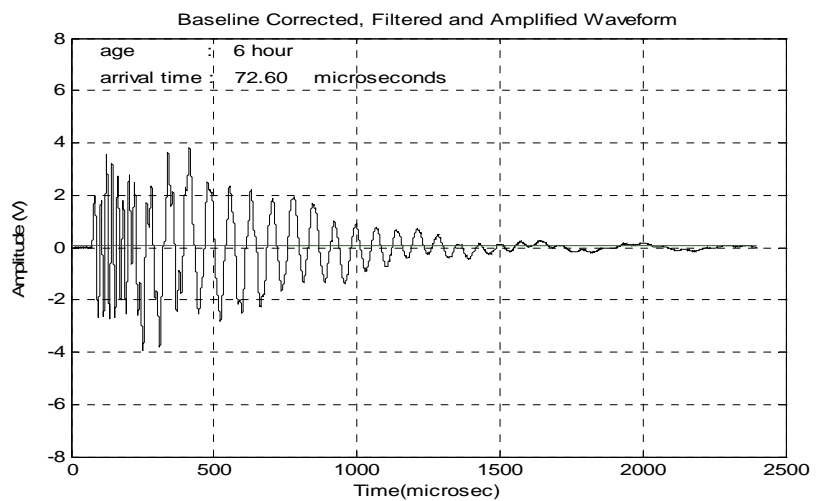
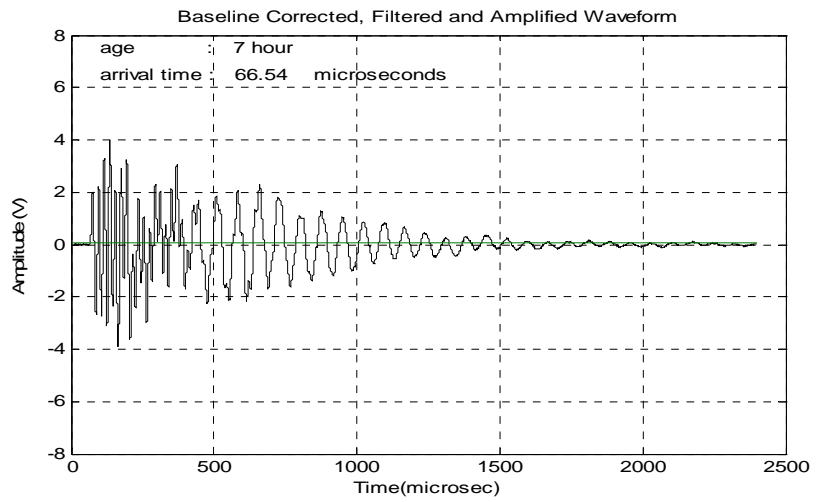
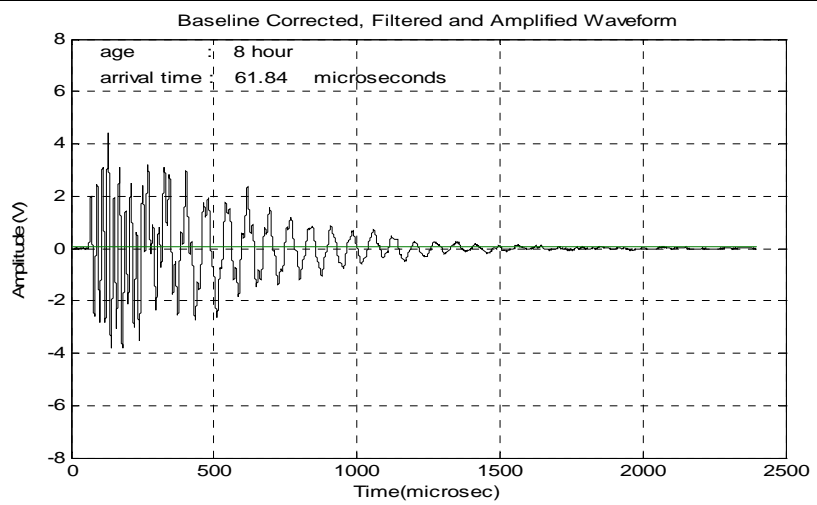


Figure 5.3. (continued)

7 hours



8 hours



10 hours

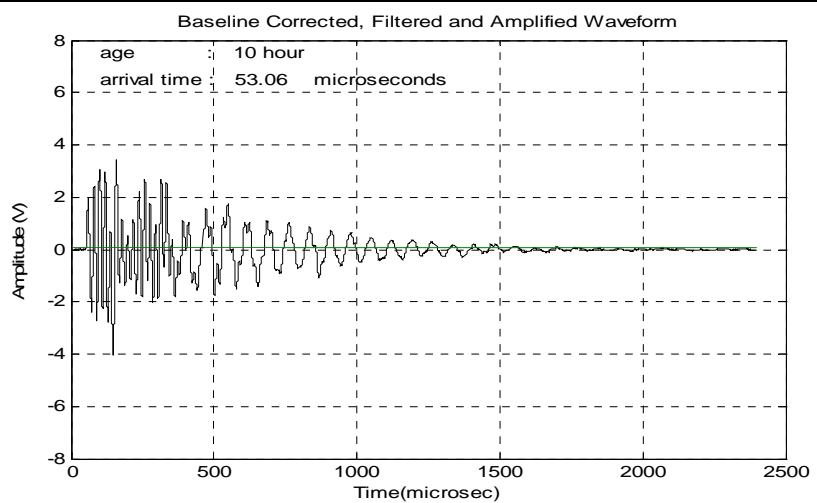
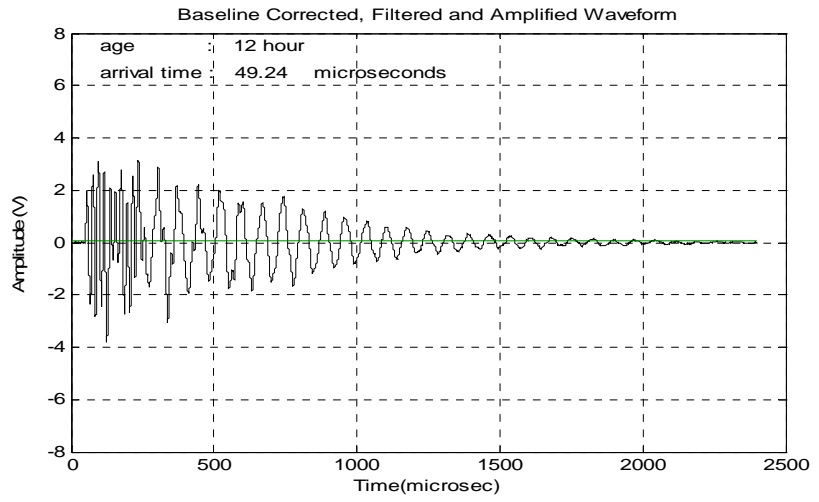
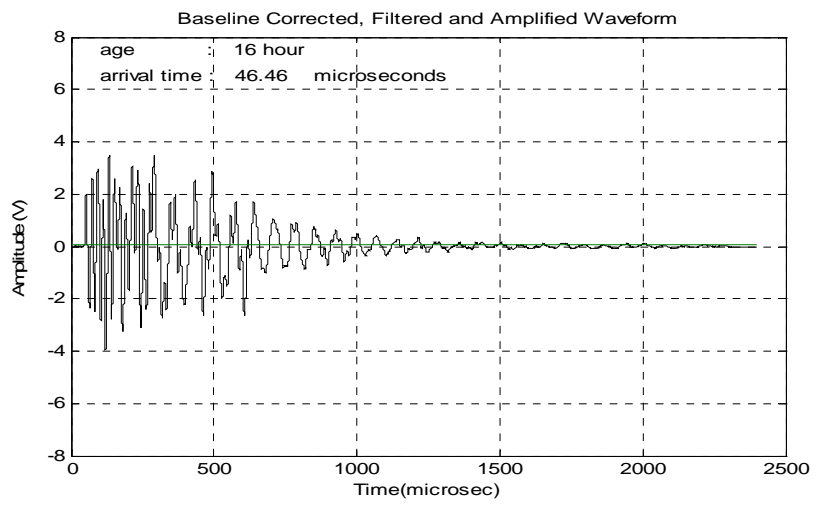


Figure 5.3. (continued)

12 hours



16 hours



20 hours

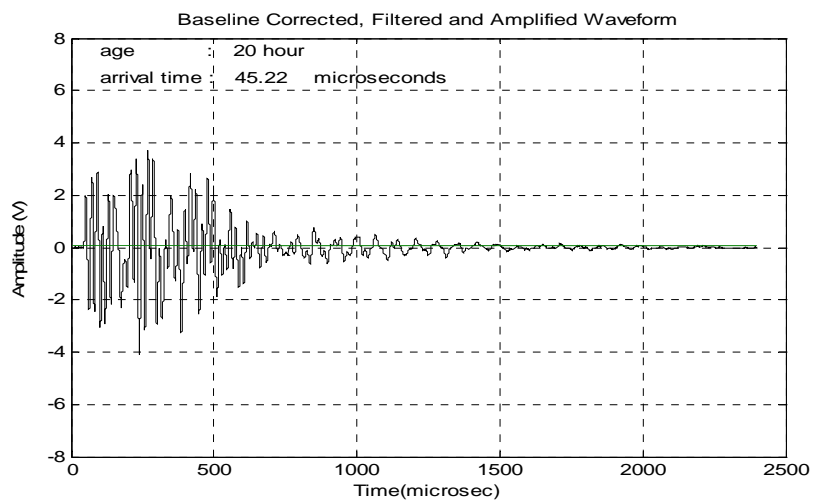
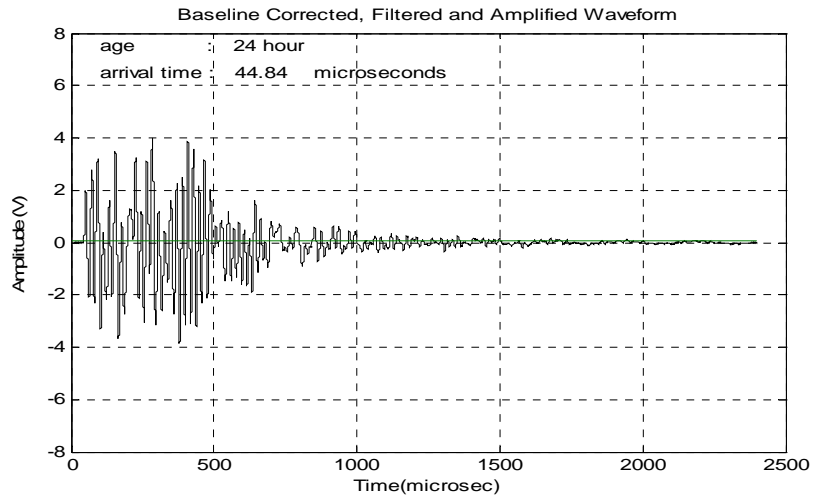
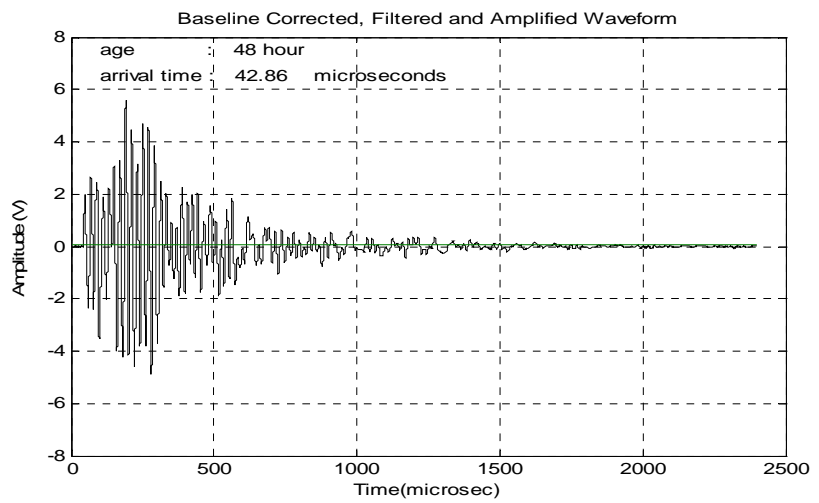


Figure 5.3. (continued)

24 hours



48 hours



72 hours

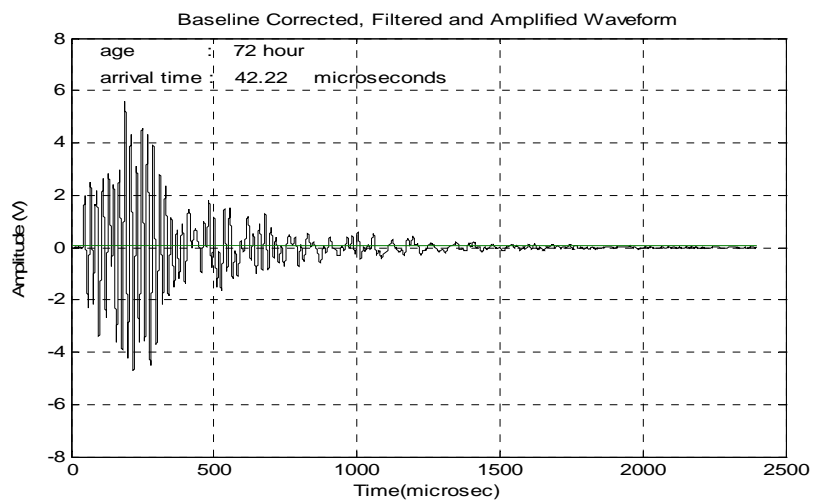


Figure 5.3. (continued)

### 5.3 Development of Ultrasonic Pulse Velocity in Cement Pastes

Ultrasonic pulse velocity (UPV) measurements were carried out in cement pastes having three different w/c ratios for the first 24 hours after mixing with a time interval of 15 minutes. The change of UPV with time for the three w/c ratios used is shown in Figure 5.4.

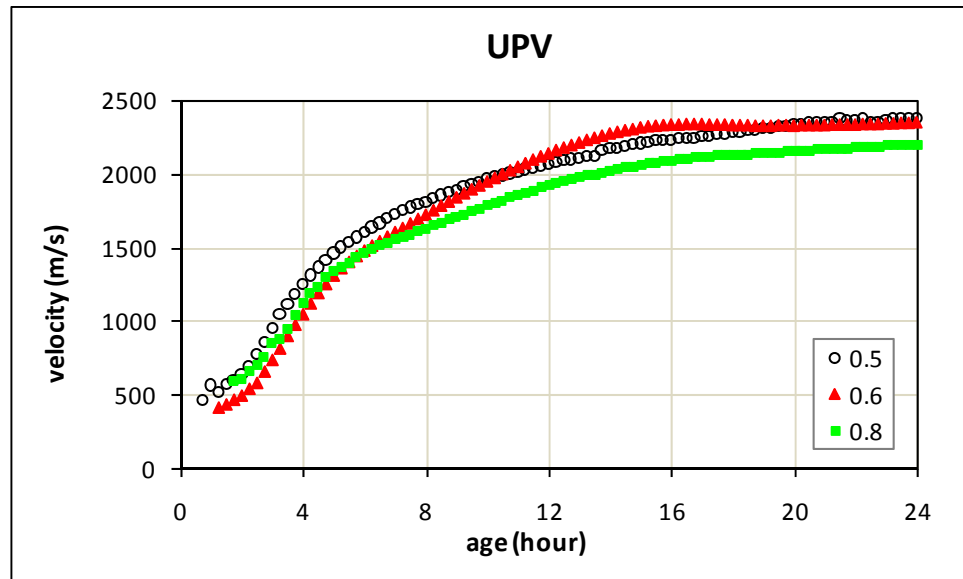
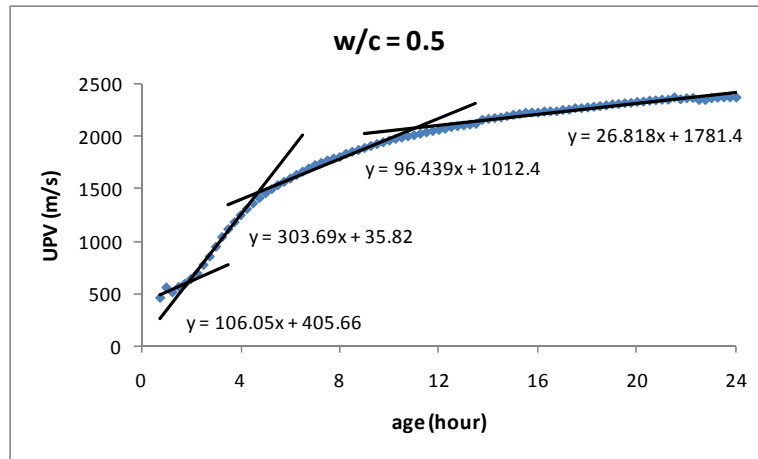


Figure 5.4. Development of UPV in cement pastes for different w/c ratios

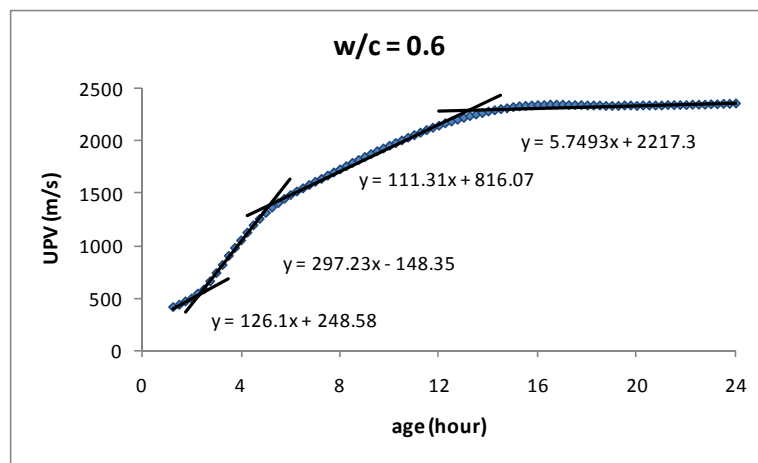
From Figure 5.4, it is seen that UPV increases with time following an S-shaped curve. The relationship of UPV and age can be separated into four distinct portions which are almost linear. The portions for each w/c ratio are shown in Figure 5.5, separately. First of all, the behavior for about the first hour after mixing could not be observed with the experimental set-up used. This most probably resulted from the fact that the waves could not be distinguished from the electrical noise during the very early stages of hydration due to high attenuation. Just after mixing, the solid particles of the cementitious system are not interconnected, therefore, there is high attenuation and the wave velocities cannot be measured accurately. The first meaningful velocity measured in the cement pastes is about 500 m/s. After the first point the velocity could be determined, the UPV increases at a slow rate which is

shown as the first linear portion. However, as the behavior before that portion could not be determined accurately, the lines fitted on the first few measurements are not reliable. During this portion the dormant period still continues. The slight increase in UPV might be due to the settlement of the cement paste as a result of its own weight. However, the number of data from this region is limited, so making conclusions based on this portion is not reasonable. The following three linear portions are more important in interpreting the results of the investigation. In the second stage, the UPV starts to increase with a steep slope as a result of the formation of hydration products after the dormant period. The rate of change of UPV is highest in this part. The following portion has a milder slope as compared to second portion defined in the UPV development curves. Lastly, the slope of UPV becomes very mild in the fourth region. However, the increasing of UPV indicates that the formation of hydration products still continues. On the other hand, the decreasing slopes in the linear portions of the UPV development with respect to time could be an indication of reaching an asymptotic value in time. The value obtained at the end of 24-hour hydration shows that this asymptotic value will depend on the w/c ratio of the cement paste as the rate of UPV development is very small in the last stage as compared to previous stages.

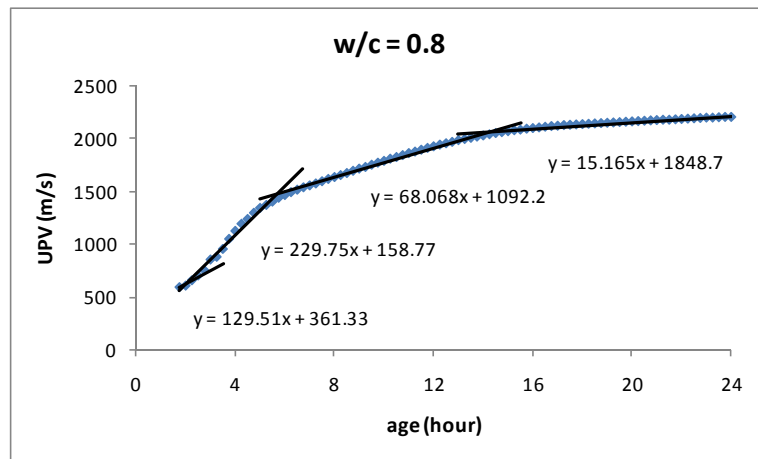
At the end of 24 hours, the cement paste with w/c ratio of 0.5 reaches a UPV value of 2375 m/s, while the cement paste with w/c ratio of 0.6 reaches a UPV of 2350 m/s and cement paste with w/c ratio of 0.8 reaches a UPV of 2200 m/s. This indicates that the UPV development is dependent on w/c ratio of the paste. High w/c ratio usually results in low UPV values in the pastes. Additionally, when the slopes of the portions of the UPV development curves are compared, it is seen that the slope of the second part is higher for the paste with lower w/c ratio. This portion is defined as the stage when the hydration products formation is fastest.



a) w/c ratio = 0.5



b) w/c ratio = 0.6



c) w/c ratio = 0.8

Figure 5.5. The stages of UPV development in cement pastes with different w/c ratios

After mixing the cement with water, the cement particles are initially almost evenly distributed within the liquid phase. In first few minutes some flocculation of the cement particles because of opposite zeta potentials and Van der Waals forces occurs. However, these flocculations may easily be destroyed upon ultrasound applications to the paste (Odler, 2005). Although the viscosity of the water-cement mixture increases due to flocculation of cement particles, this process is reversible upon ultrasound application. This can be one of the reasons for the unreasonable ultrasonic velocity measurements within the first few hours.

With progressive hydration, the precipitation of hydration products on the surfaces of the cement particles causes some roughening of these surfaces. Continuing growth of hydration products results in the contact of individual cement particles covered with these. Eventually, the number of contacts between the cement particles increases to form a three-dimensional network of solids. This phenomenon stops the unlimited deformability of the paste by increasing its viscosity. Still however, the solid network can be broken down easily because there is almost no strength of the paste. As the hydration progresses, amount of hydrated materials increases and the pore space reduces. The bond between solid particles will further strengthen resulting in hardening and load carrying capacity. These features can also be observed in the ESEM micrographs of very early age cement pastes given in Figure 5.2.

The rate of increase in UPV development changes as hydration progresses in cement pastes. As the UPV increases with progress of hydration, the rate of UPV could be related to the rate of hydration reactions. In order to observe how the rate of UPV behaves, the first derivative of UPV curves with respect to time was calculated numerically. The difference in UPV between two measurements was divided by the time interval between the two adjacent measurements. Curve smoothening technique of moving average with two-points was applied to the results. The results are shown in Figure 5.6 for each w/c ratio.

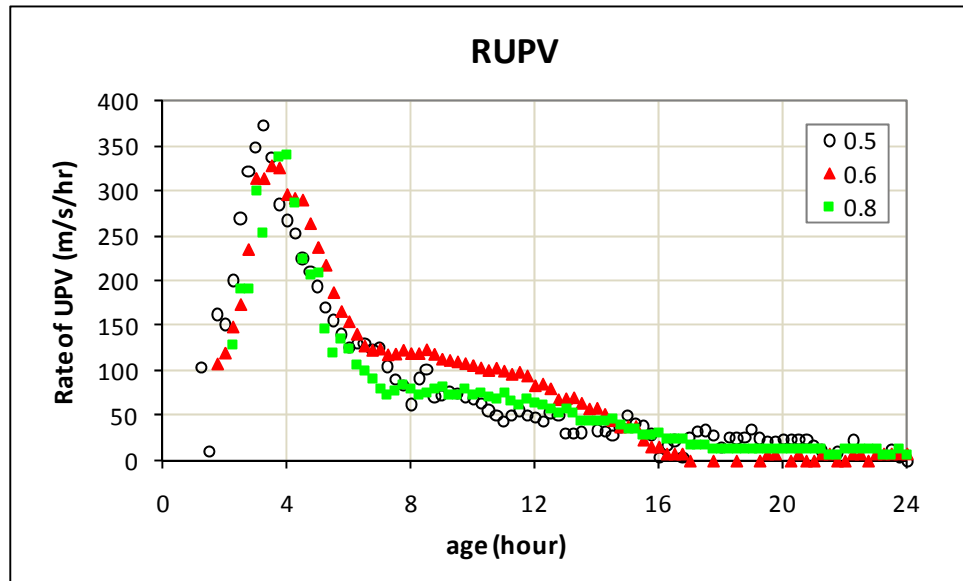


Figure 5.6. Rate of UPV change with time in cement pastes for different w/c ratios

In Figure 5.6, it is seen that the rate of increasing of UPV changes interestingly during the hydration process of cement pastes. After a steep increase, it starts to decrease with different slopes at different stages. Finally, it reaches to a value around zero. The peak seems to occur between 3 and 4 hours in all cement pastes. Although the occurrence time seems to change in a very narrow range, it is seen in the curves that as the w/c ratio increases, the peak is shifted slightly to the later ages.

Actually when the curves in Figure 5.6 are examined, 5 different stages can be distinguished in the rate of UPV curves for each w/c ratio. In the first stage the rate of UPV increases steeply. After reaching a peak value at about 3 to 4 hours it starts to decrease with a steep slope. Thirdly, a short constant portion is observed. The length of constant portion seems to be dependent on w/c ratio of the paste. In the fourth stage, the rate of UPV development starts to decrease until about 16 hours. Lastly, the rate of UPV approaches an asymptotic line around zero which means at that period the UPV does not change significantly.

## 5.4 Setting Time Test Results in Cement Pastes

The initial and final setting time values of cement paste specimens were determined by Vicat apparatus for each w/c ratio. The change of initial and final setting times determined by Vicat apparatus applied to pastes with different w/c ratios are shown in Figure 5.7.

As expected, increasing w/c ratio results in longer setting time. For both initial and final setting times, almost a perfect linear relationship is observed between the w/c ratio and setting time. The slope for final setting time is greater than the slope of initial setting time. This means end of setting is delayed more when w/c ratio is increased as compared to start of setting in cement pastes. For small w/c ratios, the start and end of setting are closer to each other.

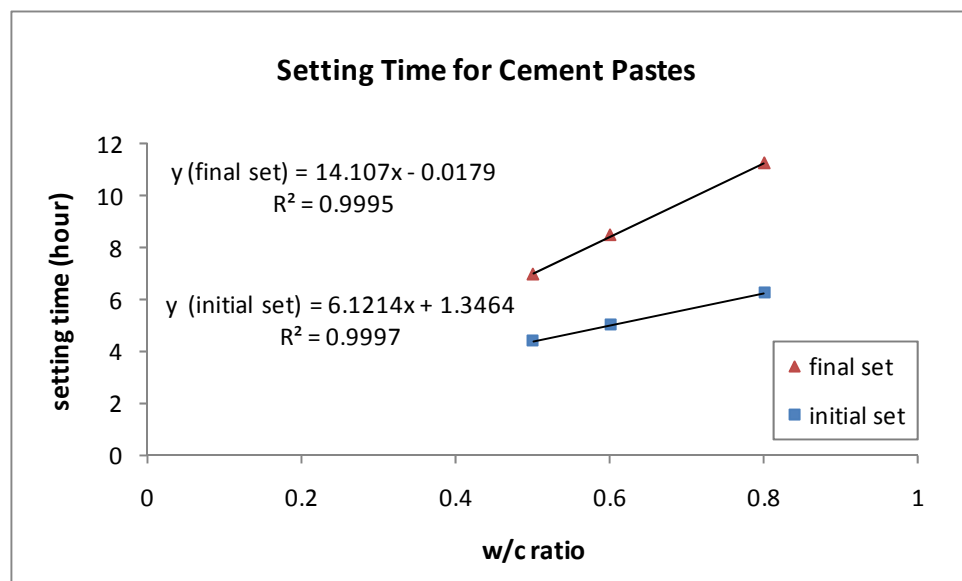


Figure 5.7. Setting time values for each w/c ratio

The UPV values corresponding to initial and final setting times were determined from UPV-time curves for each cement paste with different w/c ratios. The setting time results and the corresponding UPV values are listed in Table 5.1. The averages of the UPV values for start and end of setting are also shown in the table.

Table 5.1. Setting time test results and corresponding UPVs

w/c ratio	Initial set (h)	UPV <sub>@initialset</sub> (m/s)	Final set (h)	UPV <sub>@finalset</sub> (m/s)
0.5	4.42	1346	7.00	1729
0.6	5.00	1309	8.50	1785
0.8	6.25	1490	11.25	1873
average		1382		1793

As seen in Table 5.1, initial setting time occurs when the medium reaches a UPV in the range of 1309-1490 m/s. The average of values for three w/c ratios corresponds to 1382 m/s. On the hand, during the final setting time, the medium has an UPV in the range of 1729-1873 m/s. The average for final setting time corresponds to 1793 m/s. Therefore, it could be concluded that the initial setting time for cement pastes occurs when the UPV reaches a velocity about 1380 m/s while final setting time occurs when the UPV reaches a velocity about 1790 m/s regardless of the w/c ratio of the paste.

#### 5.4.1 Determination of initial setting time from UPV curves in cement pastes

It was aimed to estimate the initial setting time directly from the UPV measurements. From the UPV-time curves of cement pastes, it is obvious that the development of UPV is related to the hydration process of the paste. As shown in Figure 5.5, UPV development curves can be divided into four linear portions. As the UPV is related to density and modulus of elasticity of the materials, the points where the slopes change could correspond to some critical points of hydration. Therefore, it could be useful to determine those points of intersection of linear portions. The points were determined from the line equations fitted to portions which are shown on the graphs of Figure 5.5. The intersection times and the corresponding UPV values are given in Table 5.2 for each w/c ratio. In the table, the average of UPV values for each intersection, the maximum difference and the

percentage of the maximum difference with respect to average values are also shown.

Table 5.2. The intersection points of linear portions and corresponding UPVs

w/c ratio	Int. of 1-2 (hr)	UPV (m/s)	Int. of 2-3 (hr)	UPV (m/s)	Int. of 3-4 (hr)	UPV (m/s)
0.5	1.87	617	4.71	1407	11.04	2108
0.6	2.32	551	5.19	1348	13.27	2232
0.8	2.02	612	5.77	1439	14.30	2038
Average (m/s)		593		1398		2126
Range (m/s)		66		91		194
Range/average*100 (%)		11.1		6.5		9.1

If the UPV values corresponding to the critical points of UPV development curves are examined, it is seen that those points occur at similar velocities. As the UPV is related to the physical properties of the medium, it can be concluded that at the intersections of linear portions the materials have similar properties regardless of the w/c ratio. This result is a proof that UPV can be a reliable tool in monitoring the hydration process of cement pastes.

The average of UPVs corresponding to the intersection of 2<sup>nd</sup> and 3<sup>rd</sup> linear portions of UPV development curves is 1398 m/s. This value is quite close to the value given in Table 5.1 for initial setting time. The initial setting time values determined from Vicat apparatus and the point where the second slope change on the UPV development curves occurs (i.e. intersection of 2<sup>nd</sup> and 3<sup>rd</sup> linear portions as seen in Figure 5.5) are compared in Table 5.3.

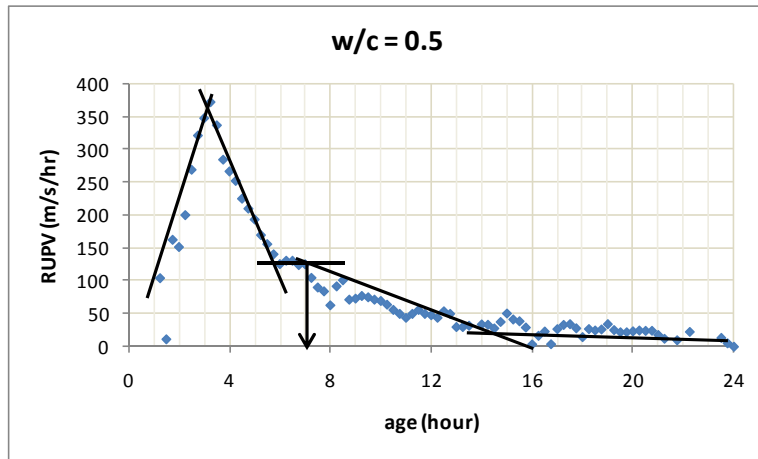
Table 5.3. Comparison of Vicat and UPV for initial setting time determination

w/c ratio	Initial set (h)	UPV <sub>@initialset</sub> (m/s)	Int. 2-3 (h)	UPV <sub>@int.</sub> (m/s)	Difference (h)	Difference %
0.5	4.42	1346	4.71	1407	0.31	7.01
0.6	5.00	1309	5.19	1348	0.19	3.80
0.8	6.25	1490	5.77	1439	-0.48	-7.68
Average (m/s)		1382		1398		

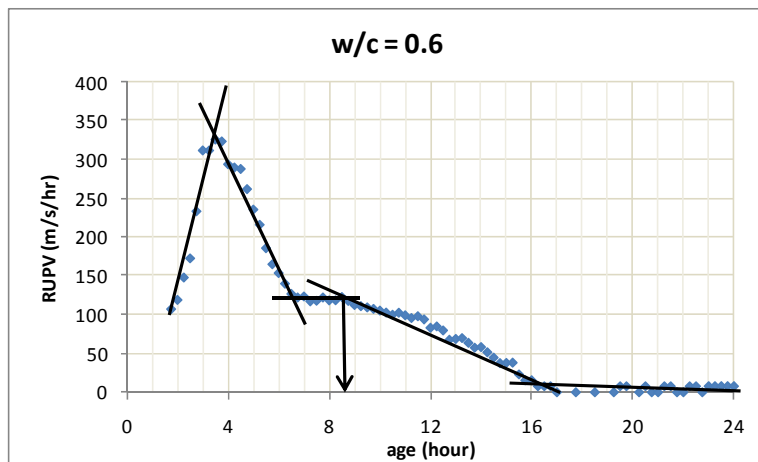
The percent difference was calculated with respect to initial setting time as determined from the standard Vicat test method. The maximum difference is less than 8% which is a quite good approximation for non-destructive test methods. Therefore, it can be stated that the initial set occurs in cement pastes at the point where the second change in the slope of idealized UPV curves occurs. At that point the UPV is around 1400 m/s in all cases independent of the w/c ratio of the paste. Ultrasonic test seems to be a good method for initial setting time determination.

#### 5.4.2 Determination of final setting time from UPV curves in cement pastes

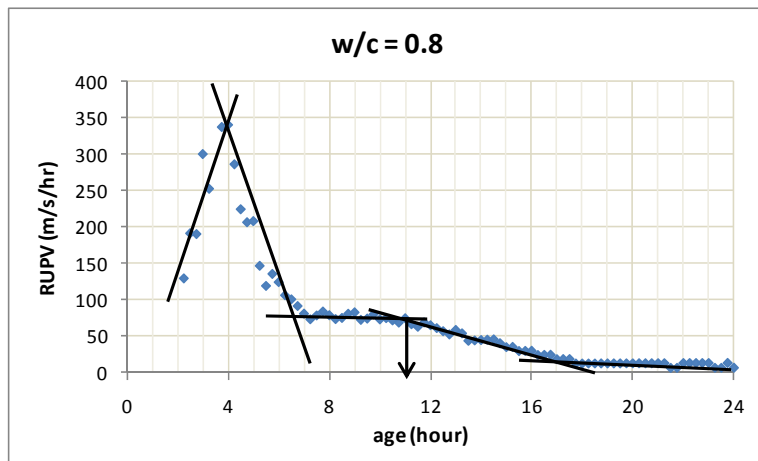
The final setting time of cement paste could not be determined directly from the characteristic points of UPV development curves. However, the rate of UPV development curve gives valuable information about the setting behavior. As explained in Figure 5.6, the rate of UPV development curves can be divided into five distinct linear stages. Those stages of rate of UPV development curves are shown in detail in Figure 5.8 for each w/c ratio, separately.



a) w/c ratio = 0.5



b) w/c ratio = 0.6



c) w/c ratio = 0.8

Figure 5.8. The stages of RUPV development curves of cement pastes with different w/c ratios

In the rate of UPV development curves, the peak which is the intersection of 1<sup>st</sup> and 2<sup>nd</sup> linear portions, the beginning of the plateau which is the intersection of 2<sup>nd</sup> and 3<sup>rd</sup> linear portions, the end of plateau which is the intersection of 3<sup>rd</sup> and 4<sup>th</sup> linear portions and the intersection point of 4<sup>th</sup> and 5<sup>th</sup> linear portions were determined. The results and the corresponding UPV values are given in Table 5.4 for each w/c ratio. In the table, besides the values of UPV, the averages and the deviations are also given for each characteristic point.

Table 5.4. The characteristic points of RUPV curves and the corresponding UPVs

w/c ratio	1-2 (hr)	UPV (m/s)	2-3 (hr)	UPV (m/s)	3-4 (hr)	UPV (m/s)	4-5 (hr)	UPV (m/s)
0.5	3.25	1042	6.00	1601	7.00	1729	14.60	2191
0.6	3.50	899	6.50	1543	8.60	1796	16.50	2339
0.8	3.75	1049	7.00	1554	11.00	1858	17.25	2122
Average (m/s)		997		1566		1794		2217
Range (m/s)		150		58		129		217
Range/average*100 (%)		15.0		3.7		7.2		9.8

As in the case of the characteristic points of UPV development curves, similar UPV values were obtained for the characteristic points of rate of UPV development curves. As UPV depends on the density, elastic modulus and Poisson's ratio of the body, it can be concluded that at those points the pastes have similar physical and elastic properties whatever the w/c ratio of the material is.

For the determination of final setting time of cement pastes, the results listed in Table 5.1 and 5.4 were compared. The results showed that the final setting time as determined by Vicat apparatus is close to the point where the horizontal platform in rate of UPV development curve ends. The comparison of results is given in Table 5.5. The differences between two determinations were also calculated. Additionally, the difference in percentage in determining the final setting time from

rate of UPV development curves was also given with respect to the final setting time as determined by Vicat test method.

Table 5.5. Comparison of Vicat and UPV Methods for final setting time determination

w/c ratio	Final set (h)	UPV <sub>@finalset</sub> (m/s)	End of Platform (h)	UPV <sub>@plt</sub> (m/s)	Difference (h)	Difference %
0.5	7.00	1729	7.00	1729	0.00	0.00
0.6	8.50	1785	8.60	1796	0.10	1.18
0.8	11.25	1873	11.00	1858	-0.25	-2.22
Average (m/s)		1793		1794		

As seen in Table 5.5, the difference is quite small. Therefore, it can be concluded that final setting time can be determined from UPV measurements. Additionally, it is seen that the UPV when the final setting time occurs is around 1800 m/s for any w/c ratio.

As a result of above discussions, it can be stated that determination of setting times in cement paste by ultrasonic test method is quite a reliable method. The standard Vicat test describes two arbitrary rheological changes occurring in the viscosity of the paste during the course of hydration as the initial and final setting. On the other hand, estimation of setting through UPV is something that depends on the physical changes that occur in the paste. As mentioned previously, UPV depends on density ( $\rho$ ), elastic modulus (E) and Poisson's ratio ( $\nu$ ) of the material. As the density of fresh cement paste does not change significantly within the first 24 hours, it is the E and  $\nu$  that affect the UPV and its development rate during the hydration process. As long as the UPV is determined accurately, it seems to be a dependable method. From the test results it could be claimed that initial setting in cement paste occurs around a UPV of 1400 m/s and final setting occurs around a UPV of 1800 m/s.

Additionally, those points could be determined as the characteristic points of UPV and rate of UPV development curves. The initial setting time corresponds to the point of second change of the slope of the idealized UPV development curve, while the final setting time corresponds to the end point of the horizontal platform in the rate of UPV development curves.

Besides the setting time, other changes in the cement paste structure seem to be reflected to UPV measurements. For this purpose, both the UPV and rate of UPV curves will be compared with the rate of heat of hydration curves for cement pastes in the following section.

### 5.5 Heat of Hydration and Rate of Heat of Hydration Test Results

The rate of heat of hydration of cement pastes with different w/c ratios were determined by isothermal conduction calorimetry method for the first 72 hours after the mixing operation. The results for each w/c ratio are given in Figure 5.9 in a graphical form.

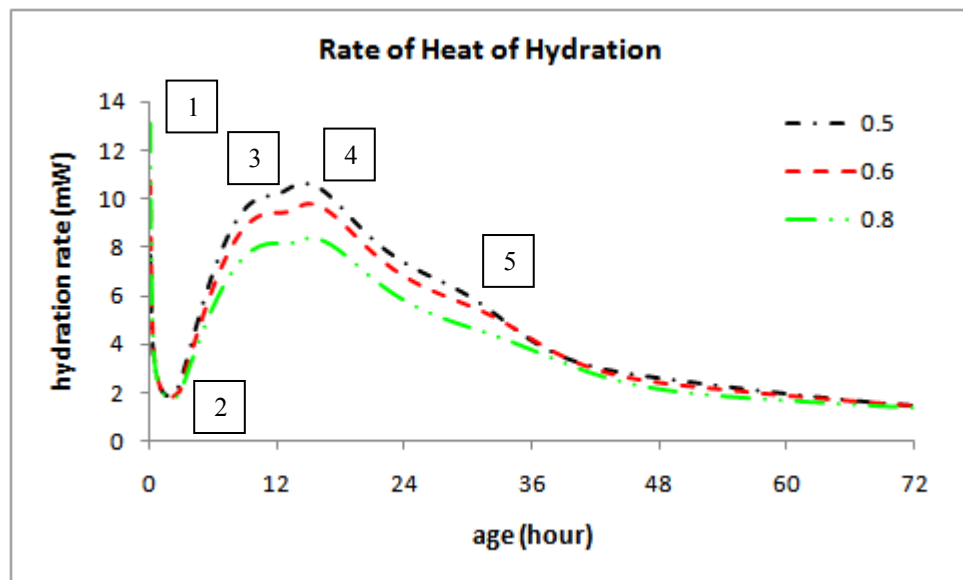
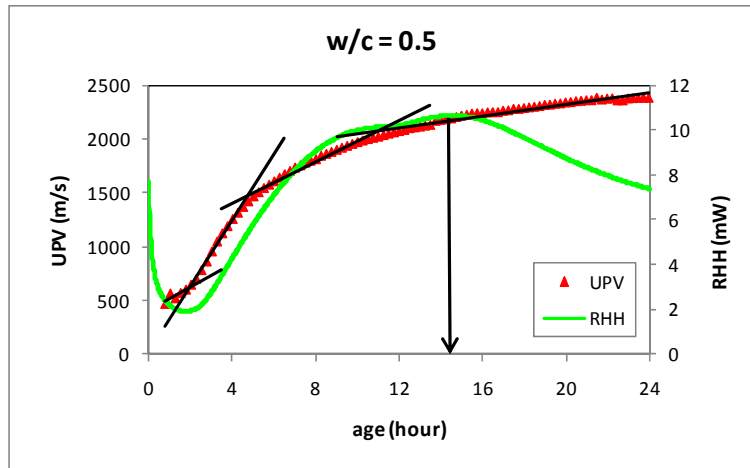


Figure 5.9. Rate of heat of hydration of cement for different w/c ratios

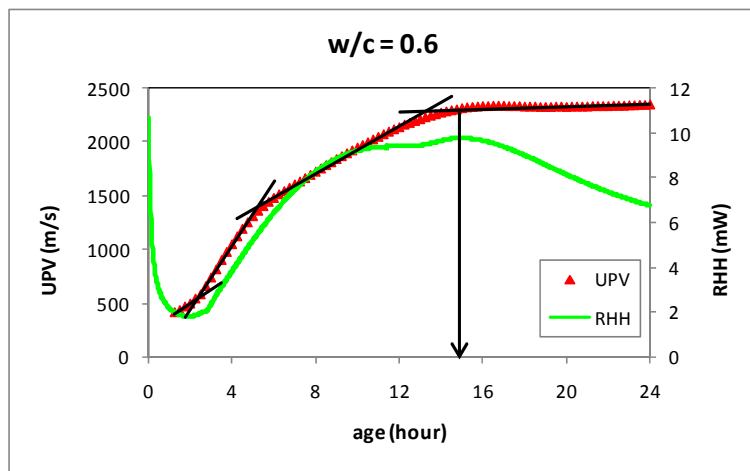
As seen in Figure 5.9, in cement pastes with lower w/c ratios, the hydration progresses faster due to higher amounts of cement particles. Actually, the difference in the rate of hydration is very significant for different w/c ratios during the acceleration stage of hydration of cement particles. During this stage, pastes with smaller w/c ratio hydrate faster.

In Figure 5.9, the stages of hydration explained in Chapter 2 can be identified in the rate of heat of hydration curves. The labeling is similar to the labeling of Figure 2.1. Stage 1 corresponds to pre-induction period. In this stage the ionic species in the cement dissolves. However, as this stage lasts only a few minutes, during the preparation of the specimen and the installation of the apparatus this stage may not be able to be monitored exactly. Stage 2 is the dormant period. As explained in Chapter 2, in this stage hydration slows down. In the acceleration stage, the state of hydration of  $C_3S$  increases and some hydration of  $C_2S$  starts; therefore, the rate of heat evolution increases. Setting occurs within this stage. The peak as shown as Point 3 corresponds to hydration of  $C_3S$ . Sometimes a second peak in rate of hydration curve is obtained which corresponds to formation of renewed Aft which is labeled as Point 4 in Figure 5.9. The shoulder in the figure which is designated as Point 5 describes the time when Aft-Afm transformation occurs.

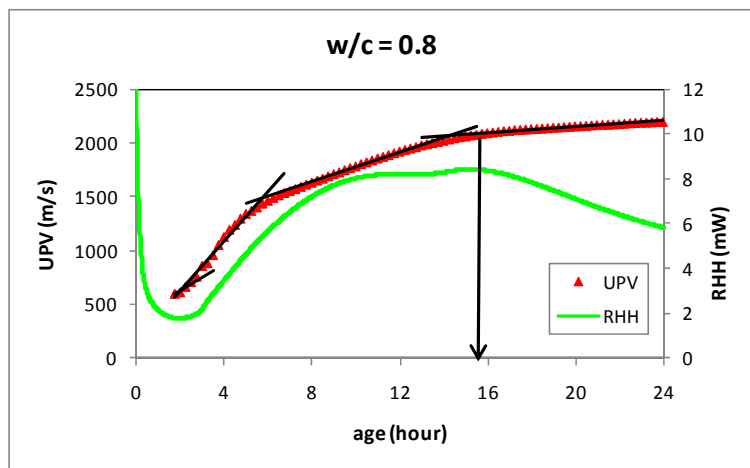
Rate of heat of hydration results shows how the hydration reactions progress in the cement paste. On the other hand, UPV also reflects various changes in the cement paste structure during hydration process. In order to check whether UPV measurements are sensitive to other changes in the cement paste besides setting process, UPV development and rate of heat of hydration curves are compared for different w/c ratios in Figure 5.10. On the figure, UPV and rate of heat of hydration (RHH) curves are shown on the same graph for the first 24 hours after mixing. The left vertical axis shows UPV results, while the right vertical axis shows RHH test results, the horizontal axis is the age of the specimen.



a)  $w/c=0.5$



b)  $w/c=0.6$



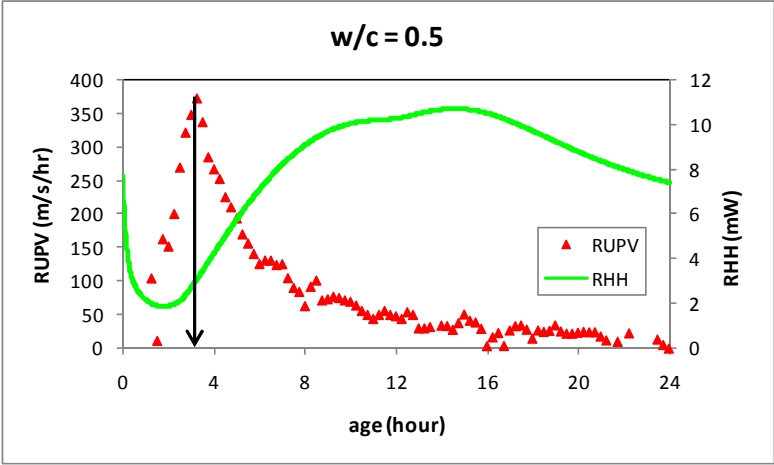
c)  $w/c=0.8$

Figure 5.10. Comparison of UPV and RHH development in cement pastes

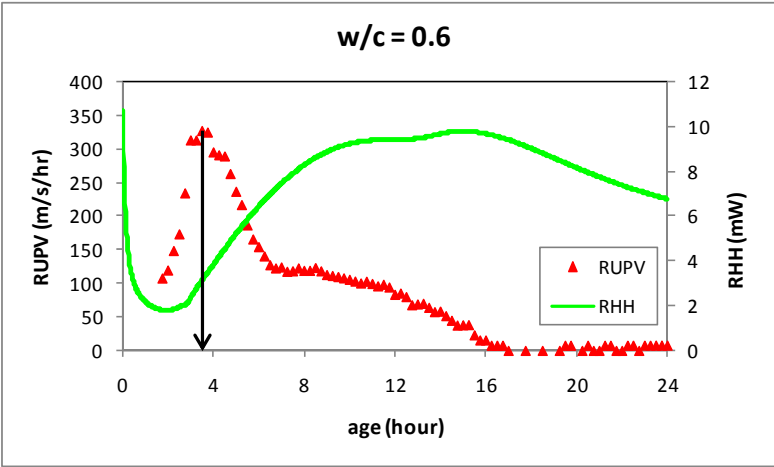
UPV development curves were divided into four linear portions. The slope of the last portion is very mild as compared to the other three parts for each w/c ratio. This indicates that the increase in UPV is small after that time. From Figure 5.10, it is seen that the start of 4<sup>th</sup> portion of the UPV curves corresponds roughly to the start of post-acceleration stage as shown in Figure 2.1. The deceleration period starts at approximately 14.5 hours, 15.0 hours and 15.5 hours after mixing in cement pastes with w/c ratios of 0.5, 0.6 and 0.8, respectively. The corresponding UPV values for those points are 2185 m/s, 2316 m/s, 2080 m/s, respectively. Therefore, it could be stated that the deceleration period starts when UPV is around 2100 m/s. However, as after that point the increase in UPV is small, this value might be dependent on the w/c ratio of the material. Beyond that point the hydration reactions also start to slow down.

During the acceleration stage of the hydration process, the hydration of C<sub>3</sub>S compound is accelerated. Considering that the hydration products formed in this stage are C-S-H, Aft and CH, acceleration of C<sub>3</sub>S hydration will result in higher density and higher modulus of elasticity of the paste as hydration continues. Although it is not possible to give a quantitative explanation for the increasing rate of UPV within this stage, it can be stated that besides the decreasing porosity, the increasing amount of C-S-H and CH upon accelerated C<sub>3</sub>S hydration at expense of Aft formation will obviously result in higher density and modulus of elasticity of the fresh paste since the density and modulus of elasticity of (C-S-H + CH) is approximately 1.3 and 15 times greater than those of Aft, respectively (Odler, 2005; Mindess and Young, 1981).

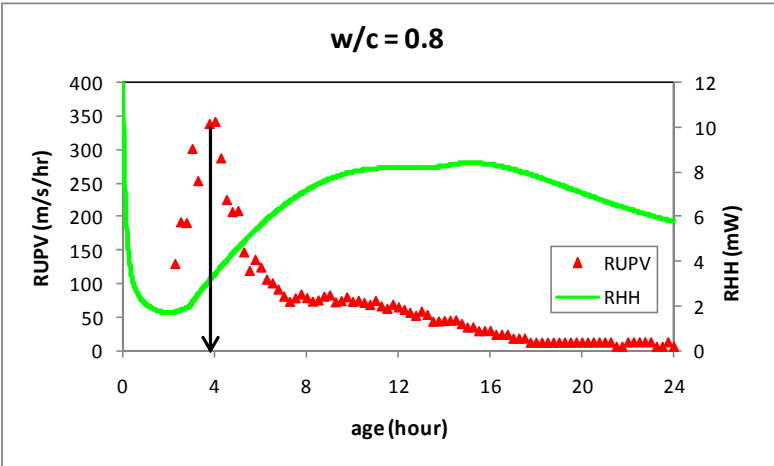
The rate of heat of hydration curves of cement pastes were also compared with the rate of UPV development curves for each w/c ratio. The comparison is shown in Figure 5.11 for each w/c ratio, separately. On the figures the left vertical axis shows the rate of UPV (RUPV) results, while the right vertical axis shows the rate of heat of hydration (RHH) results.



a) w/c=0.5



b) w/c=0.6



c) w/c=0.8

Figure 5.11. Comparison of RUPV and RHH development in cement pastes

As it was previously stated the rate of UPV development curves can be idealized by five linear portions. The first two parts intersect making a peak at the initial stages of the hydration reactions. The occurrence of peak and the corresponding UPV values were already listed in Table 5.4. The peak occurs at 3.25 hours, 3.50 hours and 3.75 hours for cement pastes having w/c ratio of 0.5, 0.6 and 0.8, respectively. As given in Table 5.4, the corresponding UPV values are 1042 m/s, 899 m/s and 1049 m/s, respectively. The comparison of RUPV and RHH reveals that the initial peak in RUPV curves can be taken as the end of the dormant period as determined from RHH curves. From the UPV values, it could also be stated that the dormant period ends and the acceleration period starts when the UPV in the cement pastes reaches approximately 1000 m/s.

The heat of hydration of cement pastes were obtained by taking the integral of the rate of heat of hydration curves with respect to time. The heat of hydration results are given in Figure 5.12 for each w/c ratio.

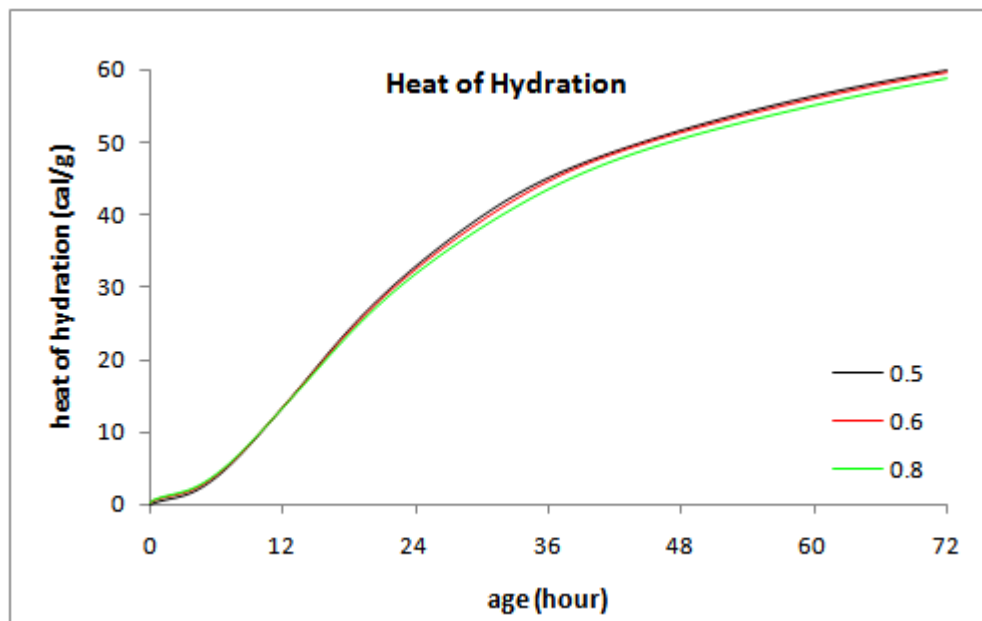


Figure 5.12. Heat of hydration of cement pastes for different w/c ratios

As seen in Figure 5.12, the total heat of hydration in cement pastes increases as the hydration progresses. The increase in heat evolution is slow at the beginning. After about 4 hours, the rate of heat evolution increases, and the hydration progresses more rapidly. As time passes the rate of heat evolution decreases, and the increase in heat of hydration continues with a milder slope. Additionally, the heat evolution during hydration process is a little higher in cement pastes with low w/c ratio. However, the effect of w/c ratio on heat of hydration of cements is not as significant as the effect on the rate of heat of hydration of cements. Therefore, it can be stated that rate of heat of hydration results describes the hydration process better than the heat of hydration results.

### 5.6 Development of Ultrasonic Pulse Velocity in Cement Mortars

The development of ultrasonic pulse velocity (UPV) in cement mortars was determined for 28 days after mixing. Mortars having three different w/c ratios of 0.5, 0.6, and 0.8 were tested. The molds used in UPV testing of mortars had the dimensions of 15\*15\*15 cm. The development of UPV in cement mortars is given in Figure 5.13 for each w/c ratio.

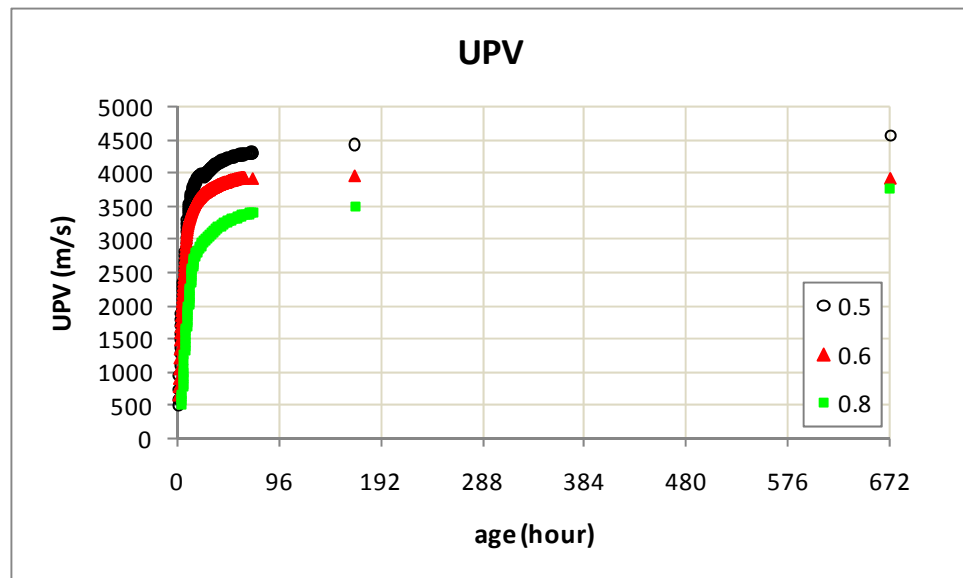


Figure 5.13. Development of UPV in cement mortars for different w/c ratios

In Figure 5.13, it is seen that UPV is higher for the mortars with low w/c ratios and lower for the mortars with high w/c ratios. The UPV depends on the density and dynamic elastic modulus of the medium. As the amount of voids increases when the w/c ratio increases, it is expected that the ultrasonic waves propagate slower in the mortars of higher w/c ratios.

As also seen in Figure 5.13, UPV increases with time as the hydration progresses in cement mortars. However, the increase is faster at early ages and slower at later ages at each w/c ratio. At the initial stages, the hydration process progresses rapidly, as time passes the rate of hydration starts to slow down. During the early stages at which UPV increases rapidly, the formation rate of hydration products is high. However, as hydration progresses, the production rate decreases. From Figure 5.13, it can be concluded that UPV development is more sensitive to the early-age changes in the cement mortars rather than later-age changes. Although the compressive strength development in cement mortars continues, the UPV does not change significantly after about 24 hours after mixing. Therefore, the UPV development with time seems to be more responsive to the hydration process rather than strength development in cement mortars. As a result, it can be concluded that ultrasonic test method could be a suitable testing method to monitor the hydration process in cementitious materials.

In order to observe the development of UPV in cement mortars at early ages, a closer look at the initial stages of hydration is needed. Therefore, the development of UPV in mortars for the first 24 hours after mixing will be examined. During the first 72 hours, the measurements were taken with 15-minutes time interval. Therefore, it could be said the UPV was determined continuously during hydration. The results for the first 24 hours after mixing of the mortars are shown in Figure 5.14 for the three w/c ratios.

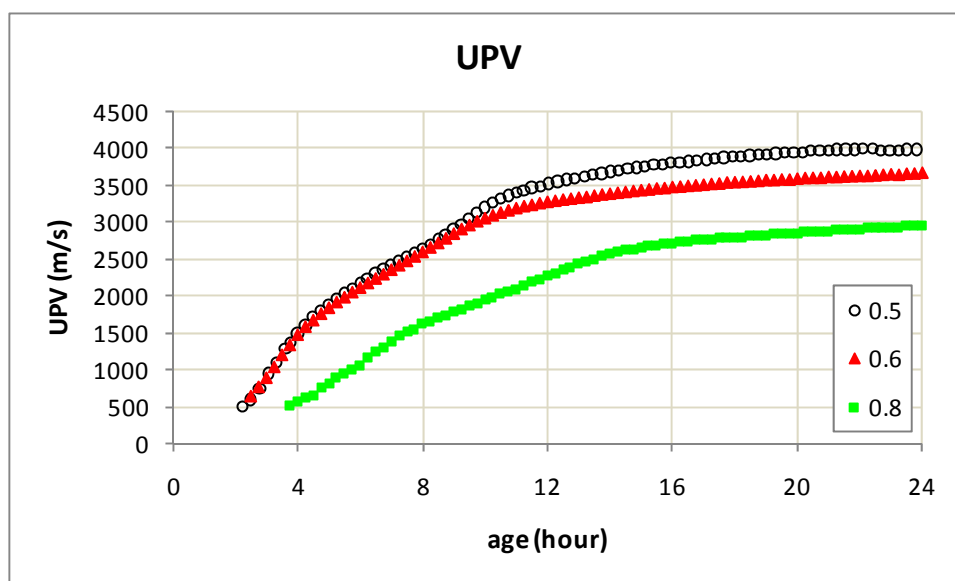
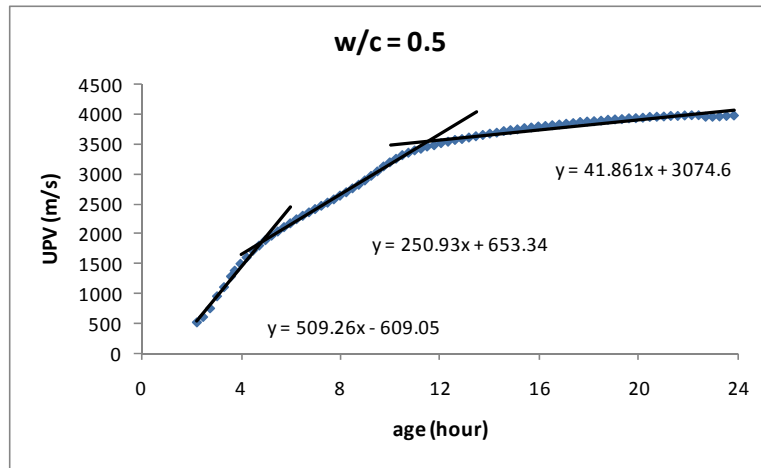
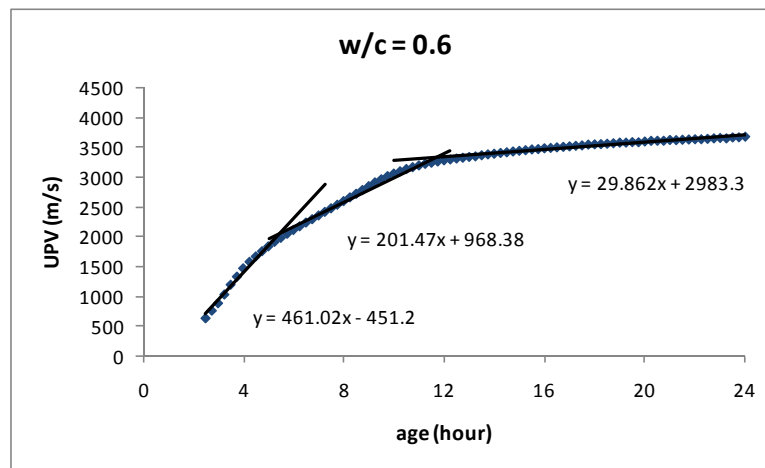


Figure 5.14. Development of UPV in cement mortars for the first 24 hours

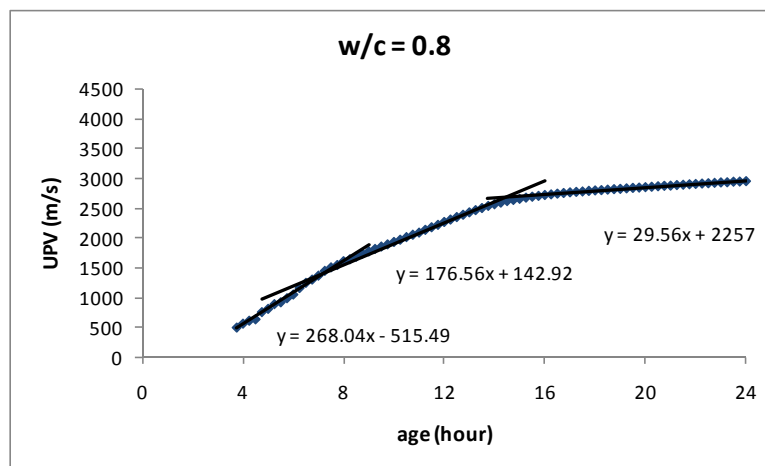
Comparison of Figures 5.4 and 5.14 indicates that the shape of the UPV development curve in hydrating cement mortars is similar to the shape of UPV development curves in hydrating cement pastes. However, in cement mortars, most probably due to the longer travel path and higher attenuative character, the first few hours of hydration during which the UPV development is very slow, could not be captured. In cement mortars, the first waveforms that could be distinguished from the electrical noise were obtained at somewhat later ages. The first readings of UPV in cement mortars were obtained at about 500 m/s for each w/c ratio. However, the time for this gets longer as the w/c ratio of the mortar sample increases. The initial UPV readings of mortars having 0.5 w/c ratio started at 2.25 hours, that of mortars having 0.6 w/c ratio started at 2.50 hours and finally, that of mortars having 0.8 w/c ratio started at 3.75 hours. The velocity values reached at 24 hours are much higher than the velocity values obtained in cement pastes at the same age. The UPV is also sensitive to w/c ratio, for higher values of w/c ratio, UPV is smaller as in the case of cement paste specimens. At the end of 24 hours, the UPV is about 4000 m/s for the mortars having w/c ratio of 0.5, while it is about 3700 m/s and 3000 m/s for the mortars having w/c ratio of 0.6 and 0.8, respectively.



a) w/c ratio = 0.5



b) w/c ratio = 0.6



c) w/c ratio = 0.8

Figure 5.15. The stages of UPV development in mortars for each w/c ratio

From Figure 5.14, it is seen that the UPV development curves of mortars could be defined by three distinct lines. Although the UPV curves were divided into four portions in cement pastes, the first linear part could not be obtained in mortars as at very early ages the UPV could not be measured precisely. The linear portions are shown in Figure 5.15 for each w/c ratio together with the equations of the lines.

As seen in Figure 5.15, the slopes of the linear portions in the UPV development curves decrease step-wisely. The UPV increase is the fastest at the first stage. The slope of second linear portion is milder as in the case of pastes. The third linear portion has a very mild slope. As in the case of cement paste hydration, the increase in UPV is an indication for the formation of hydration products and development of elastic properties in the body. The slopes of the lines of each portion for each w/c ratio are listed in Table 5.6.

Table 5.6. Slopes of linear portions in UPV development curves

w/c ratio	Part 1	Part 2	Part 3
0.5	509.26	250.93	41.861
0.6	461.02	201.47	29.862
0.8	268.04	176.56	29.560

In Table 5.6, the changes in the slopes of the lines fitted to the three stages of UPV development curves of the mortar mixtures having different w/c ratios are listed. As seen in the table, the slope decreases step-wise at each portion. Additionally, as w/c ratio increases, the rate of UPV development decreases in all stages. This is reasonable, as for smaller w/c ratios hydration progress faster; therefore, UPV also increases faster as compared to mortar samples with higher w/c ratios.

The points where the slope of UPV changed were also determined. The intersection points of linear portions and the corresponding UPV values are listed in Table 5.7 for each w/c ratio.

Table 5.7. The intersection points of linear portions and corresponding UPVs

w/c ratio	Int. of 1-2 (hr)	UPV (m/s)	Int. of 2-3 (hr)	UPV (m/s)
0.5	4.89	1827	11.58	3465
0.6	5.47	1976	11.74	3260
0.8	7.20	1441	14.38	2609
Average (m/s)		1748		3111
Range (m/s)		535		831
Range/average*100(%)		30.1		27.5

The occurrence of slope change in UPV development curves of mortars is dependent on the w/c ratio of the specimens. For higher w/c ratio, those points were obtained at later ages. The corresponding UPV values are also given in Table 5.7. Although the UPVs are similar for mortars having w/c ratios of 0.5 and 0.6; the values for 0.8 w/c ratio are considerably smaller. The average and the range of UPVs are also given in the same table. It is seen that the range is quite high for each characteristic point. The UPV values for mortars of 0.8 w/c ratio are smaller than the other specimens for all ages due to the larger amount of voids and less amount of solid particles especially at the early stages. After hardening the amount of pores is also large due to high w/c ratio. Additionally, for higher w/c ratios as the cement content was kept constant, the amount of aggregate is decreased. This smaller amount of aggregate also results in lower UPV values. Therefore, it could be concluded that the UPV is dependent on w/c ratio and the amount of aggregates and pores for the each stage of the hydration process.

As in the case of cement pastes, rate of UPV development curves were also obtained numerically from the UPV data of mortar specimens for the first 24 hours after mixing. Same technique was used for smoothening of the resultant curves. The rate of UPV development curves for mortars of different w/c ratios are shown in Figure 5.16.

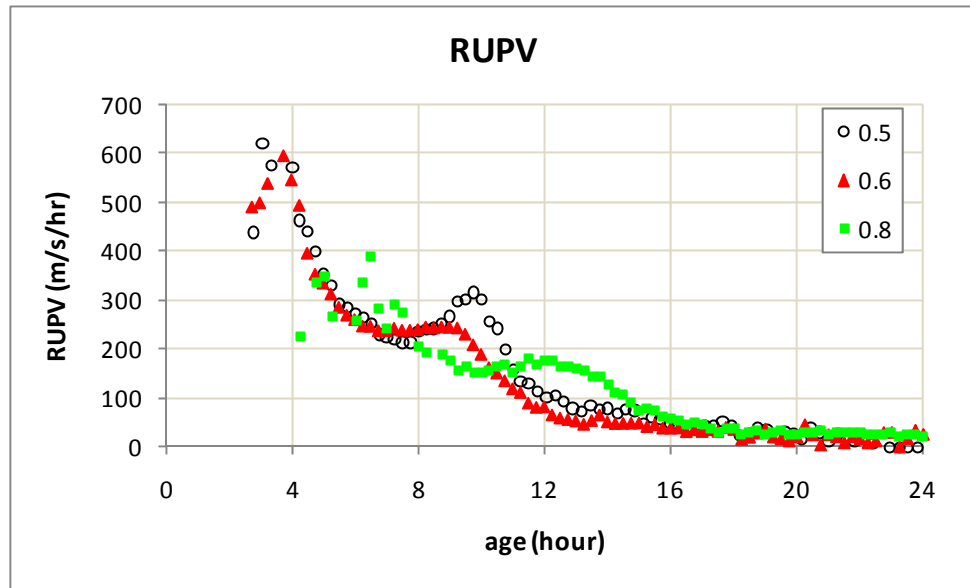


Figure 5.16. Rate of UPV change with time in mortars for different w/c ratios

The rate of UPV development curves with respect to time in mortar samples resembles generally the rate of UPV in cement paste samples. At the initial stage a peak is observed in all w/c ratios. After the first peak, the rate starts to decrease. Unlike the pastes, instead of making a plateau, the RUPV reaches a minimum and then starts to increase slightly until reaching a second small peak. Later on, RUPV starts to decrease approaching an asymptotic value around zero. It is seen in Figure 5.16 that for high w/c ratios, the rate of UPV development is smaller especially at the initial stages. Additionally, for the mortar samples with high w/c ratio, the characteristic points of rate of UPV development curves are generally shifted to later ages. This could be accepted as an indication of slower hydration process in mortars with higher w/c ratios.

The time for the first peak and the minimum points of rate of UPV development curves were determined for each w/c ratio. In order to designate those points 2<sup>nd</sup> degree polynomials were fitted to the related portions. The UPVs corresponding to each point were also calculated from the UPV development curves. The results are given in Table 5.8.

Table 5.8. The characteristic points of RUPV development curves and corresponding UPVs

w/c ratio	1 <sup>st</sup> maximum (hr)	UPV (m/s)	1 <sup>st</sup> minimum (hr)	UPV (m/s)
0.5	3.40	1144	7.45	2509
0.6	3.54	1223	7.49	2475
0.8	5.84	1023	10.20	1969
Average (m/s)		1130		2227
Range (m/s)		200		540
Range/average*100 (%)		17.7		24.2

As seen from Table 5.8, the time of occurrence for first maximum and minimum points of RUPV development curves are dependent on the w/c ratio; for higher w/c ratios those points obtained at later ages. When the UPV values are examined, at the peak of the RUPV development curves, the UPV values are around 1100 m/s; while at the minimum point, the range in UPV measurements is larger. While for 0.5 and 0.6 w/c ratios the UPV is approximately 2500 m/s at the minimum point of RUPV development curve, it is approximately 2000 m/s for 0.8 w/c ratio.

### 5.7 Determination of Setting Time in Mortars

The initial and final setting times of mortar specimens were determined by Penetration Resistance (PR) test according to ASTM C 403. The results for each mortar type and the corresponding UPV values are summarized in Table 5.9. The averages of the corresponding UPV values for each w/c ratio are given in the table. The range of the change in UPV values are also listed.

Table 5.9. Initial and final setting times of mortars and corresponding UPVs

w/c ratio	Initial set (h) $t_i$	UPV <sub>ti</sub> (m/s)	Final set (h) $t_f$	UPV <sub>tf</sub> (m/s)
0.5	3.06	953	5.49	2035
0.6	3.52	1212	5.73	2047
0.8	5.75	1001	9.44	1853
Average (m/s)		1055		1978
Range (m/s)		259		194
Range/average*100 (%)		24.5		9.8

Although the range in UPV measurements for initial setting time as determined by penetration resistance test is high, it might be said that UPV should reach a value around 1000 m/s when the setting starts in cement mortar. Additionally the setting ends when the mortar reaches a UPV about 2000 m/s. However, this value is slightly smaller for 0.8 w/c ratio. On the other hand, since such high w/c ratios are not generally used in concrete industry, it would be appropriate to use 2000 m/s as the criterion for final setting time in ultrasonic testing method.

For the initial setting time of mortars, examination of Tables 5.8 and 5.9 yields that the setting in mortars starts when the rate of UPV development curve makes the first peak. This was also concluded in the previous studies related to this subject as summarized in Chapter 3. The description of initial setting time as the first peak of rate of UPV development curves is compared with the initial setting time as determined from standard test method. The result is given in Table 5.10. In the table the difference between the two methods is given as the percentage of setting time determined by the standard penetration resistance test method.

Table 5.10. Initial setting time as determined by standard method and UPV method

w/c ratio	UPV Method (hr)	Standard Method (hour)	Difference (minutes)	Difference (%)
0.5	3.40	3.06	20.4	11.1
0.6	3.54	3.52	1.2	0.6
0.8	5.84	5.75	5.4	1.6

From the results of Table 5.10, it is seen that the difference is quite small. Therefore, it can be concluded that the initial setting time as defined by standard penetrometer test method can also be estimated by UPV test method as the peak in rate of UPV development curve.

This peak in rate of UPV is named as the inflection point of UPV curves. The inflection point is the point at which the curve changes from concave to convex or vice versa. It is calculated from the second derivative of the curve. When the second derivative changes its sign, the first derivative makes a maximum or a minimum. That is the inflection point of the curve.

### **5.8 Alternative Approach for the Setting Time of Cement Mortars**

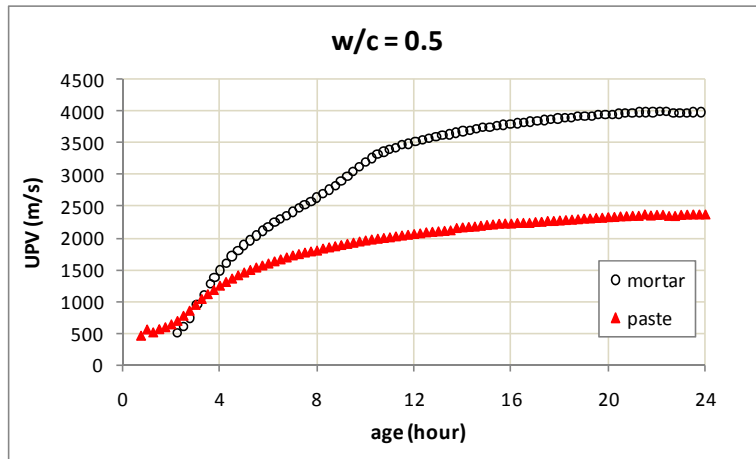
As discussed previously, it is possible to estimate the setting time of mortars as determined from the standard penetration resistance test method by UPV measurements during early stages. However, standard penetrometer test method defines initial and final setting times as two arbitrary points of setting according to the penetration resistance shown against the penetration of the apparatus into the mortar specimen. The initial setting is defined as the time when the medium gains a penetration resistance strength of 3.5 MPa while final setting is defined as the time corresponds to 27.6 MPa penetration resistance strength. Those values are given in ASTM C 403. However, it is not possible to determine exactly when the setting process starts and ends in the mortar or concrete mixtures. Therefore, the

penetration resistance values mentioned in the standard test method are arbitrarily chosen values.

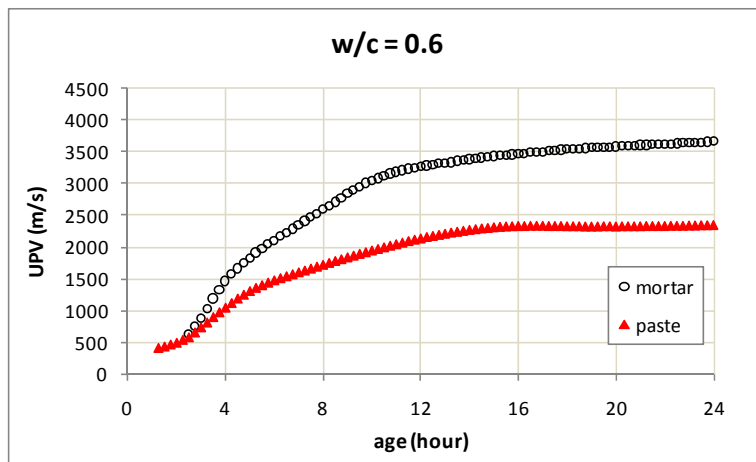
Setting is a phenomenon that occurs in the cement paste portion of mortars and concretes as the result of hydration reactions that take place between cement particles and water. Therefore, setting time of mortars should be similar to setting time of pastes under the same conditions. As it was seen that UPV development curves are sensitive to the structural changes during the hydration of pastes, the setting time of mortars should also be defined by UPV measurements as in the case of pastes. The comparisons of UPV development and rate of UPV development in pastes and mortars are given in Figures 5.17 and 5.18 for each w/c ratio, respectively.

As seen from Figure 5.17, although at the initial stages there are some differences; generally UPV in mortar is greater than the UPV in pastes due to the presence of aggregates. The behavior of UPV with time seems to be similar in pastes and mortars for 0.5 and 0.6 w/c ratios. However, at 0.8 w/c ratio, this similarity could not be obtained at the initial stages. Before final setting, the mortar and paste of 0.8 w/c ratio show different behaviors.

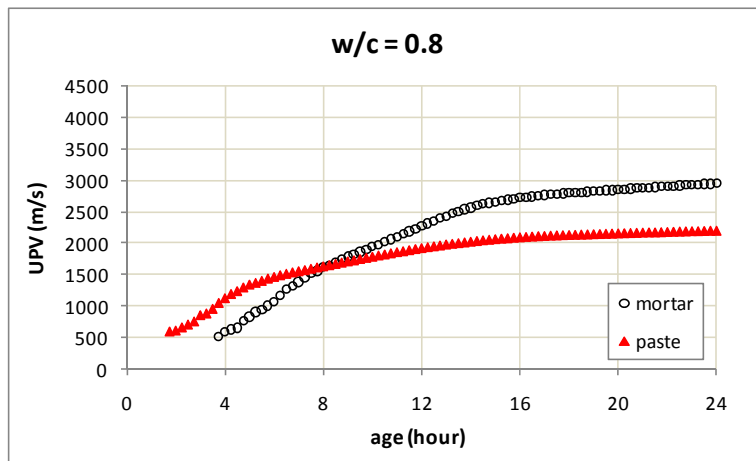
Also similar conclusions could be obtained from the RUPV development curves shown in Figure 5.18. The curves are similar for 0.5 and 0.6 w/c ratios; however, the initial peaks in pastes and mortars with w/c ratio of 0.8 do not seem to occur at the same ages. This was also expected from the UPV curves.



a) w/c ratio = 0.5

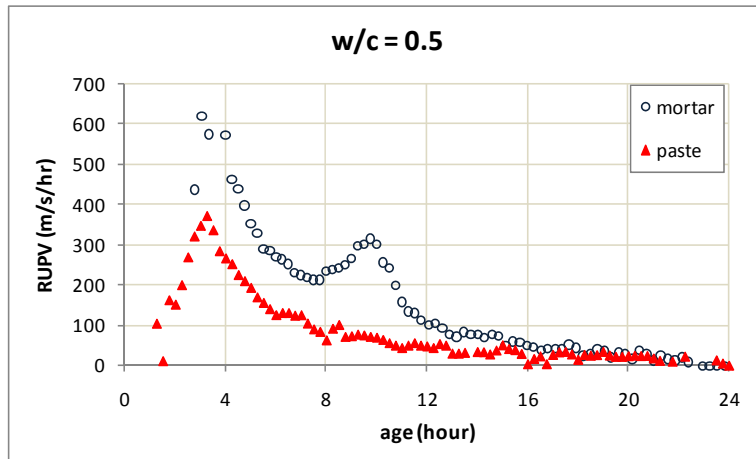


b) w/c ratio = 0.6

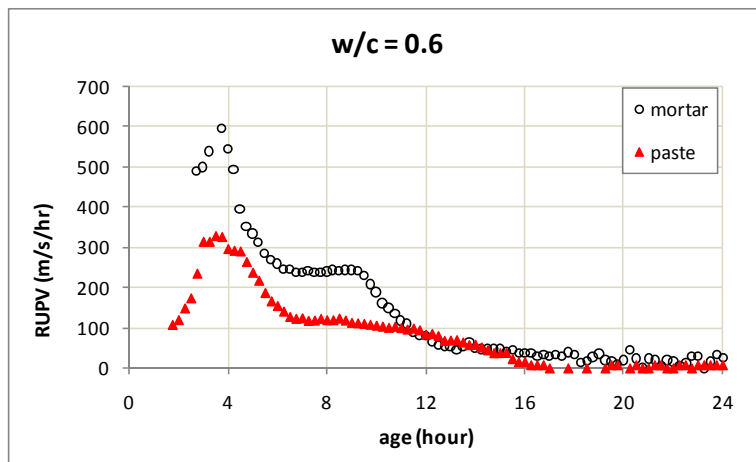


c) w/c ratio = 0.8

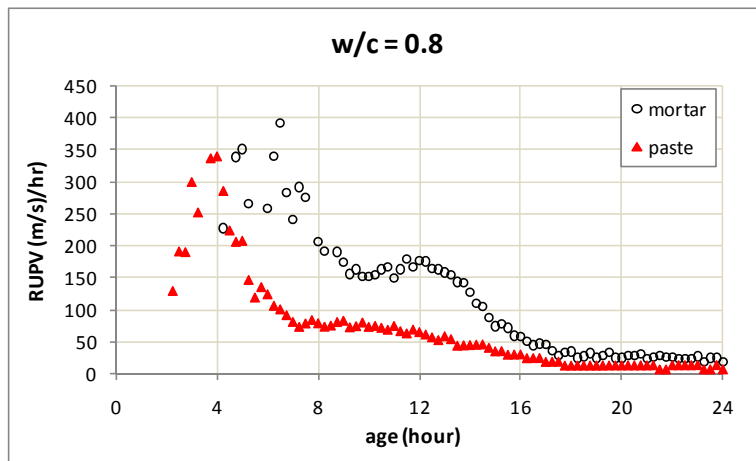
Figure 5.17. Comparison of UPV development in pastes and mortars for different w/c ratios



a) w/c ratio = 0.5



b) w/c ratio = 0.6



c) w/c ratio = 0.8

Figure 5.18. Comparison of RUPV development in pastes and mortars for different w/c ratios

In Section 5.4, determination of initial setting time by UPV test method is described for cement pastes. The UPV development curves of cement pastes were idealized by four linear portions. The intersection point of 2<sup>nd</sup> and 3<sup>rd</sup> linear portions which can also be defined as the point where the slope of the curve changes second time, is found out to be the initial setting time in cement pastes. The UPV corresponding to the initial setting time is stated to be approximately 1400 m/s.

On the other hand, in case of mortars, the first linear portion of the UPV development curves could not be observed. Therefore, unlike pastes, the UPV curves were idealized by three linear portions. Similar to the pastes, setting in paste portion of mortar should start around the intersection point of 1<sup>st</sup> and the 2<sup>nd</sup> linear portions. This point can also be defined as the point where the slope of the UPV changes drastically. The results for this point are given in Table 5.7 for each w/c ratio.

The final setting time in cement pastes was defined by RUPV development curves in Section 5.4. The RUPV curves were seen to make a plateau after a first peak and then to start to decrease. The length of constant portion seemed to depend on the w/c ratio of the specimen. The end of this plateau was defined as the final setting time of the cement pastes. However, in the mortars, the shape of RUPV development curves is a little different. Instead of a constant portion, the RUPV curves make a minimum after the first peak. This point of minimum is used to define the final setting time in the mortar specimens. The results for this point are also given in Table 5.8 for each w/c ratio.

The setting time results according to the newly defined approach are listed in Table 5.11 for both initial and final setting times together. The corresponding UPV values for newly defined initial and final setting times are also shown in the table for each w/c ratio.

Table 5.11. Initial and final setting times of mortars according to new approach

w/c ratio	Initial Setting		Final Setting	
	Time (hr)	UPV (m/s)	Time (hr)	UPV (m/s)
0.5	4.89	1827	7.45	2509
0.6	5.47	1976	7.49	2475
0.8	7.20	1441	10.20	1969

Although the results for setting time given in Table 5.11 are quite different from those obtained by standard penetration resistance test method in mortars, they can be accepted to be close to the values obtained by Vicat apparatus in cement pastes of same w/c ratio. Except for initial setting of the mixture having 0.8 w/c ratio, the results are similar to those obtained from UPV development curves of cement pastes.

When the UPV values corresponding to the defined times are examined, it is seen that the results are similar for 0.5 and 0.6 w/c ratio, while the values are smaller in 0.8 w/c ratio. This could be due to the different amount of aggregates in the mixtures. However, interestingly there is approximately a 550 m/s difference in UPV measurements between the proposed initial and final setting times.

### **5.9 Factors Affecting the Velocity Measurements on Fresh Mortars**

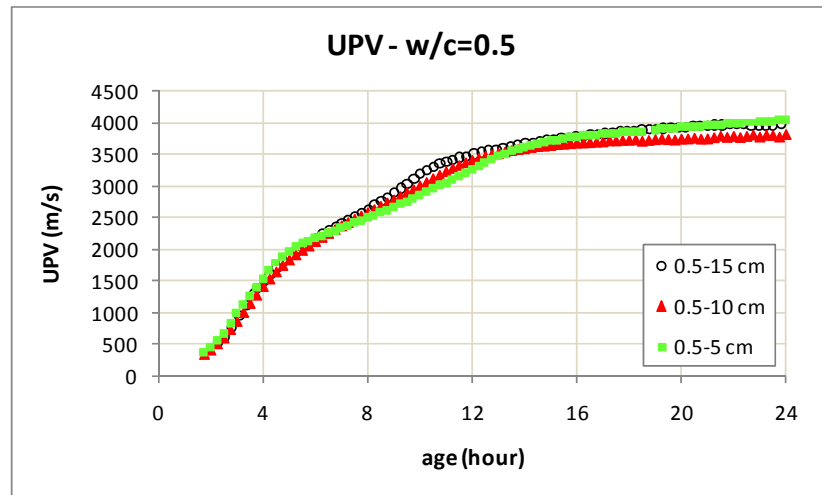
As a new method is being developed, the effects of some factors related to the experimental test set-up should be controlled in order to improve the test method. For this purpose, the effect of path length travelled by ultrasonic pulse waves and the effect of frequency of transducers used for wave transmitting and receiving were tested in fresh mortar specimens.

### **5.9.1 Effect of path length**

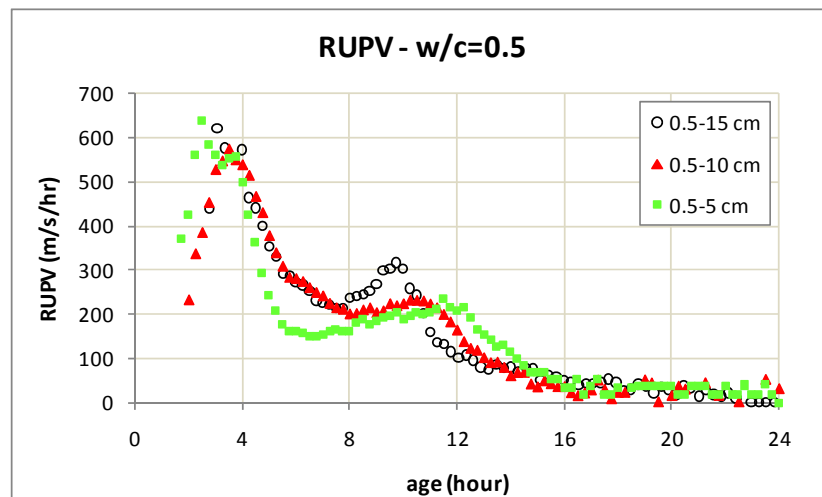
When the attenuation and the near-field effects are considered, travel path distance of the ultrasonic pulse waves is an important parameter that needs to be considered. Some of the energy of the ultrasonic wave is lost during the propagation through the material due to attenuation. If the length traveled by the wave is too long, the wave could attenuate totally, or could decline so that it could not be able to be distinguished from the electrical noise. On the other hand, too short path lengths are also undesirable in ultrasonic testing due to near-field effect which was explained in Chapter 2. The ultrasonic pulses are generated at several points in the transducer and during travelling through the material these pulses merge to form a single wave. This distance is related to the transducer dimension and wavelength. If the measurements are taken within the limits of near-field, the results are not reliable. Additionally, ASTM C 597 restricts the least dimension of the test object to a value greater than the wavelength to eliminate the effect of waves reflected from the boundaries. Therefore, it is obvious that path length can be an important parameter in ultrasonic testing.

In this part of the research, it is aimed to investigate the effect of travel path length on the development of UPV in hydrating cement mortars. For this purpose, the experiments applied on mortar specimens with different w/c ratios were repeated for three different path distances. The path distances which correspond to longitudinal dimension of the mold were chosen as 15, 10 and 5 cm. The effects of path distance were tested for each w/c ratio, separately. During these experiments only one dimension of the test mold was changed, i.e. the other two dimensions of the mold were 15 cm, in order to eliminate the effect of lateral dimensions on the ultrasonic measurements. 15 cm length for the lateral dimensions of the mold is an appropriate value as it is recommended that the least dimension should be greater than one wavelength. This value supplies this condition for each frequency applied at the measured velocity range.

In order to observe the effect of travel path distance on the results of non-destructive testing of fresh cement mortars, development of ultrasonic pulse velocity and the rate of ultrasonic pulse velocity development with respect to time were compared for different path lengths at each w/c ratio, separately. For each w/c ratio, the UPV and rate of UPV development curves are shown together in Figures 5.19 – 5.21.



a) UPV development



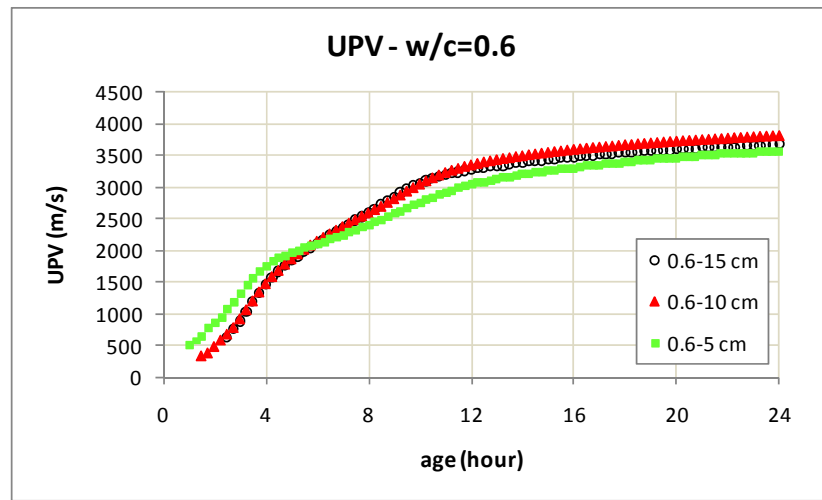
b) Rate of UPV development

Figure 5.19. Effect of path distance on UPV and RUPV of mortars with 0.5 w/c ratio

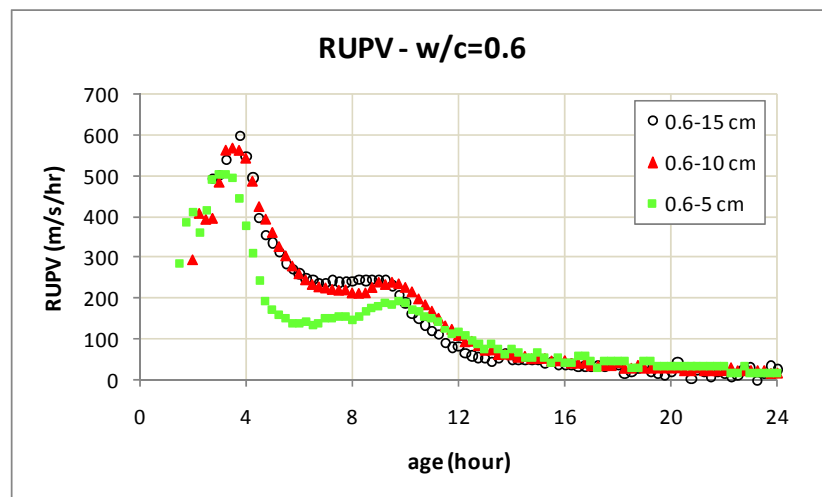
Figure 5.19 shows the effect of travel path length of ultrasonic waves for 0.5 w/c ratio during the first 24 hours after mixing. From Figure 5.19-a, the UPV development curves seem to be similar for all lengths. However, the starting point of UPV measurements differ according to the travel length; first meaningful velocity value was obtained for 15 cm at 2.25 hours after mixing, while it was obtained at 1.75 hours for 10 cm and at 1.25 hours for 5 cm. The effect of attenuation is seen obviously for longer distances. Additionally, when the UPV values at 24 hours are compared, there is only a maximum difference of 200 m/s. This difference only corresponds to about 5% for a velocity level of 4000 m/s. However, when Figure 5.19-b is investigated, the result of small differences in UPV development curves can be realized in the RUPV development curves for different travel lengths. Although the initial part which contains the first peak is similar for 10 and 15 cm test parameter, it occurs earlier for the test specimen having 5 cm travel path length. The second peaks also do not occur at the same time for the three trials. Therefore, it could be concluded that although the UPV curves seem to be similar for different mold dimensions, the RUPV development curves show some differences for test specimens having different sizes.

The effect of travel path in ultrasonic testing of fresh mortars is seen for w/c ratio of 0.6 in Figure 5.20. In UPV development graphs, the curves are similar for 15 and 10 cm except for the initial readings. On the other hand, the behavior for 5 cm travel path is different; at the initial stages the UPV values are greater, however, after 5 hours the velocity values are smaller as compared to other two travel path test results. When the initial reading time is compared, it is seen that first reading was taken at 2.5 hours after mixing for 15 cm, 1.5 hours for 10 cm and 1.0 hour for 5 cm travel path. The difference between the maximum and minimum UPV values obtained in this group is about 250 m/s at 24-hours which is about 6 % for a velocity level of 4000 m/s. In Figure 5.20-b, the RUPV development curves are again similar as in the case of UPV curves for 15 and 10 cm travel lengths while it is quite different for 5 cm path. For 5 cm measurements, the initial peak was

obtained earlier while the second peak was obtained later than the other two travel path distances.

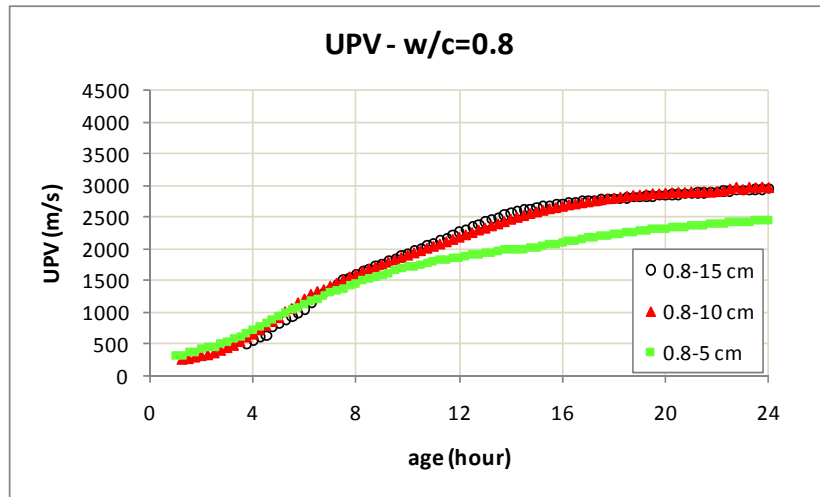


a) UPV development

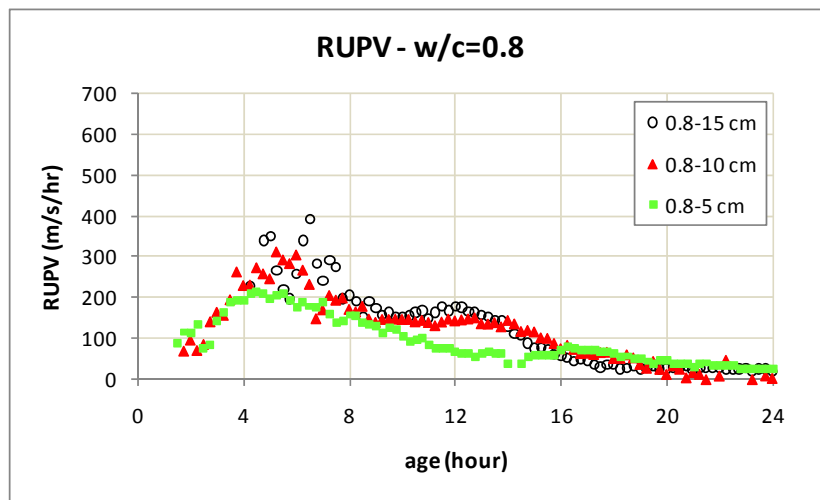


b) Rate of UPV development

Figure 5.20. Effect of path distance on UPV and RUPV of mortars with 0.6 w/c ratio



a) UPV development



b) Rate of UPV development

Figure 5.21. Effect of path distance on UPV and RUPV of mortars with 0.8 w/c ratio

The curves in Figure 5.21 also reveal similar results. The results are quite similar for 10 and 15 cm travel path lengths, however, the curve is quite different for 5 cm travel length especially after 7 hours. The UPV values are very small as compared to others for the 5 cm mold. The initial readings could be taken at 3.75 hours after mixing for 15 cm, at 1.25 hours for 10 cm and at 1 hour for 5 cm. For the RUPV development curves, again similar conclusions could be made. However, the curves are less smooth, especially at the initial stages of hydration.

From Figures 5.19-5.21, similar conclusions regarding travel path distance were made for each w/c ratio. Moreover, it should be mentioned that the tests were applied on different batches of cement mortars as it was not possible to test multiple systems at the same time. Therefore, small differences in the test results were expected; because it was likely to have some small differences in the properties of specimens from different batches.

In order to compare the test results, the characteristic points of UPV and RUPV development curves which were mentioned in the previous section and the corresponding UPV values are listed for each travel path length in Tables 5.12 and 5.13, respectively. The important points for UPV development curves were the intersections of the linear portions which were used to idealize the curves. In RUPV development curves, the initial peak and the minimum point of the curves were used to define the hydration process.

Table 5.12. Comparison of intersection points of linear portions in UPV curves

w/c ratio	15 cm		10 cm		5 cm	
	Int. 1-2	Int. 2-3	Int. 1-2	Int. 2-3	Int. 1-2	Int. 2-3
0.5	4.89 h 1827 m/s	11.58 h 3465 m/s	4.88 h 1781 m/s	12.37 h 3448 m/s	4.30 h 1906 m/s	14.05 h 3688 m/s
0.6	5.47 h 1976 m/s	11.74 h 3260 m/s	5.48 h 2017 m/s	12.08 h 3364 m/s	4.56 h 1882 m/s	13.43 h 3153 m/s
0.8	7.20 h 1441 m/s	14.38 h 2609 m/s	7.52 h 1505 m/s	15.92 h 2654 m/s	8.21 h 1507 m/s	16.15 h 2118 m/s

Table 5.13. Comparison of characteristic points of linear portions in RUPV curves

w/c ratio	15 cm		10 cm		5 cm	
	Maximum	Minimum	Maximum	Minimum	Maximum	Minimum
0.5	3.40 h 1144 m/s	7.45 h 2509 m/s	3.68 h 1229 m/s	7.73 h 2517 m/s	3.08 h 1309 m/s	7.52 h 2501 m/s
0.6	3.54 h 1223 m/s	7.49 h 2475 m/s	3.73 h 1338 m/s	7.84 h 2564 m/s	2.96 h 1292 m/s	7.31 h 2289 m/s
0.8	5.84 h 1023 m/s	10.20 h 1969 m/s	5.65 h 1105 m/s	10.76 h 2000 m/s	5.40 h 1029 m/s	14.09 h 1996 m/s

As seen from tables and figures, in all mortar specimens the travel path distances of 15 and 10 cm lengths give similar results, while the travel path length of 5 cm gives different results. Therefore, it could be concluded that using very short lengths is not recommended for ultrasonic testing of fresh cement mortars. This can be explained by two reasons; near-field effect and the least dimension restriction. The near-field regions and the wavelengths for different velocity levels are listed in Table 2.1. As seen from Table 2.1, the near-field region is greater than 5 cm for low velocities. However, in the case of higher velocities, wavelength starts to be greater than 5 cm. On the other hand, longer path distances result in high attenuation which hinders the observation during very early stages of hydration. It was seen that 10 or 15 cm travel path distance is appropriate for the test method. However, attenuation is more effective when travel path is chosen as 15 cm. Although the time difference for the initial reading is smaller between 5 and 10 cm, the time difference is greater between 10 and 15 cm travel lengths. The attenuation is more effective when higher w/c ratios are used. Therefore, the travel path distance of waves should be chosen carefully for ultrasonic testing of fresh cementitious materials depending on wavelength, near-field and attenuation.

### **5.9.2 Effect of frequency range of transducers**

As mentioned in Chapter 2, frequency and wavelength are in inverse relation so that the product of the two parameters equals to wave velocity. This means that for a given wave velocity, at higher frequencies the wavelength decreases. Additionally, for a constant frequency application, the wavelength increases as the ultrasonic pulse velocity increases.

In ultrasonic testing, the wavelength is important in order to assume the medium as homogeneous as long as the wavelength is greater than the maximum particle size. For testing concrete, the wavelength of the ultrasonic pulse waves should be greater than the maximum aggregate size. Unless this requirement is supplied, the

applicability of the method becomes questionable as the initial assumptions could not be fulfilled.

In hydrating cementitious materials, the UPV of the medium starts at very low values increasing up to about 4000-5000 m/s as time passes depending on the properties of the material. Therefore, the wavelength of the ultrasonic pulse wave propagating through the medium increases with time if narrow-band transducers are used. For different velocity levels, the wavelength generated through the medium is listed in Table 5.14 for different frequency applications.

Table 5.14. The wavelength for different velocity and frequency

UPV (m/s)	Frequency (kHz)		
	54	82	150
100	0.18 cm	0.12 cm	0.07 cm
200	0.37 cm	0.24 cm	0.13 cm
500	0.93 cm	0.61 cm	0.33 cm
1000	1.85 cm	1.22 cm	0.67 cm
2000	3.70 cm	2.44 cm	1.33 cm
4000	7.41 cm	4.88 cm	2.67 cm
4500	8.33 cm	5.49 cm	3.00 cm

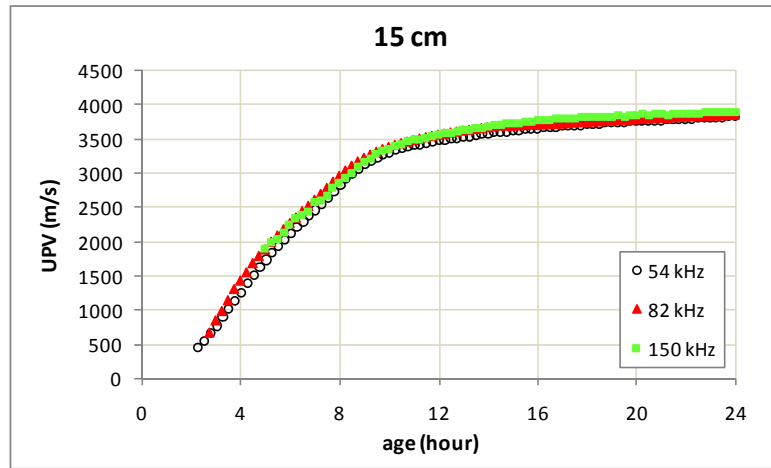
In fresh concrete the test frequency is limited by the maximum aggregate size as in the case of the hardened concrete. However, the limitation is much more severe in fresh concrete as the initial velocities are very low as compared to hardened case as seen in Table 5.14. For example, in the case of cement mortars with maximum aggregate size of 4.75 mm, the wavelength starts to be greater than the maximum aggregate size after the medium reaches a velocity level of 255 m/s for frequency of 54 kHz; while 715 m/s for frequency of 150 kHz. As a result, it could be concluded that the applied level of frequency could be quite important for low values of UPV in order to supply the assumptions of elastic wave theory. If high

frequency wave is applied to the fresh cement mortar, the wavelength could be smaller than the particle size of the medium especially at the initial stages where the wave velocity is very small.

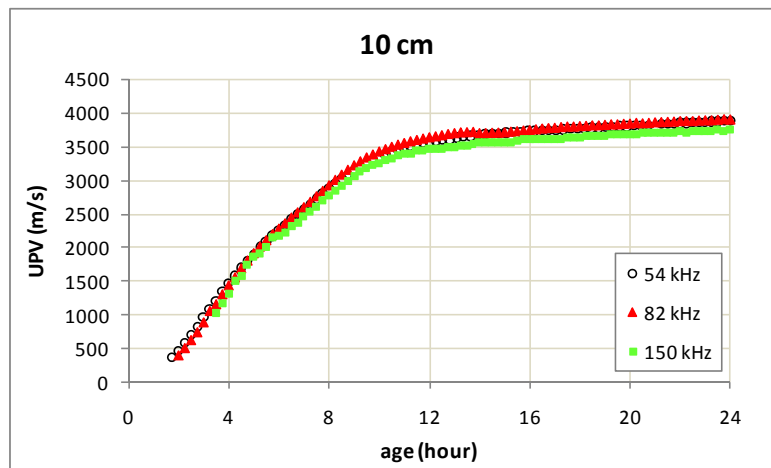
In this study, narrow-band transducers were used for generating the ultrasonic pulses through the cementitious medium. For ultrasonic testing of hardened concrete, a frequency of about 50 kHz is accepted to be suitable due to wavelength, particle size, and lateral dimension limitation. However, in this research program, cement pastes and mortars of which particle sizes are much smaller compared to concrete were tested. Therefore, applications of higher frequency levels are possible. In the experiments narrow-band transducers having 54, 82 and 150 kHz frequency were utilized in order to check the effect of frequency in the test results. In all test specimens the lateral dimensions were 15 cm, therefore, the least lateral dimension was expected not to create any problem for the applicability of the ultrasonic test method. The important factor in this application seems to be the comparison of the particle size dimension and the wavelength.

In order to investigate the effect of frequency on the experimental test set-up and on the development of UPV of the hydrating materials, a new group of experiments was planned. For this purpose, mortar specimens with w/c ratio of 0.5 were prepared. The UPV development in mortars was observed for the first 24 hours after mixing by utilizing transducers with different frequencies. At the same time the effect of path length was also investigated by applying each frequency for travel distances of 15, 10 and 5 cm.

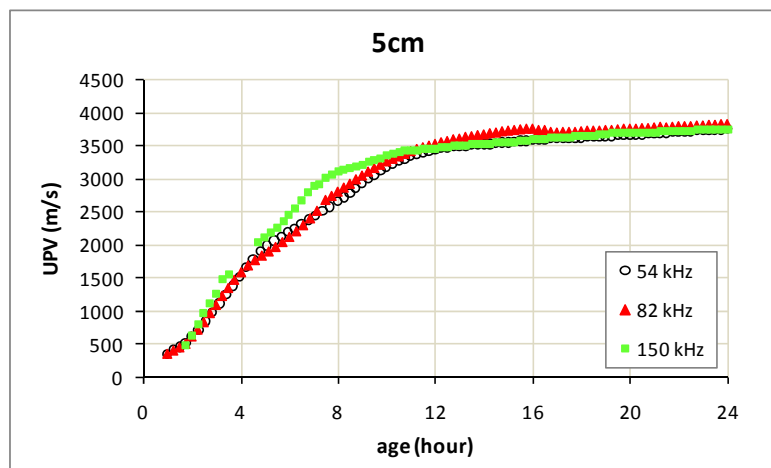
The development of UPV in mortar specimens obtained by different transducers with different frequencies for different path lengths and the development of RUPV were investigated. The development of UPV in cement mortar is given in Figure 5.22 for each frequency and travel path distance.



a) Travel path, 15 cm



b) Travel path, 10 cm

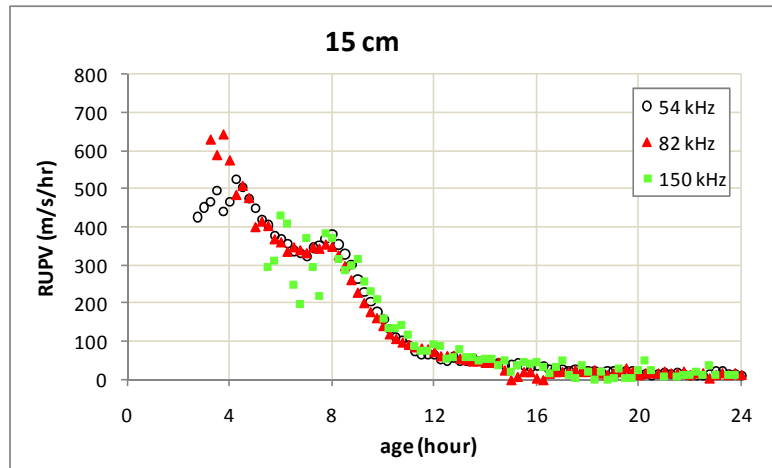


c) Travel path, 5 cm

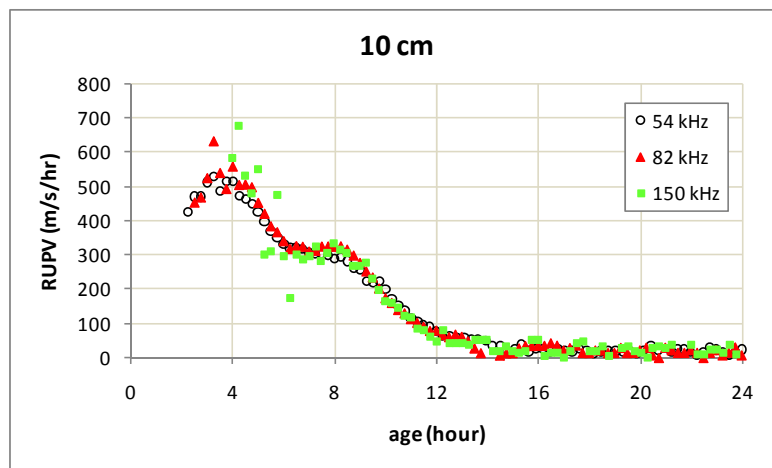
Figure 5.22. Effect of frequency on UPV development for each travel path

In Figure 5.22, the shapes of the curves are similar in all hydrating cementitious materials. For 15 cm travel path length, the curves for each frequency behave quite similar during hydration of mortar. However, when 150 kHz frequency is applied, due to high attenuation, the initial reading could not be taken until the medium gained a UPV of about 2000 m/s. The initial readings in 82 kHz frequency started also later as compared to 54 kHz, however, the difference was not much. The similar results are also true for travel path distance of 10 cm. However, in this case, the curve for 150 kHz frequency seems to be a little different from the other two frequencies. The high attenuation in high frequency could also be observed in this set of test results from the starting time of first readings. In the case of 5 cm travel path length, the curves for each frequency application are not as similar as each other compared to other travel path distances. Due to smaller travel distance of ultrasonic pulses the effect of attenuation is not as high as longer lengths. However, the curves are not very smooth. This could be arisen from the near-field effect and least dimension restriction. Especially, for lower velocity values, as the wavelength is small the near-field is larger. In order to take accurate and reliable readings, the readings must be taken beyond this region. However, in the case of high velocities, the wavelength is high. As seen in Table 5.14, the wavelength can exceed 5 cm. However, according to ASTM C 597, in order to eliminate the effect of reflected waves, the least dimension must be greater than one wavelength. On the other hand, attenuation is more effective in high frequencies. As wavelength is smaller in high frequency, during travelling through the medium the wave attenuates and the wavelength of the wave decreases so it becomes difficult to capture and separate from the electrical noise. Therefore, for testing the fresh cement mortars, the travel path and frequency should be appropriately chosen if narrow-band transducers are used.

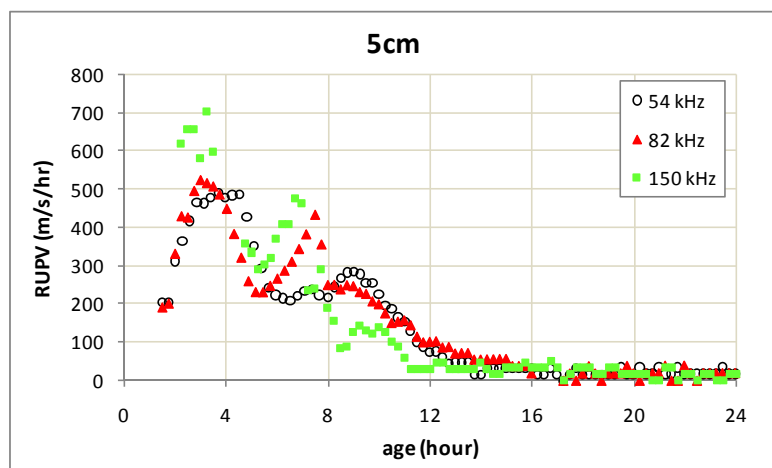
As discussed in the previous sections, the RUPV change with respect to time gives valuable information about the hydration process. The rate of UPV development curves obtained for different frequency transducers are shown in Figure 5.23 for each travel path distance.



a) Travel path, 15 cm



b) Travel path, 10 cm



c) Travel path, 5 cm

Figure 5.23. Effect of frequency on RUPV development for each travel path

In Figure 5.23, the general trend of RUPV development curves is obtained at each trial. There is an initial peak which occurs approximately 3.5 hours after mixing. After reaching that initial peak, the rate starts to decrease, and then it tends to make another peak which is not very clear in all tests. As hydration reactions slow down, the rate approaches to zero. For 15 cm travel path (5.23-a), the initial peak is most clear in 54 kHz frequency transducer. On the other hand, meaningful data started to be obtained far beyond the time for initial peak with 150 kHz frequency testing. The early readings obtained with 150 kHz are quite dispersed. This is most probably due to the difficulty of distinguishing the real waveform from the electrical noise because of the small wavelengths at the beginning stages. At the beginning, the generated ultrasonic pulse waves are not be able to be transmitted through the medium from sender to receiver due to attenuation. However, as hydration proceeds, the attenuative character of the medium decreases while the wavelength increases due to increasing wave velocity. Therefore, at the beginning of the test the wave could not be monitored for a while depending on the frequency and travel path length. As the travel path and frequency increase the time period needed for the initial monitoring of the waves also increases.

As seen in Figure 5.23, 15 and 10 cm travel path curves are quite similar in 54 and 82 kHz; however, 5 cm travel path test results behave differently in all cases. Additionally, in 5 cm travel path distance test set-up, the characteristic points of rate of UPV development curves do not coincide well in all frequency transducers tested.

For the determination of initial and final setting time of cement mortars by UPV test, a method has been proposed for mortars in Section 5.8. According to the proposed method the initial setting occurs when the slope of idealized lines of UPV development curves changes, while final setting occurs when the RUPV curves makes a minimum point as described in cement pastes. In order to check the effect of different frequencies, those values were compared for each frequency and travel path distance. The results are given in Table 5.15.

Table 5.15. Comparison of determined setting times with different frequencies

Frequency (kHz)	Proposed initial setting			Proposed final setting		
	15 cm	10 cm	5 cm	15 cm	10 cm	5 cm
54	4.94 h	4.86 h	4.74 h	7.48 h	7.58 h	7.34 h
	1723 m/s	1855 m/s	1878 m/s	2630 m/s	2750 m/s	2511 m/s
82	5.02 h	5.09 h	4.50 h	7.21 h	7.28 h	5.68 h
	1905 m/s	1960 m/s	1752 m/s	2687 m/s	2693 m/s	2040 m/s
150	*	5.07 h	4.48 h	**	7.12 h	5.35 h
		1885 m/s	1949 m/s		2510 m/s	2230 m/s

\*The value could not be determined as the readings had not started yet

\*\* The value could not be determined as a polynomial could not be fitted to the data

As seen from Table 5.15, if high frequencies are utilized with long travel path distances, the setting times may not be determined as the initial reading starts very late due to high attenuation. On the other hand, the setting times determined from the short path lengths (5 cm) are generally different from the results obtained by other two path lengths most probably due to near-field effect and least dimension restriction. The results for initial setting time seem to be a little longer and for final setting time seem to be a little shorter as frequency increases for 15 and 10 cm travel path distances; however, the differences are acceptable as the maximum value is about 16 minutes.

As a result it can be claimed that using high frequency transducers is not suitable for testing fresh cement mortars due to high attenuation and small wavelength which makes it difficult to distinguish from electrical noise especially at the initial stages. Secondly, using short travel distance makes the measured data less reliable due to near-field effect at low velocities and due to least dimension restriction at high velocities. However, using very long travel distances especially with high frequencies is also not desirable for monitoring the hydration stages, because due to attenuation the observation of the ultrasonic pulses may become impossible

especially at the very early stages of the hydration. Therefore, for the test set-up a suitable frequency range and travel distance should be chosen if narrow-band frequency transducers are used. Depending on the parameters used in this investigation, frequencies of 54 and 82 kHz can be used reliably for travel path lengths of 15 and 10 cm.

### 5.10 Repeatability of the UPV Testing of Fresh Mortars

In order to test the repeatability of UPV measurements in fresh cement mortars, the tests were repeated for mortars having w/c ratio of 0.5. The mortar mixtures were prepared from the same materials with the same proportions at different times. The ultrasonic test was applied with 54 kHz frequency transducers. The tests were repeated twice for the three travel path lengths. The UPV development with time in the two repetitions was compared for different travel path lengths, separately.

In order to check the repeatability of the test method, the initial and final setting time results obtained from UPV measurements as proposed in Part 5.8 are given in Table 5.16.

Table 5.16. Comparison of determined setting times at different times

Path length (cm)	Proposed initial setting		Proposed final setting	
	1 <sup>st</sup> trial	2 <sup>nd</sup> trial	1 <sup>st</sup> trial	2 <sup>nd</sup> trial
15	4.89 h	4.94 h	7.45 h	7.48 h
	1827 m/s	1723 m/s	2509 m/s	2630 m/s
10	4.88 h	4.86 h	7.73 h	7.58 h
	1781 m/s	1855 m/s	2517 m/s	2750 m/s
5	4.30 h	4.74 h	7.52 h	7.34 h
	1906 m/s	1878 m/s	2501 m/s	2511 m/s

As seen in Table 5.16, the results are quite similar for different measurements in the case of 15 and 10 cm travel path lengths. However, the values obtained in the case of 5 cm travel length differ not only from the measurements of other path distances but also between the two different measurements of the same length. Therefore, it can be concluded that the repeatability of the results is not good if short path lengths are used. This is due to the inaccuracy of the measurements due to the near-field effect.

It can be calculated from Table 5.16 that the initial setting time differs maximum 3 minutes and final setting time differs maximum 9 minutes between two measurements when the same path length dimension is considered. As the values are also similar for different travel path applications of 15 and 10 cm, if the differences are calculated regardless of the path length, it is obtained that the maximum difference in initial setting time determination is about 5 minutes and in final setting time determination it is about 16 minutes. Therefore, it can be said that the UPV method is repeatable and accurate if the appropriate path length dimension is chosen for the test.

### **5.11 Properties of Hardened Mortars**

In the research program beyond the properties of fresh cementitious materials, some properties in hardened state were also examined in order to correlate with UPV development and control the similarities between different batches. For this purpose, compressive strength and total volume of permeable pores were determined during 28 days for mortars having different w/c ratios. The UPV of the cement mortars were also determined on the 7<sup>th</sup> and 28<sup>th</sup> days in addition to the first 72 hours. For the UPV determination tests, a 54 kHz frequency was applied. In order to measure the UPV at later ages, the mortar specimens were left inside the mold after 72-hours continuous measurements. The upper faces of the specimens were sealed with stretch film in order to prevent moisture loss. All test specimens were kept in the same place under similar conditions until the test age. As the UPV

measurements were applied to the specimens having three different sizes, there are three UPV measurements for different travel path lengths of 15, 10 and 5 cm against a single compressive strength and permeable pore volume at each test day. Although the compressive strength and pore volume tests were repeated for each batch which had to be prepared for UPV measurements of different path lengths, as the results are similar the average of the results were taken for each w/c ratio at each test age. This is an indication for obtaining similar properties for different batches of same mortars. The results of compressive strength and volume of permeable pores tests are given in the following sections and their correlation with UPV results are also examined.

#### **5.11.1 Strength test results**

In order to determine the compressive strength of mortar specimens 4\*4\*16 cm prismatic specimens having w/c ratios of 0.5, 0.6 and 0.8 were prepared. Before applying compressive strength test, the prisms were divided into two pieces by flexural test and the flexural strength values were also determined. The strength values of mortar specimens were obtained at 1, 2, 3, 7 and 28 days. Until the test age, the specimens were cured in lime-saturated water in the same temperature conditions as the UPV test specimens were kept. The average of results of nine specimens mixed at three different batches was taken at each age for each w/c ratio. The results of flexural and compressive strength tests are listed in Table 5.17.

Table 5.17. Flexural and compressive strength test results of mortar specimens

Age (day)	w/c=0.5		w/c=0.6		w/c=0.8	
	Flex. Str. (kgf/cm <sup>2</sup> )	Compr. Str. (kgf/cm <sup>2</sup> )	Flex. Str. (kgf/cm <sup>2</sup> )	Compr. Str. (kgf/cm <sup>2</sup> )	Flex. Str. (kgf/cm <sup>2</sup> )	Compr. Str. (kgf/cm <sup>2</sup> )
1	48.79	194.19	41.86	170.96	21.08	57.08
2	64.15	250.56	53.38	246.82	31.40	82.17
3	67.65	294.08	57.91	265.23	34.36	100.59
7	74.96	321.96	66.38	289.84	45.76	142.13
28	81.59	382.98	76.00	317.50	59.34	188.18

In Table 5.17, it is seen that the compressive strengths of specimens are higher than flexural strength as expected. As hydration proceeds, the compressive and flexural strength increase naturally. In order to observe how the strength develops with time in mortar specimens, the changes of compressive and flexural strength with time are shown graphically in Figures 5.24 and 5.25.

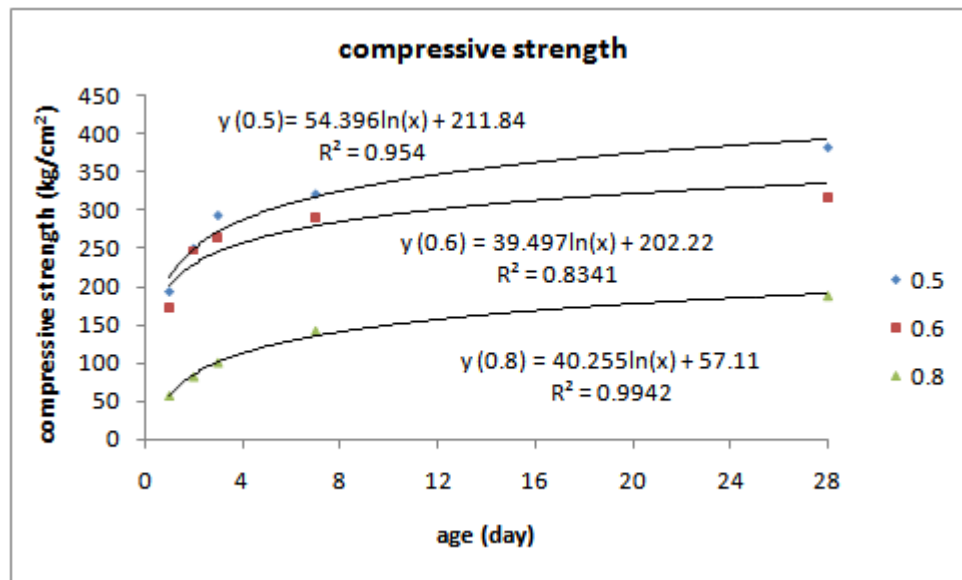


Figure 5.24. Development of compressive strength in mortar specimens

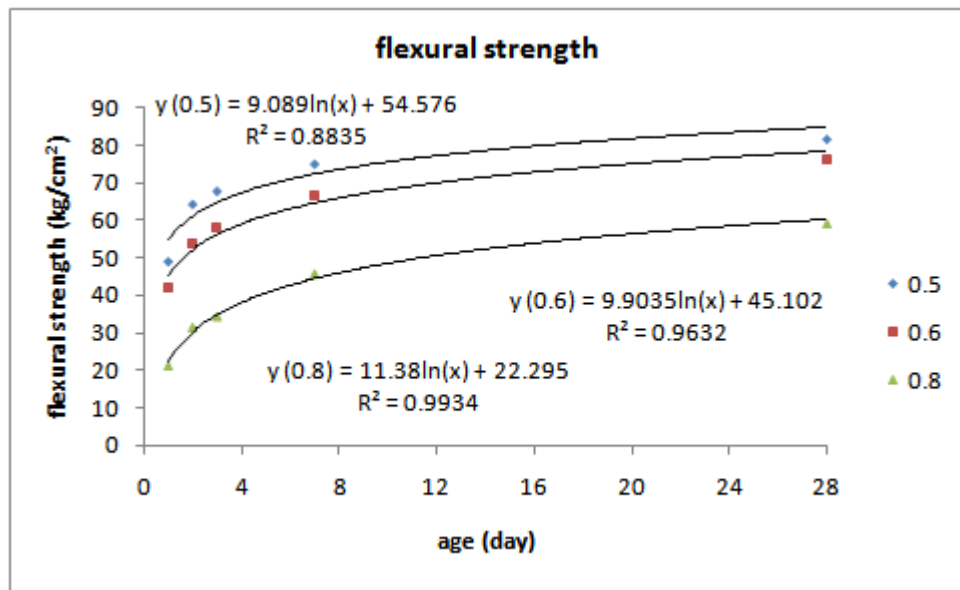


Figure 5.25. Development of flexural strength in mortar specimens

Both the flexural and compressive strength are known to be related to the w/c ratio of the material; the higher the w/c ratio, the lower the strength. As seen in Figures 5.24 and 5.25, both flexural and compressive strength increase logarithmically with time. Due to the similar behavior of both parameters with respect to time, their correlation with each other is also investigated and shown graphically in Figure 5.26.

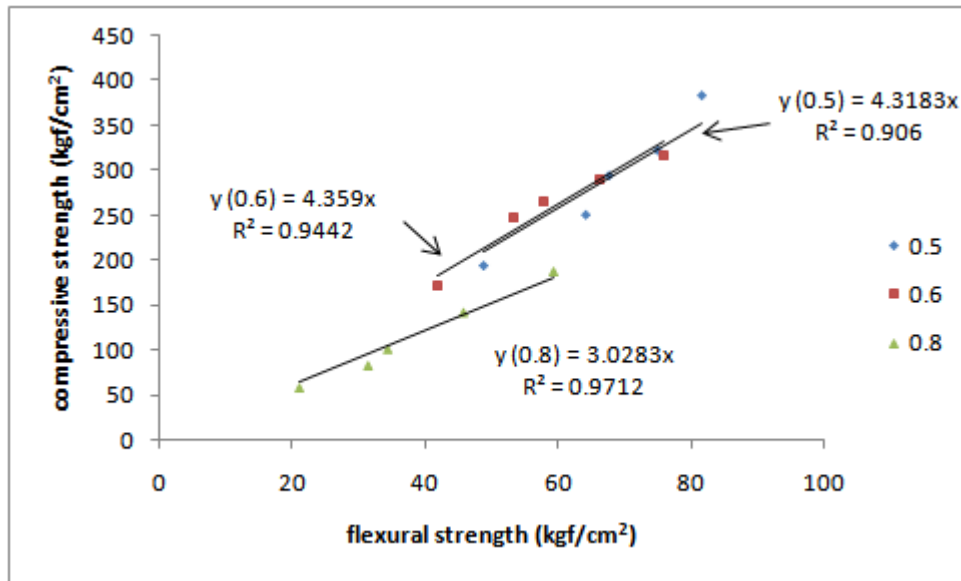


Figure 5.26. Relation between flexural and compressive strength in mortar specimens

As seen in Figure 5.26, a linear relationship is obtained between compressive and flexural strength for each w/c ratio. The lines were drawn such that they passed through the origin, because unless the strength was started to develop in the mortar, both the compressive and flexural strength of the specimen were zero. The slopes of the lines seem to be dependent on the w/c ratio of mortar specimens. The lines for mortars having w/c ratio of 0.5 and 0.6 are very close to each other. As the strength values are very small as compared to other mortar specimens, the line for mortars with 0.8 w/c ratio stays below the other two lines.

The UPV of mortar specimens were also determined at hardened state with the experimental set-up used to monitor the UPV development during the hydration of fresh mortars. The UPV measurements of freshly mixed mortar specimens were carried continuously for the first 72 hours, so the values corresponding to 24, 48 and 72 hours were taken as the 1<sup>st</sup>, 2<sup>nd</sup> and 3<sup>rd</sup> day readings. The 7<sup>th</sup> and 28<sup>th</sup> day UPV measurements were taken on the same specimens with the same set-up. Therefore, UPV readings were measured for three different travel path lengths. Results of UPV measurements for the 1, 2, 3, 7 and 28 days are shown in Figure

5.27 for the 15 cm travel path length as an example of UPV development in hardened cement mortars prepared with different w/c ratios.

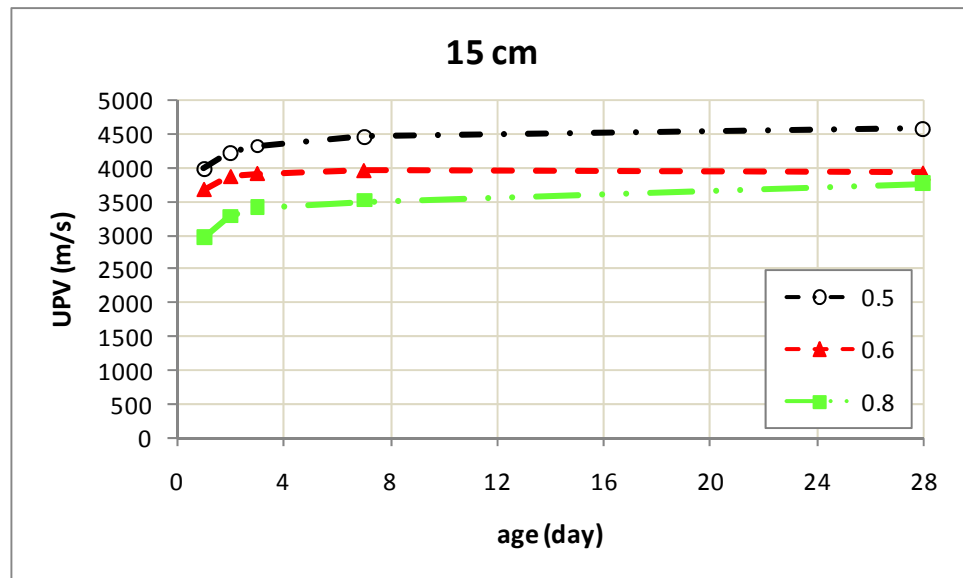
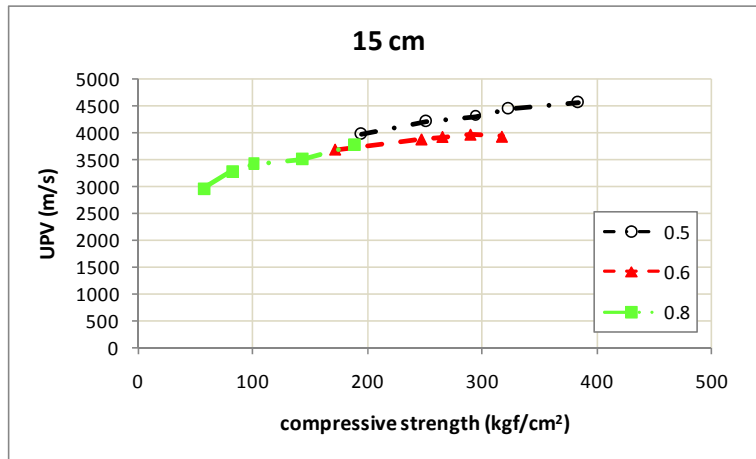


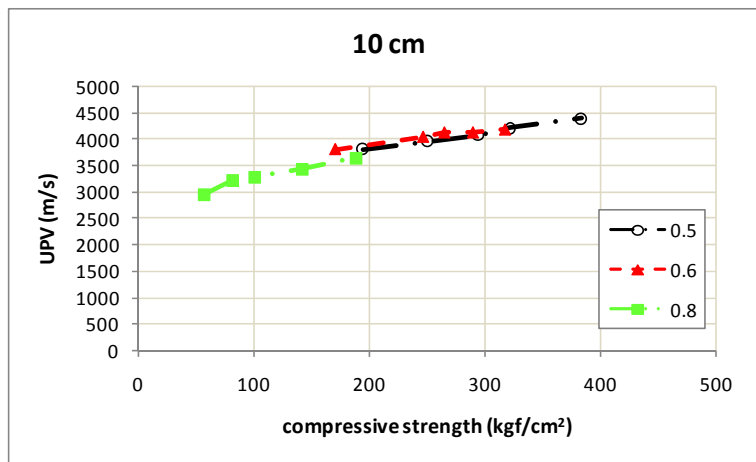
Figure 5.27. Development of UPV in hardened cement mortars

The UPV in cement mortars increases logarithmically with time in hardened specimens as seen in Figure 5.27. However, compared to development of UPV in fresh concrete during the first 24 hours after mixing (Figure 5.14), the amount of increase in UPV is very small between 1<sup>st</sup> and 28<sup>th</sup> days. As also observed in the fresh state, UPV is higher for lower w/c ratios at all ages.

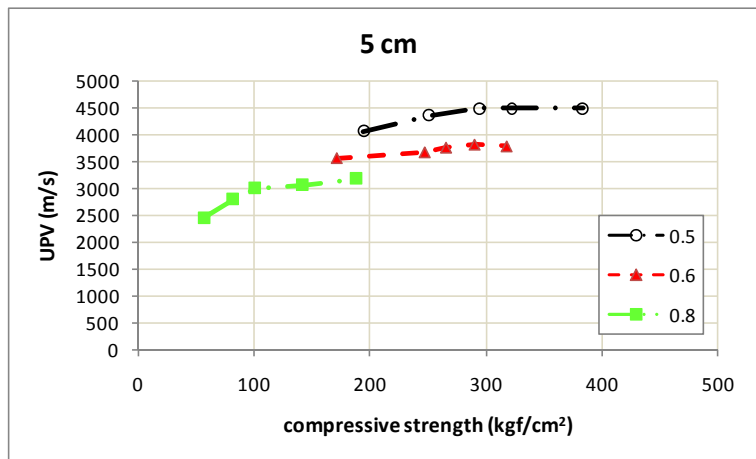
The development of strength and UPV with age of mortar is similar in different w/c ratios as seen from the above figures. The change of UPV with respect to compressive strength of mortar specimens with different w/c ratios is given in Figure 5.28 for the three travel path lengths, separately.



a) Travel path length, 15 cm



b) Travel path length, 10 cm



c) Travel path length, 5 cm

Figure 5.28. Relation between UPV and compressive strength for different travel path lengths

As seen in Figure 5.28, the smaller the compressive strength the lower the UPV value in all w/c ratios and travel path lengths. In Figures 5.28-a and 5.28-b, the relation between UPV and compressive strength seems to be independent of the w/c ratio of the specimen produced from the same aggregate and cement. The effect of w/c ratio is seen only on the values of the UPV and strength not on the relation between UPV and strength. However, when Figure 5.28-c is considered, for the travel path length of 5 cm, the relationship is not such similar for different w/c ratios. For the same strength value, the possible value of UPV differs in a wider range as compared to other two travel paths.

The UPV development with respect to strength value could be examined together for all mortar types according to travel path distances. For this purpose, the UPV-strength curves were obtained from the results of mortars having three different w/c ratios. The results for compressive strength of mortar specimens are shown graphically in Figure 5.29. In this figure, three series of data are given representing each travel path length. Lines are fitted by least-squares regression to each series of data. The coefficients of correlation ( $R^2$ ) are determined in order to check how well the fitted lines define the real data points.

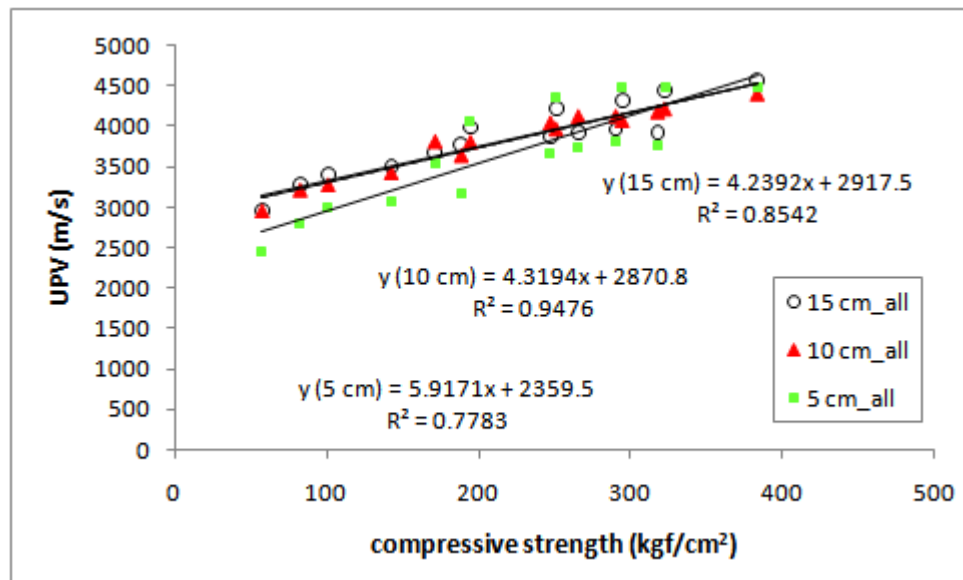


Figure 5.29. Relationships between UPV and compressive strength

As seen in Figures 5.29, the UPV and the strength of the mortar specimens seem to be linearly related to each other. Especially for 10 and 15 cm travel path lengths, the lines are very close and the coefficients of the lines are similar. However, the UPV - strength relation for 5 cm travel path length behaves slightly different. Although there is approximately a linear relation, the correlation coefficient is also small as compared to other two test types. Therefore, it could also be concluded that using very small specimens is also not suitable for testing of hardened specimens as in the case of fresh specimens, most probably due to the effect of the reflected waves from the boundaries as wavelength becomes greater than the least dimension.

As a result, it could be claimed that with the prepared experimental set-up the monitoring of the cementitious specimens could also be continued in the hardened state after observing the fresh state properties. The development of UPV in the cementitious materials could be measured as long as desired without interrupting the testing.

### **5.11.2 Volume of permeable pore determination test results**

As the second property of the hardened cement mortars, the total volume of permeable voids in the mortar specimens was determined according to ASTM C 642. Beyond the volume of permeable pores, the determination of water absorption, bulk density and apparent density of the mortar specimens were also possible according to this standard test method. For this purpose 4\*4\*16 cm prismatic specimens were prepared at three different w/c ratios. The specimens were water-cured at the same conditions as the compressive strength test specimens. The test was applied to 1, 2, 3, 7 and 28 day-old specimens. At each age three specimens were used to determine the properties for each batch of one type of mortar. As three batches were prepared for each w/c ratio, the final results obtained are the average of the results of nine specimens as the values are quite similar to each other for different batches of the same w/c ratio. The test results are

summarized in Table 5.18. In the table volume of permeable pores, absorption, apparent and bulk density of the mortar specimens at different ages are given.

Table 5.18. Volume of permeable pores, absorption, apparent and bulk density

<b>w/c</b>	<b>Age (day)</b>	<b>Vol. of Perm. Pores (%)</b>	<b>Absorption (%)</b>	<b>Apparent Density (g/cm<sup>3</sup>)</b>	<b>Bulk Density (g/cm<sup>3</sup>)</b>
<b>w/c=0.5</b>	<b>1</b>	18.6	8.6	2.60	2.12
	<b>2</b>	17.7	8.3	2.57	2.12
	<b>3</b>	17.3	8.1	2.57	2.12
	<b>7</b>	17.4	8.2	2.57	2.12
	<b>28</b>	15.9	7.4	2.54	2.14
<b>w/c=0.6</b>	<b>1</b>	24.4	12.2	2.64	1.99
	<b>2</b>	24.4	12.2	2.63	1.99
	<b>3</b>	24.4	12.2	2.64	2.00
	<b>7</b>	24.1	12.1	2.63	1.99
	<b>28</b>	23.9	11.8	2.66	2.02
<b>w/c=0.8</b>	<b>1</b>	30.6	17.0	2.55	1.77
	<b>2</b>	29.9	16.2	2.59	1.82
	<b>3</b>	29.5	15.7	2.55	1.80
	<b>7</b>	29.6	16.4	2.54	1.78
	<b>28</b>	28.6	15.3	2.62	1.87

From Table 5.18, it is seen that the properties are dependent on the w/c ratio of the mortar specimens. As w/c ratio of the mortar increases, volume of permeable pores and water absorption also increase while bulk density decreases. On the other hand, the relation between apparent density and w/c ratio is not clear.

In Table 5.18, the effect of age on the properties can also be seen between the 1<sup>st</sup> and 28<sup>th</sup> days. However, during this time period the change in properties is quite small. It could be said that after hardening, the volume of permeable pores, absorption and density of the mortar specimens do not change much although the degree of hydration increases. The changes in values are so small that the difference could not be measured accurately between short time periods. The change in absorption and volume of permeable pores of mortars during the first 28 days of hardened mortars are shown graphically in Figures 5.30 and 5.31, respectively.

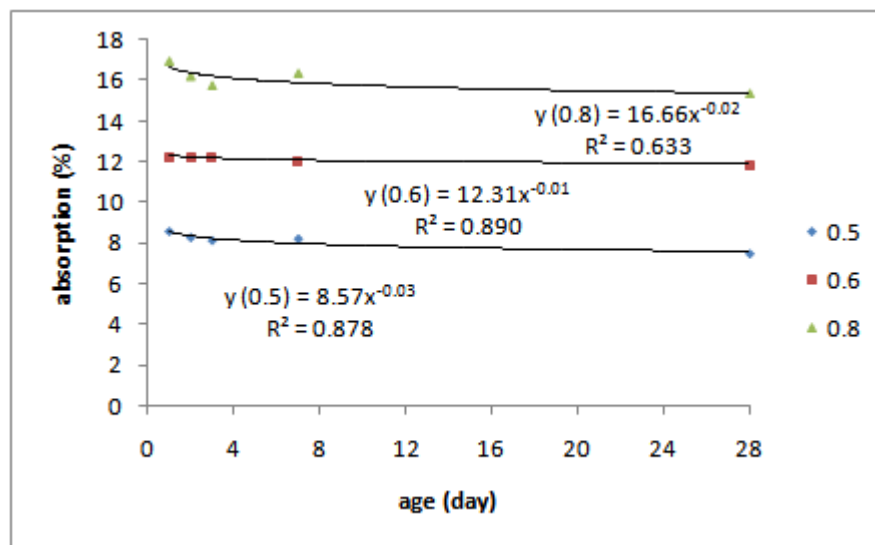


Figure 5.30. Absorption of mortar specimens

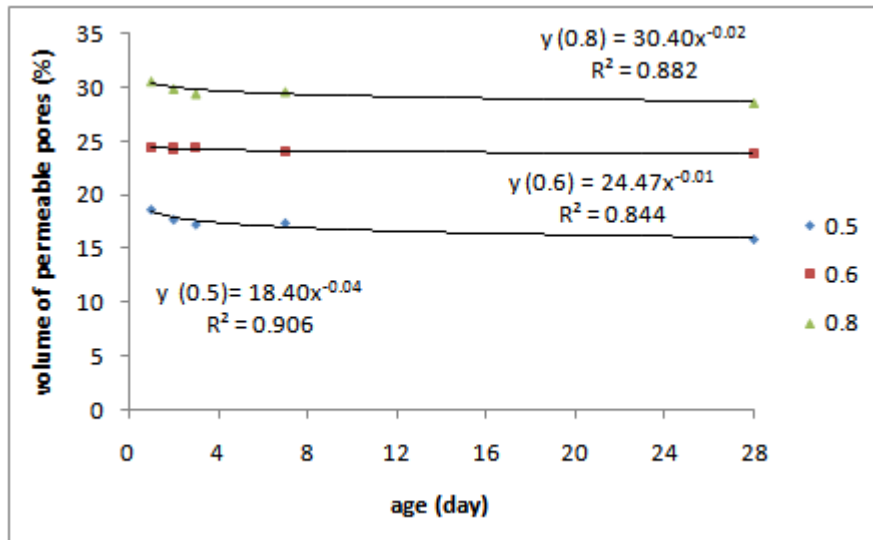


Figure 5.31. Volume of permeable pore space of mortar specimens

As seen in Figures 5.30 and 5.31, the main effective factor in determining the absorption and permeable pore volume is the w/c ratio of the mortar rather than the age. A power equation is the best suited relation for both parameters in all mortars. However, the power term is negative and small in all cases. The constants are related to the w/c ratio of the mortars. It is also obvious from the figures that absorption and permeable pore space behave similarly with respect to time.

The relation between permeable pore volume and the w/c ratio is shown for each test age separately in Figure 5.32.

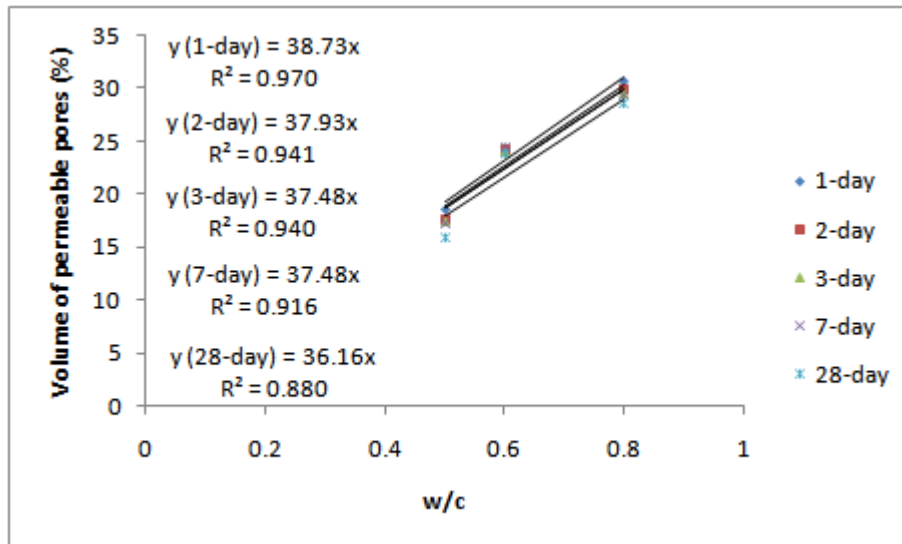
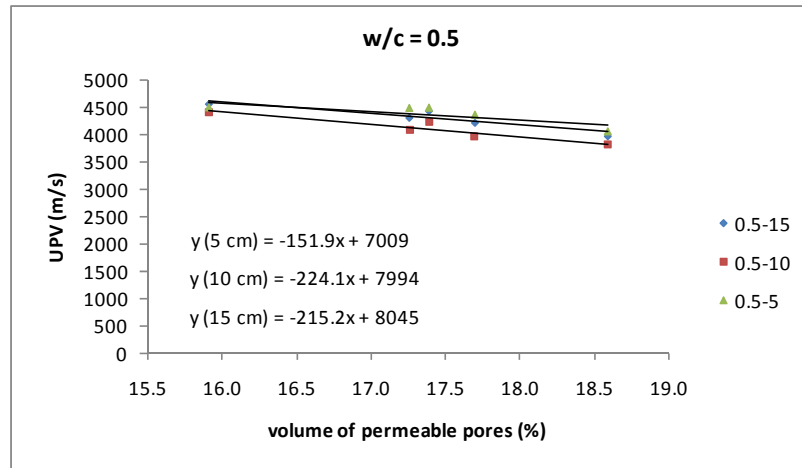


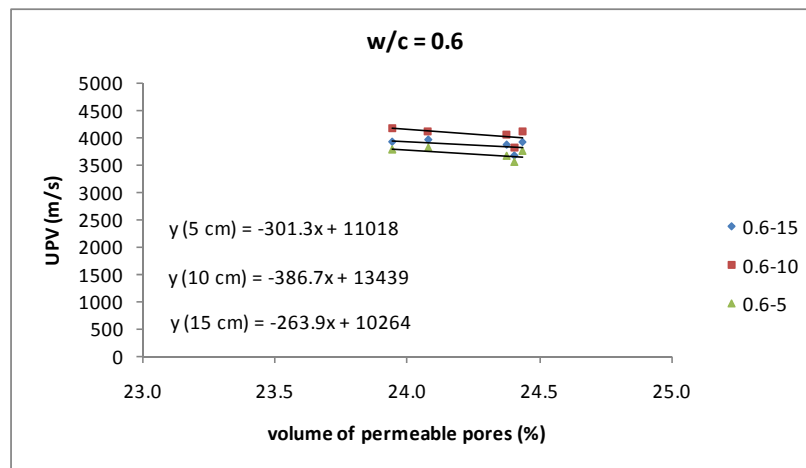
Figure 5.32. Relation between volume of permeable pores and w/c ratio

In Figure 5.32, volume of permeable pores is linearly related to w/c ratio of the mortar at all ages with high  $R^2$  values. The lines corresponding to each test age are very close to each other, especially the results obtained on the 2<sup>nd</sup>, 3<sup>rd</sup> and 7<sup>th</sup> days are nearly same. The coefficients of the line equations are also close to each other, decreasing slightly with increasing age. It could be claimed that for the determination of permeable space volume of the mortar specimens, the test age does not affect the result as long as the material is in the hardened state.

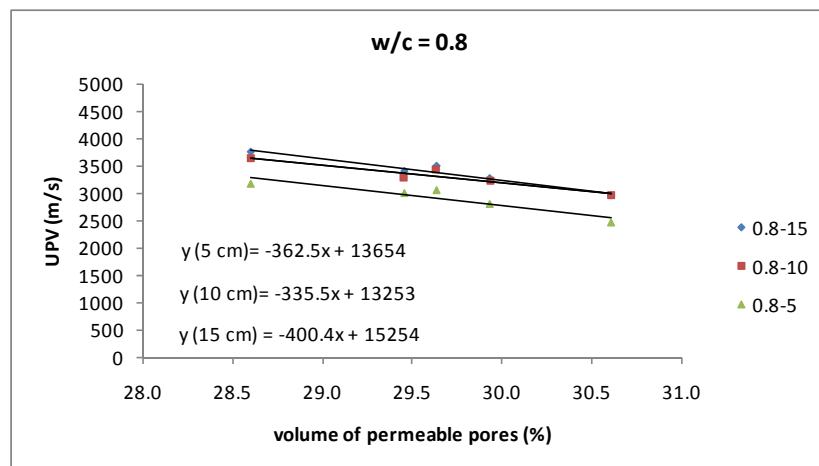
The porosity of materials is one of the parameters that determine the velocity of the ultrasonic pulses (UPV) in the medium. High amount of porosity means the waves propagate slower as the waves cannot propagate through voids but travel around them. The results of experiments applied during this research also proved this statement. In mortars with higher w/c ratio, it was found out that the volume of permeable pores was also high. Additionally, in mortars with high w/c ratio, the UPV measured was also slow at all ages. The change of UPV with respect to volume of permeable pores of the mortar specimens is given in Figure 5.33 for different travel path lengths used in UPV measurements of mortars with given w/c ratio.



a) w/c ratio = 0.5



b) w/c ratio = 0.6



c) w/c ratio = 0.8

Figure 5.33. Relation between UPV and permeable pore volume in mortars

According to Figure 5.33, a linear relationship is seen between UPV and volume of permeable pores for each w/c ratio and travel path length. In this relation travel path length is only effective on UPV measurements, the path length is not a parameter for volume of permeable voids determination. The parameters for permeable pore volume determination are the mortar type and age. In the graphs, it is seen that volumes of permeable pores change rather in a small range.

As a result, it could be repeated that the volume of permeable pores is directly related to the w/c ratio of the mortar. UPV is also dependent on the w/c ratio of the medium. Therefore, it is clear that the UPV of hardened mortar specimens is also related to the volume of permeable pores.

## **CHAPTER 6**

### **CONCLUSIONS**

The aim of this study was to monitor the development of properties in fresh cementitious materials continuously. In order to monitor the hydration process in cements, first, a non-destructive test method depending on ultrasonic measurements was developed. After the experimental set-up was established, cement pastes and mortars with different w/c ratios were tested so that the UPV (Ultrasonic Pulse Velocity) development curves with time were obtained. The properties of specimens were also determined by standard test methods to correlate with the UPV measurements. The rate of heat of hydration and the setting time of cement pastes were determined. The ESEM images before and after setting of paste sample were obtained for observing the hydration process. For the mortars, beyond the setting time, the strength and the volume of permeable pores up to 28 days were also measured in order to compare with the UPV measurements. The effect of frequency range of the transducers and the travel path length used in the established experimental set-up were also checked.

The UPV and rate of UPV (RUPV) development curves were analysed and correlated with the traditional test results in order to explain the hydration process. The results yielded valuable information for the monitoring of hydration.

As the result of this investigation, the following conclusions have been derived:

1. The ESEM micrographs of cement paste having 0.5 w/c ratio were obtained at dormant period, initial setting and final setting during the early hydration. The images showed the stages of the hydration process clearly. During the dormant period, the particles are not connected so that ultrasonic pulses cannot properly propagate through the material. At initial setting the hydration products precipitated on adjacent cement particles seem to touch each other and an interconnected system is started to be formed. After final setting the amount of hydration products increases and the voids between the particles are filled so that ultrasonic pulses can be transmitted faster.
2. The UPV values were obtained from the waveforms. At very early stages which correspond to the dormant period, the waveforms are not very clear. The waves travelled through the medium and captured by the receiving transducer are very weak during the early ages due to the attenuation and the electrical noise, therefore, the UPV measured at this stage is not very accurate. However, after the initial set, due to the formation of interconnected system, the waves start to be clearer with increasing amplitudes. As the hydration proceeds, the medium becomes more solid and the UPV increases. After the medium sets completely, the change in the waveforms becomes less significant.
3. From the UPV development test results in cement pastes and mortars it is seen that generally the higher w/c ratios yield smaller UPV values not only at later ages but also at early ages of hydration.
4. The UPV development curves in cement pastes show typical S-curves for all w/c ratios. The UPV curves can be idealized by four distinct approximately linear portions. However, the first portion is not very reliable as the very early ages could not be determined accurately by the set-up. The 2<sup>nd</sup> portions have the highest slopes which reveal that the hydration products start to form very rapidly. The slopes of 3<sup>rd</sup> portions are milder. Lastly, the fourth linear parts have very mild slopes which can be an indication of slowing down of the hydration reactions.

5. In the RUPV development curves of cement pastes, which were determined from UPV values by numerical derivative with respect to time, 5 stages could be distinguished. Firstly, the rate increases steeply. After making a peak, it starts to decrease. Later it has a constant portion the length of which is dependent on the w/c ratio of the specimen. Then, the rate of UPV development starts to decrease approaching to zero in two steps.
6. The comparison of UPV and RUPV development curves with setting time measurements and rate of heat of hydration curves shows that the proposed test method defines the hydration process in cement pastes quite well. From this comparison the following results are obtained:
  - The initial setting time of cement pastes can be defined as the point at which the slope of UPV development curves changes distinctly a second time. This point is determined as the intersection of the 2<sup>nd</sup> and 3<sup>rd</sup> linear portions of UPV development curves. The maximum difference for the initial setting time as determined from UPV method and Vicat apparatus is less than 8%. At the initial setting time the medium gains a UPV value of approximately 1400 m/s regardless of the w/c ratio of the sample.
  - The final setting time occurs when the plateau in RUPV development curve ends. The maximum difference for the final setting time as determined from UPV method and Vicat apparatus is less than 3% in the tested samples. Additionally, at final setting time it is seen that UPV is approximately 1800 m/s at any w/c ratio.
  - The dormant period in cement pastes seems to end when the RUPV curves reaches its first peak and the UPV of the medium reaches about 1000 m/s.
  - The start of deceleration period in cement pastes seems to coincide with the start of 4<sup>th</sup> linear portion of the idealized UPV curves. After this point, the increase in UPV is very slight as characterized by the very mild slope.

7. The UPV measurements were applied up to 28 days in mortar specimens. The increase in UPV is very limited after 24 hours as compared to increase during the first 24 hours. Therefore, it can be concluded that the UPV measurements are more sensitive to change in fresh state properties rather than the hardened state properties.
8. The UPV development curves in mortars for the first 24 hours are similar to those in cement pastes. However, the UPVs reach higher values in mortars as compared to pastes. On the other hand, due to higher attenuation and longer path distances the initial linear portions could not be observed in mortar samples. Therefore, the UPV curves are idealized by three distinct linear portions. The 1<sup>st</sup> portion in mortars corresponds to 2<sup>nd</sup> portion of the pastes. Similar to pastes, the slope is the highest in the first portion and becomes milder at each stage in all w/c ratios. Additionally, the slopes are smaller for the higher w/c ratios.
9. The RUPV development curves of mortars are slightly different from those of pastes. After making an initial peak as in the case of pastes, RUPV starts to decrease. However, instead of making a plateau, it makes a minimum point and then increases slightly reaching a second small peak. Afterwards it decreases approaching zero asymptotically.
10. The comparison of setting times as determined by Penetration Resistance Test (PR) with UPV and RUPV results yields the followings:
  - The initial setting time seems to occur around the initial peak of RUPV curves. This approach in determining initial setting time results in an error of about 12 %.
  - For final setting time determination, a UPV of 2000 m/s seems to be a good approximation for w/c ratios of 0.5 and 0.6. However, in case of mortars with 0.8 w/c ratio, this value is around 1800 m/s. Depending on the assumption that such high w/c ratios are not generally used in conventional concrete industry, UPV of 2000 m/s might be accepted as a suitable approximation.

11. PR test defines setting as the two arbitrary stages of hydration in cement mortars. However, the setting phenomenon is related only to the paste portion of the mortars. Therefore, the setting times in mortars should not be much different than those of pastes. Depending on this assumption, the setting times of mortars were defined by UPV test method similar to the definitions in pastes.

- The initial setting is defined as the point where the slope of UPV curve changes drastically as in the case of pastes. This point is determined as the intersection of 1<sup>st</sup> and 2<sup>nd</sup> linear portions of the UPV curves (make attention that the UPV in mortars were idealized by three linear portions unlike the four linear portions in UPV of pastes). The UPV values at that point is approximately 1900 m/s for mortars of 0.5 and 0.6 w/c ratio, while it is about 1450 m/s for mortar having 0.8 w/c ratio.
- The final setting time is supposed to occur when the RUPV development curves reaches its minimum point. The UPV is approximately 2500 m/s for 0.5 and 0.6 w/c ratio; and 2000 m/s for 0.8 w/c ratio.
- The initial and final setting time values as obtained by this alternative method are dependent on w/c ratio of the samples as expected; the higher the w/c ratio, the longer the setting time.
- The UPV increases approximately 550 m/s between the beginning and end of setting.
- The initial and final setting times as determined from the UPV method in mortars are close to the setting times as determined by Vicat apparatus in cement paste with the same w/c ratios.
- The UPVs are higher in mortars due to the presence of aggregate particles as compared to paste samples. However, the amount of aggregate is different in different mortar types depending on the w/c

ratio for constant cement content. Therefore, having different UPVs at the similar stages of hydration is acceptable.

12. Although the travel path length is not expected to affect the UPV values, excessively long distances result in higher attenuation, while excessively short distances result in inaccurate results due to the near-field effect and reflected waves from the boundary. In the path distances tested in this study, 15 cm and 10 cm travel length (i.e. mold dimension) reveals similar results. On the other hand, in the case of 5 cm travel path length usually, the results are different. Additionally, in the case of 15 cm travel path distance, the initial stages of hydration could not be observed especially for high w/c ratios due to high attenuation.
13. Higher frequencies result in smaller wavelengths and hence higher attenuation due to scattering. Especially for very small UPVs, the wavelength could be smaller than the particle dimensions in the mortars. As the frequency applied increased, the initial readings were delayed in mortars, which means high frequencies are not suitable to monitor the very early stages. Additionally, the effect of frequency seems to be more severe for smaller travel path distances. Therefore, it could be stated that a suitable frequency and travel path length should be chosen.
14. The UPV measurements obtained at different times for different batches prepared with the same materials and same proportions seems to be similar for 15 and 10 cm travel path lengths with a maximum difference of 5 minutes in initial setting time estimation and 16 minutes in final setting time estimation. This small difference in UPV measurements for two repetitions in different batches makes the method repeatable and reliable as long as the appropriate path length dimension is chosen for the test.
15. Samples with smaller w/c ratio result in higher strength and higher UPV as expected when all the ages and w/c ratios are considered. A linear relationship is obtained between UPV and strength. This relationship is quite similar in the case of 15 and 10 cm travel path lengths. Therefore, it

could be concluded that very small specimen dimensions are also not suitable in the hardened state as in the case of fresh state.

16. The volume of permeable pores is higher for the specimens of higher w/c ratio. A linear relationship is also obtained between the UPV and permeable pore volume at each w/c ratio of the samples. The UPV is directly dependent on the amount of voids; the higher the amount of voids, the slower the UPV. However, the effect of hydration degree in total volume of permeable pores in the mortar specimens is not significant. As the age of the specimen increases the total volume of permeable pores decreases slightly. This also explains the reason for only the slight increase in UPV at hardened state as compared to fresh state.
17. The UPV can be a suitable and reliable test method in monitoring the hydration process in cements. It is also superior to traditional test methods as it is possible to test the specimens as long as desired; not only in the fresh state but also in the hardened state. The results in hardened state also give useful information about the properties of the specimens. Therefore, it can be stated that the method is a compatible test procedure for continuous monitoring of the properties of cementitious materials.

## **CHAPTER 7**

### **RECOMMENDATIONS**

Ultrasonic pulse velocity method can be used to describe the hydration process of cements. In this research program the method was applied to cement pastes and mortars having different w/c ratios. The results were encouraging to expand the application to different cementitious materials. Depending on the evaluation of the results of this study, the following recommendations for the future studies can be made:

1. Some further software studies may be helpful for improving the analysis part of the data obtained from data acquisition system. The UPV and RUPV development curves and the characteristic points related to those curves could be determined faster and more systematically if a suitable computer program could be established.
2. The application of the method on different types of cements can be studied. The effect of several chemical and mineral admixtures on hydration properties can also be monitored by UPV method.
3. The monitoring of hydration in concrete samples and extending the usage to the construction site should be the ultimate goal in order to standardize the UPV method in hydrating materials.

## REFERENCES

Akkaya, Y., Voigt, T., Subramaniam, K. V., and Shah, S. P., "Nondestructive measurement of concrete strength gain by an ultrasonic wave reflection method", *Materials and Structures*, V. 36, No. 262, 2003, pp. 507-514

Arnaud, L., and Thinet, S., "A device to monitor continuously by the setting of concrete", 15<sup>th</sup> World Conference on Non-Destructive Testing, Rome, 2000

Arnaud, L., "P- and S- waves to determine the rheological properties of heterogeneous materials with evolving properties", 16<sup>th</sup> World Conference on Non-Destructive Testing, Montreal, Canada, 2004

ASTM C-186, "Standard Test Method for Heat of Hydration of Hydraulic Cement", American Society for Testing and Materials, 2002

ASTM C 191-01a, Standard Test Method for Time of Setting of Hydraulic Cement by Vicat Needle, Annual Book of ASTM Standards, 2002

ASTM C 403/C 403M-99, Standard Test Method for Time of Setting of Concrete Mixtures by Penetration Resistance, Annual Book of ASTM Standards, 2002

ASTM C 597-97, Standard Test Method for Pulse Velocity Through Concrete, Annual Book of ASTM Standards, 2002

ASTM C 642-97, Standard Test Method for Density, Absorption, and Voids in Hardened Concrete, Annual Book of ASTM Standards, 2002

ASTM D 2845-95, Standard Test Method for Laboratory Determination of Pulse Velocities and Ultrasonic Elastic Constants of Rock, American Society for Testing and Materials, 2000

Belie, N. De, Grosse, C. U., Kurz, J., and Reinhardt, H. W., "Ultrasound monitoring of influence of different accelerating admixtures and cement types for shotcrete on setting and hardening behavior", *Cement and Concrete Research*, V. 35, 2005, pp. 2087-2094

Beutel, R., Öztürk, T., Grosse, C. U., "Comparative evaluations of cementitious materials on early age with ultrasonic wave transmission, wave reflection and impact-echo measurements", *Otto-Graf-journal*, V. 16, 2005, pp. 213-224

Boumiz, A., Vernet, C., and Cohen Tenoudji, F., "Mechanical properties of cement pastes and mortars at early ages: evolution with time and degree of hydration", *Advanced Cement Based Materials*, V. 3, 1996, pp. 94-106

Boutin, C., and Arnaud, L., "Mechanical characterization of heterogeneous materials during setting", *European Journal of Mechanics A/Solids*, V. 14, 1995, pp. 633-656

D'Angelo, R., Plona, T. J., Schwartz, L. M., and Coveney, P., "Ultrasonic measurements on hydrating cement slurries: Onset of shear wave propagation", *Advanced Cement Based Materials*, V. 2, 1995, pp. 8-14

Erdoğan, T. Y., 2002, Materials of Construction, Metu Press Publishing Company, Ankara, Turkey

Grosse, C. U., Weiler, B., Herb, A. T., Schmidt G., and Hofler, K., "Advances in ultrasonic testing of cementitious materials", *Festschrift zum 60. Geb. von Prof. Reinhardt (C. U. Grosse, Ed.)*, Libri-Verlag, Hamburg, 1999, pp. 106-116

Grosse, C. U., and Reinhardt, H. W., "Ultrasound technique for quality control of cementitious materials", *Proc. of 15. World Conf. On NDT, Rom, 2000* ([www.ndt.net](http://www.ndt.net))

Grosse, C.U., Koble, S. U., and Reinhardt, H. W., "Ultrasound scanning electron microscopy and nuclear magnetic resonance spectroscopy- comparison of results of investigating the hydration process in cementitious materials", NDT.net, V.6, May 2001

Grosse, C. U., Reinhardt, H. W., "Fresh concrete monitored by ultrasound methods", Otto-Graf-Journal, V. 12, 2001, pp. 157-168

Grosse, C. U., "About the improvements of US measurement techniques for the quality control of fresh concrete", Otto-Graf-journal, V. 13, 2002, pp. 93-110

Grosse, C., and Reinhardt H. W., "Advanced testing methods for cement based materials during setting and hardening", Concrete Plant International, V. 5, October 2005, pp. 66-80

Houf, J. W., "Practical contact ultrasonics- defining terms and principles", The NDT Technician, V.2, October 2003

Irwin, D., Pessiki, S., "Nondestructive evaluation of concrete strength in precast plant using impact-echo method", ATLSS Report No. 04-10, Center for Advanced Technology for Large Structural Systems, April 2004, 59 pp

Kaczmarek, M., "Ultrasound- A useful tool to investigate complex materials", Periodica Polytechnica Ser. Chem. Eng., V.45, No. 2, 2001, pp. 111-129

Kamada, T., Uchida, S., Rokugo, K., "Nondestructive evaluation of setting and hardening of cement paste based on ultrasonic propagation characteristics", Journal of Advanced Concrete Technology, V. 3, No. 3, October 2005, pp. 343-353

Keating, J., Hannant, D. J., and Hibbert, A. P., "Comparison of shear modulus and pulse velocity techniques to measure the build-up of structure in fresh cement pastes used in oil well cementing", Cement and Concrete Research, V. 19, 1989a, pp. 554-566

Keating, J., Hannant, D. J., and Hibbert, A. P., "Correlation between cube strength, ultrasonic pulse velocity and volume change for oil well cementing", Cement and Concrete Research, V. 19, 1989b, pp. 715-726

Krautkrämer, J. and Krautkrämer, H., 1983, Ultrasonic Testing of Materials, Springer-Verlag, New York, USA

Labouret, S., Looten-Baquet, I., Bruneel, C., and Frohly, J., “Ultrasound method for monitoring rheology properties evolution of cement”, *Ultrasonics*, V. 36, 1998, pp. 205-208

Lee, H. K., Lee, K.M., Kim, Y. H., Yim, H., and Bae, D. B., “Ultrasonic in-situ monitoring of setting process of high-performance concrete”, *Cement and Concrete Research*, V. 34, 2004, pp. 631-640

Malhotra V. M. And Carino N. J. (Editors), 2004, Handbook on Nondestructive Testing of Concrete, 2<sup>nd</sup> Edition, CRS Press LCC, USA

Mehta, P. K., and Monteiro, P. J. M., 2006, Concrete: Microstructure, Properties, and Materials, The McGraw-Hill Companies, New York, USA

Mindess, S., and Young, J. F., 1981, Concrete, Prentice-Hall Inc., Eaglewood Cliffs, New Jersey, USA

Neville, A. M., 2003, Properties of Concrete, 4<sup>th</sup> Edition, Pearson Education Limited, Harlow, England

NT Built 505, “Measurement of Heat of Hydration of Cement with eat Conduction Calorimetry”, Nordtest Method, approved 2003-12

Odler, I. “Hydration, Setting and Hardening of Portland Cement”, 2005, Lea’s Chemistry of Cement and Concrete, 4<sup>th</sup> Edition ( Ed. Hewlett, P. C.), Elsevier Butterworth-Heinemann, Oxford

Öztürk, T., Rapoport, J., Popovics, J. S., Shah, S. P., “Monitoring the setting and hardening of cement-based materials with ultrasound”, *Concrete Science and Engineering*, V. 1, No. 2, 1999, pp. 83-91

Öztürk, T., Kroggel, O., Grübl, P., Popovics, J. S., “Improved ultrasonic wave reflection technique to monitor the setting of cement-based materials”, *NDT&E International*, V. 39, 2006, pp. 258-263

Penguin English Dictionary, 2<sup>nd</sup> Edition, Slovakia, 2004

Pessiki, S. P., and Carino, N. J., “Setting time and strength of concrete using the impact-echo method”, *ACI Materials Journal*, September-October 1988, pp. 389-399

Pessiki, S., Johnson, M., “Nondestructive evaluation of early-age concrete strength in plate structures by impact-echo method”, *ACI Materials Journal*, Vol. 93, No. 3, May-June 1996, pp. 260-271

Pessiki, S., Rowe, M., “Influence of steel reinforcing bars on the evaluation of early-age concrete strength using impact-echo method”, *ACI Structural Journal*, Vol. 94, No. 4, July-August 1997, pp. 378-388

Rapoport, J. R., Popovics, J. S., Subramaniam K. V., and Shah S. P., “Using ultrasound to monitor the stiffening process of Concrete with Admixtures”, *ACI Materials Journal*, V. 97, 2000, pp. 675-683

Reinhardt, H. W., and Grose, C., “Setting and hardening of concrete continuously monitored by elastic waves”, *NDTnet*, V.1, July 1996

Reinhardt, H. W., Grose, C., Weiler, B., Bohnert J., and Windisch N., “P-wave propagation in setting and hardening concrete”, *Otto-Graff Journal*, V. 7, 1996, pp. 181-189

Reinhardt, H. W., and Grosse, C. U.,” Continuous monitoring of setting and hardening of mortar and concrete”, *Construction and Building Materials*, V. 18, 2004, pp. 145-154

RILEM Report 31, Advanced Testing of Cement-Based Materials during Setting and Hardening – Final Report of RILEM TC 185-ATC, Editors: H.W. Reinhardt, and C. U. Grosse, September 2005, 362 pages

RILEM TC 119-TCE1, (chairman: R. Springenschmid), “Adiabatic and semi-adiabatic calorimetry to determine the temperature rise in concrete due to hydration heat of the cement”, *Materials and Structures*, V. 30, 1997, pp. 451-464

Sanchez de Rojas, M. I., Luxen, M. P., Frias M. and Garcia N., “The influence of different additions on portland cement hydration heat”, *Cement and Concrete Research*, V.23, 1993, pp.46-54

Sansalone, M., “Impact-echo: The complete story”, *ACI Structural Journal*, November-December 1997, pp. 777-786

Sayers, C. M., and Dahlin A., “Propagation of ultrasound through hydrating cement pastes at early times”, *Advanced Cement Based Materials*, V. 1, 1993, pp. 12-21

Sayers, C. M., and Grenfell, R. L., “Ultrasonic propagation through hydrating cements”, *Ultrasonics*, V. 31, 1993, pp. 147- 153

Schindler A. K., Dossey, T., and McCullough, B. F., “Temperature Control During Construction to Improve the Long-term Performance of Portland Cement Concrete Pavements”, Research report number 0-1700-2, Center for Transportation Research, the University of Texas at Austin, May 2002

Stepisnik, J., Lukac, M. and Kocuvan, I., “Measurement of cement hydration by ultrasonics”, *Ceramic Bulletin*, V. 60, 1981, pp. 481-483

Tharmaratnam, K., and Tan, B. S., “Attenuation of ultrasonic pulse in cement mortar”, *Cement and Concrete Research*, V.20, No. 3, 1990, pp. 335-345

Voigt, T., Akkaya, Y., Shah, P. S., “Nondestructive Testing of Concrete Using Ultrasound”, *Leipzig Annual Civil Engineering Report*, Lacer No. 6, 2001, pp. 349-362

Voigt, T., Akkaya, Y., Shah, P. S., “Determination of early age concrete strength by a reflective ultrasonic technique”, 6<sup>th</sup> International Symposium on High Strength/High Performance Concrete, Leipzig, Germany, June 16-20 2002, pp. 1489-1501

Voigt, T., and Shah, P. S., “Nondestructive testing of setting and hardening of Portland cement mortar with sonic methods”, NDT-CE 2003a

Voigt, T., Akkaya, Y., and Shah, S. P., “Determination of early age mortar and concrete strength by ultrasonic wave reflections”, *Journal of Materials in Civil Engineering*, ASCE, 2003b, pp. 247-254

Voigt, T., and Shah, S. P., “Properties of early-age portland cement mortar monitored with shear wave reflection method”, *ACI Materials Journal*, V. 101, No. 6, November-December 2004, pp. 473-482

Voigt, T., Grosse, C. U., Sun, Z., Shah, S. P., and Reinhardt, H. W., “Comparison of ultrasonic wave transmission and reflection measurements with P- and S- waves on early age mortar and concrete”, *Materials and Structures*, V. 38, 2005, pp. 729-738

Ye, G., Laura, P., Breugel K., Fraaij, A.L.A., “Study on the development of the microstructure in cement-based materials by means of numerical simulation and ultrasonic pulse velocity measurement”, *Cement and Concrete Composites*, V. 26, 2004, 491-497

Young, J. F., Mindess, S., Gray, R. J., and Bentur, A., 1998, *The Science and Technology of Civil Engineering Materials*, Prentice Hall Inc., New Jersey, USA

## CURRICULUM VITAE

### PERSONAL INFORMATION

Surname, Name: Kasap Keskin, Özlem  
Nationality: Turkish (TC)  
Date and Place of Birth: 8 November 1978 , İzmir  
Phone: +90 506 253 79 50  
email: ozlemkasap@gmail.com

### EDUCATION

Degree	Institution	Year of Graduation
MS	METU Civil Engineering	2002
BS	METU Civil Engineering	2000
High School	İzmir Science High School	1996

### WORK EXPERIENCE

Year	Place	Enrollment
2007- 2008	Turkish Cement Manufacturers' Association	R&D Institute Expert
2000-2007	METU Department of Civil Engineering	Research Assistant

### FOREIGN LANGUAGES

Fluent English, Intermediate German

### PUBLICATIONS

#### Thesis

- Effects of Cement Type on Concrete Maturity, (M.S. Thesis), Middle East Technical University, Ankara, Turkey, 2002, 96 pages

### Journals

- M. Sahmaran, O.Kasap, K. Duru, and I.O. Yaman, “Effects of mix proportions and water-cement ratio on sulfate resistance of blended cements”, *Cement and Concrete Composites*, Vol. 29, No. 3, 2007, pp. 159-167
- M.Sahmaran, O.Kasap, K.Duru, I.O.Yaman, “Effects of chemical composition and water-cement ratio on the sulfate resistance of mortars”, *Cement and Concrete World*, V.10, No.59, 2006, pp. 66-77 (Both in English and Turkish)
- Kasap, O. and Tokyay, M., “A method for determination of equivalent age of concrete by heat of hydration of cement”, *Teknik Dergi*, V. 15, No. 2, April 2004 , pp. 3215-3227 (in Turkish)
- Kasap, O. and Tokyay, M., “Effects of cement type on concrete maturity”, *Cement and Concrete World*, V.7, No.40, 2002, pp.58-70 (Both in English and Turkish)

### Proceedings

- Ozlem Kasap, Mustafa Sahmaran, Kevser Duru, I.Ozgur Yaman, “Sulfate resistance of blended cements for different phases: paste, mortar, concrete”, *Proceedings of 3<sup>rd</sup> International Symposium in Cement and Concrete*, Editor Asım Yeğınobalı, Istanbul, Turkey, 2007, pp. 563-572
- M. Şahmaran, O. Kasap, I. O. Yaman “Sulfate performance of blended cements with fly ash and natural pozzolan”, *Sixth National Concrete Congress Proceedings*, Istanbul, Turkey, 2005, pp. 201-208 (in Turkish)
- Kasap, O. and Tokyay, M., “Effects of cement type on concrete maturity”, *Proceedings of Role of Cement Science in Sustainable Development*, Editors R.K. Dhir, M.D.Newlands and L.J.Csetenyi, Scotland, 2003, pp. 131-142